UNIVERSIDADE FEDERAL DO RIO GRANDE DO SUL

INSTITUTO DE CIÊNCIAS BÁSICAS DA SAÚDE

PROGRAMA DE PÓS-GRADUAÇÃO EM CIÊNCIAS BIOLÓGICAS:
BIOQUÍMICA

BRUNA DONIDA

DESENVOLVIMENTO DE NANOPARTÍCULA COM β-CICLODEXTRINA E AVALIAÇÃO DE SEU POTENCIAL TERAPÊUTICO PARA TRATAMENTO DA DOENÇA DE NIEMANN-PICK C.

Porto Alegre

2019

BRUNA DONIDA

DESENVOLVIMENTO DE NANOPARTÍCULA COM β-CICLODEXTRINA E AVALIAÇÃO DE SEU POTENCIAL TERAPÊUTICO PARA TRATAMENTO DA DOENÇA DE NIEMANN-PICK C.

Tese apresentada ao Programa de Pós-Graduação em Ciências Biológicas: Bioquímica do Instituto de Ciências Básicas da Saúde da Universidade Federal do Rio Grande do Sul, para obtenção do título de doutora em Bioquímica.

Orientadora: Prof^a. Dr^a. Carmen Regla Vargas
Co-orientadora: Prof^a. Dr^a. Fernanda Poletto

Porto Alegre
2019

CIP - Catalogação na Publicação

"One, remember to look up at the stars and not down at your feet. Two, never give up work. Work gives you meaning and purpose and life is empty without it. Three, if you are lucky enough to find love, remember it is there and don't throw it away."

Stephen Hawking

AGRADECIMENTOS

Primeiramente eu gostaria de agradecer à Professora Carmen Regla Vargas, minha orientadora, por confiar na minha capacidade e por se aventurar junto a mim nesse projeto envolvendo uma série de novos campos para nós duas. Gostaria de agradecer por ser minha mentora durante todos esses anos de pesquisa e por me incentivar a ir sempre além. Admiro muito tua organização, tua liderança e a forma como fazes pesquisa.

Agradeço à Professora Fernanda Poletto, minha co-orientadora, por abraçar a ideia desse projeto e pegar na minha mão para que conseguíssemos chegar até aqui. Não poderia ter escolhido ninguém melhor para me orientar nesse caminho, minha admiração por ti só cresceu nesses mais de 10 anos que trabalhamos juntas. Fazes parte da minha trajetória acadêmica e és, sem dúvida, um exemplo pra mim. Obrigada por me incentivar, por me ajudar a encontrar as saídas e por seres tantas vezes um ombro amigo. Acho que esta é uma bela maneira de fechar um ciclo de aprendizado que teve seu começo na Iniciação Científica.

Agradeço à Professora Dinara Moura da UFCSPA por ter sido praticamente minha segunda co-orientadora. Tens papel fundamental na minha formação, admiro muito teu trabalho e te agradeço por todos os ensinamentos. Não teria sido possível realizar este projeto sem a tua colaboração. Agradeço por poder utilizar teu laboratório e aprender com o teu grupo de pesquisa.

Durante os anos de doutorado tive a oportunidade de trabalhar com dois excelentes alunos de Iniciação Científica: a Bárbara Tauffner e o Marco Raabe. Vocês foram meu braço direito e muitas vezes também o esquerdo. Sem vocês o caminho teria sido muito mais árduo e muito menos gratificante. Aprendi mais com vocês do que pude ensinar.

Agradeço aos meus pais (Miguel e Maria Luiza Donida), minhas irmãs (Michelle, Alessandra e Camile) por terem segurado a barra junto comigo, por sempre me incentivarem a seguir em frente e por serem meu porto seguro quando tudo parecia desabar. Daniel, meu amor, não existem palavras para agradecer o teu apoio incondicional. Fostes meu alicerce, me ajudando a encontrar os caminhos e iluminado eles pra mim. Agradeço também à Tania,

Valmor e Paulo Henrique Vancin, minha família do coração, por me apoiarem durante toda essa jornada.

Às minhas amigas de toda a vida (Carolina, Letícia, Juliane e Lívia) e aos amigos dos laboratórios LABMET e LSCBA, obrigada por estarem sempre presentes, por me confortarem durante os dias ruins e por aplaudirem cada pequena vitória. A vida só tem sentido quando é compartilhada, obrigada por todos os momentos bons que dividimos. À Desirèe, principalmente, por ser minha irmã de coração, e por compartilhar meus anseios e angústias durante toda a graduação, mestrado e doutorado. Agradeço à Catarine e ao Rodrigo Verdi por me incentivarem tanto nesta reta final e por me ajudaram a encontrar os caminhos para continuar. Aos colegas da Unidade de Diagnóstico Especializado do HCPA (Rodrigo, Elisa, Maria Cristina, Denise, Graciela, Verdiana e Ana Paula) por todos os ensinamentos que compartilhamos e por me permitirem vivenciar a paixão pelas análises clínicas. Serei eternamente grata à Dra. Ana Paula Alegretti, que cruzou meu caminho rapidamente, mas que servirá para sempre como minha inspiração.

Por fim, mas não menos importante, agradeço a todos os colaboradores que tornaram possível a realização desse projeto:

- À Dra. Rejane Kessler, à Dra. Fernanda Timm e à Andryele Zaffari (HCPA) pela ajuda nos degelos das células dos pacientes e nas análises de Filipin;

- À Dra. Andressa Bernardi e ao Dr. Rudimar Frozza (Fiocruz/Rio de Janeiro-RJ) pela colaboração nos ensaios de vetorização *in vivo* das nanopartículas, pelas discussões por skype e por estarem sempre prontos a ajudar;

- Ao Dr. Mateus Borba Cardoso e ao Laboratório Nacional de Nanotecnologia (CNPEM/Campinas-SP) pelo acesso ao equipamento Malvern Zetasizer ZS;

- Ao Laboratório Nacional de Luz Síncrotron (CNPEM/Campinas-SP) pelo acesso à linha SAXS1 e à equipe da linha pelo suporte durante as medidas;

- Ao Dr. Rodrigo Portugal e ao Dr. Marcelo Farias (LNANO/Campinas-SP) pelas análises de criomicroscopia eletrônica de transmissão e pela ajuda na interpretação dos resultados;

- À Dra. Verônica Bidinotto Brito (UFCSPA) pela colaboração nas determinações de estresse oxidativo;

GRATIDÃO

SUMÁRIO

RESUMO

As doenças lisossômicas de depósito (DLDs) compreendem cerca de 70 desordens genéticas ocasionadas por mutações em proteínas críticas para o funcionamento dos lisossomos. Apesar de serem consideradas raras quando isoladas, as DLDs afetam coletivamente 1 a cada 5.000 nascidos vivos, tornando-as significativas doenças metabólicas da infância. Dentre as DLDs, encontra-se a doença de Niemann-Pick C (NPC), a qual é caracterizada por um engarrafamento lipídico intracelular ocasionado pela mutação nos genes *NPC1* ou *NPC2* e consequente acúmulo de colesterol e glicoesfingolipídios dentro do compartimento endossomal/lisossomal das células. A NPC apresenta, assim como a maioria das DLDs, envolvimento neurológico. Ainda não existe cura para NPC, mas inúmeros estudos vêm demonstrando a utilização benéfica da β-ciclodextrina (β-CD) devido à sua capacidade de mobilizar o colesterol acumulado dos lisossomos para a corrente sanguínea. Entretanto, a principal desvantagem apresentada pela β-CD é a sua incapacidade em atravessar a barreira hemato-encefálica (BHE). A procura por novos sistemas de liberação de fármacos tem sido muito relevante no sentido de se estabelecerem alternativas terapêuticas mais eficientes, que possibilitem administrar os fármacos com maior segurança, com efeitos colaterais minimizados e nos locais de ação específicos. Nesse sentido, a estrutura tridimensional flexível torna as nanopartículas lipídicas (fases esponja e microemulsões) formadas por monoleína excelentes candidatas ao carreamento de fármacos e enzimas. No desenvolvimento de carreadores nanométricos direcionados ao sistema nervoso central (SNC), o polissorbato 80 vem demonstrando ser o tensoativo mais indicado. Considerando o exposto, o objetivo deste trabalho foi o desenvolvimento de uma nanopartícula-plataforma, capaz de atravessar a BHE e liberar enzimas/fármacos dentro dos lisossomos. Além disso, utilizando a plataforma como ponto de partida, objetivou-se a incorporação de β-CD e assim o desenvolvimento de uma nanopartícula para o tratamento da NPC. Por fim, buscou-se avaliar o potencial citotóxico das nanopartículas previamente desenvolvidas. As nanopartículas foram caracterizadas por espalhamento dinâmico de luz (DLS), espalhamento de raios-X a baixos ângulos (SAXS) e

por criomicroscopia eletrônica de transmissão (cryo-MET). As nanopartículas consideradas como plataformas (NS) apresentaram diâmetro médio de cerca de 115 nm, enquanto que as nanopartículas contendo β-CD apresentaram (NS$_{β-CD}$) diâmetro médio de cerca de 120 nm. Os perfis de espalhamento obtidos por SAXS para ambas nanopartículas desenvolvidas ajustaram-se ao modelo matemático de Teubner-Strey, aplicado com sucesso para descrever microemulsões e fases esponja. Os resultados de cryo-TEM corroboraram os resultados de SAXS e DLS, demonstrando a presença de estruturas com fase interna bicontínua desordenada com tamanho médio próximo a 100 nm. Através da utilização de cumarina-6 foi possível determinar que as NS e NS$_{β-CD}$ atingiram os lisossomos após 1 hora de incubação na cultura celular. As nanopartículas foram rastreadas *in vivo* e se mostraram capazes de atingir o tecido cerebral, conferindo grande vantagem em relação às terapias comumente utilizadas. As nanopartículas foram capazes, também, de atingir o tecido hepático, que está amplamente comprometido em doenças como a NPC. Além disso, a NS$_{β-CD}$ mostrou atividade em reduzir os níveis de colesterol acumulado em fibroblastos dérmicos derivados de pacientes NPC. Tanto NS, quanto NS$_{β-CD}$ não causaram hemólise, um pré-requisito para administração parenteral, não apresentaram citotoxicidade e genotoxiciddade. Além disso, não causaram perturbações oxidativas/nitrativas quando incubadas com fibroblastos de pacientes NPC. As nanopartículas desenvolvidas neste projeto apresentaram resultados bastante promissores quanto à sua utilização para o tratamento de DLDs e, em particular, de NPC.

ABSTRACT

Lysosomal storage diseases (LSDs) comprise about 70 genetic disorders caused by mutations in critical proteins to lysosomes functioning. Although they are considered rare when isolated, LSDs collectively affect 1 in 5,000 live births, making them significant childhood metabolic diseases. Among the LSDs is Niemann-Pick type C (NPC) disease, which is characterized by intracellular lipid impairment caused by mutation in *NPC1* or *NPC2* genes and consequent accumulation of cholesterol and glycosphingolipids inside the endosomal/lysosomal cell compartment. NPC presents neurological impairment, as most LSDs. There is still no cure for NPC, but several studies have demonstrated the beneficial use of β-cyclodextrin (β-CD) because of its ability to mobilize accumulated cholesterol from lysosomes into the bloodstream. However, the main disadvantage presented by free β-CD is the inability to cross the blood-brain barrier (BBB). The search for new drug delivery systems has been very relevant in order to establish more efficient therapeutic alternatives, that allow to administer drugs with greater security, minimized side effects and in the specific sites of action. In this sense, the flexible three-dimensional structure makes the lipidic nanoparticles (sponge phases and microemulsions) formed by monoolein excellent candidates for the transport of drugs and enzymes. In the development of nanometric carriers directed to the central nervous system (CNS), polysorbate 80 has been shown to be the most indicated surfactant. Considering the above, the objective of this work was the development of a nanoparticle-platform, able to cross the BBB and release drugs/enzymes into the lysosomes. In addition, using the platform as a starting point, the objective was to incorporate β-CD in a nanoparticle for NPC treatment. Finally, we aimed to evaluate the cytotoxic potential of previously developed nanoparticles. The nanoparticles were characterized by dynamic light scattering (DLS), small angle X ray scattering (SAXS) and by cryogenic transmission electron microscopy (cryo-TEM). The nanoparticles considered as platforms (NS) had an average diameter of about 115 nm, whereas nanoparticles containing β-CD ($NS_{β-CD}$) had a mean diameter of about 120 nm. The scattering profiles obtained by SAXS for both nanoparticles were adjusted

to the Teubner-Strey mathematical model, successfully applied to describe microemulsions and sponge phases. The cryo-TEM results corroborated the results of SAXS and DLS, demonstrating the presence of structures with a disordered bicontinuous inner phase and with an average size close to 100 nm. By using coumarin-6 it was possible to track NS and $NS_{\beta\text{-CD}}$ into cells, and results showed that the NS reached the lysosomes after 1 hour of incubation with healthy fibroblasts, and $NS_{\beta\text{-CD}}$ remain in NPC fibroblasts for at least 3 hours. The nanoparticles were tracked *in vivo* and reached the brain tissue, which confers great advantage over the commonly used therapies. The nanoparticles were also able to target hepatic tissue, which is extensively involved in diseases such as NPC. In addition, $NS_{\beta\text{-CD}}$ induced a decrease in cholesterol accumulation when incubated with dermal NPC fibroblasts patients-derived. Both NS and $NS_{\beta\text{-CD}}$ did not cause hemolysis, a pre-requisite for parenteral administration, did not show cytotoxicity and genotoxicity. In addition, they did not cause oxidative/nitrative disturbances when incubated with fibroblasts from NPC patients. The nanoparticles developed in this project presented very promising results regarding their use for the treatment of LSDs, in particular NPC.

LISTA DE ABREVIATURAS

3β,5α,6β-triol - Colestano-3β,5α,6β-triol

7-KC - Cetocolesterol

ApoB - Apolipoproteína B

ApoE - Apolipoproteína E

ApoE-C - Apolipoproteína E ligada ao colesterol

BHE - Barreira hematoencefálica

CAT - Catalase

CE - Colesterol esterificado

CG-MS/MS - Cromatografia gasosa acoplada à espectrometria de massas em tandem

DLDs - Doenças lisossômicas de depósito

EIM - Erros Inatos do Metabolismo

ERN - Espécies reativas de nitrogênio

ERO - Espécies reativas de oxigênio

FDA - Órgão americano regulador de alimentos e medicamentos - "Food and Drug Administration"

GRAS - do inglês, geralmente reconhecido como seguro - "Generally Recognized As Safe"

H_2O_2 - Peróxido de hidrogênio

LAL - Lipase ácida lisossomal

LC-MS/MS - Cromatografia líquida acoplada à espectrometria de massas em tandem

LDL - Lipoproteína de baixa densidade

NPC - Niemann- Pick tipo C

NS - Nanopartículas

NS^F - Nanopartículas fluorescentes - coradas com cumarina-6

$NS^F_{β-CD}$ - Nanopartículas com β-ciclodextrina coradas com cumarina-6

$NS_{β-CD}$ - Nanopartículas com β-ciclodextrina

$O_2^{•-}$ - Íon superóxido

SNC - Sistema nervoso central

SOD - Superóxido dismutase

TER - Terapia de reposição enzimática

VLDL - Lipoproteína de muito baixa densidade

β-CD - β-ciclodextrina

1. INTRODUÇÃO

1.1 Erros Inatos do Metabolismo

Erros Inatos do Metabolismo (EIM) são desordens genéticas caracterizadas pela síntese alterada de uma proteína, geralmente uma enzima, que pode ter sua atividade parcial ou totalmente reduzida. O resultado dessa síntese errônea é o bloqueio de determinada via metabólica com consequente acúmulo de substratos e seus derivados e diminuição de produtos. A repercussão clínica deste bloqueio metabólico é variável, sendo geralmente grave ou letal (Scriver *et al.*, 2000).

Segundo Saudubray (2001), os EIM podem ser classificados em três grandes grupos com base em sua fisiopatologia:

a) *Distúrbios na síntese ou degradação de macromoléculas complexas*. As doenças enquadradas neste grupo apresentam sintomas permanentes, progressivos, não dependentes de eventos intercorrentes e não relacionados à ingesta alimentar. Fazem parte deste grupo as doenças lisossômicas de depósito (ex.: doença de Gaucher, doença de Fabry, mucopolissacaridoses, Niemann-Pick, etc.) e as desordens peroxissomais (ex.: adrenoleucodistrofia ligada ao cromossomo X, doença de Refsum, síndrome de Zellweger etc.).

b) *Erros inatos do metabolismo intermediário*. As doenças incluídas neste grupo podem levar à intoxicação aguda (quadros de acidose metabólica, vômitos, letargia e desidratação) ou intoxicação crônica (retardo mental, atraso no desenvolvimento psicomotor e luxação do cristalino), têm relação com ingesta alimentar e os pacientes podem apresentar intervalos livres de

sintomas. A intoxicação ocorre pelo acúmulo de componentes tóxicos e de metabólitos provenientes do bloqueio das rotas metabólicas. Fazem parte deste grupo as aminoacidopatias (ex: fenilcetonúria, doença do Xarope do Bordo, etc.), acidemias orgânicas (acidemia propiônica, acidemia metilmalônica, etc.), defeitos no ciclo da ureia (citrulonemia, argininemia, etc.) e as intolerâncias aos açúcares (galactosemia, etc.).

c) *Doenças com déficit de energia*. Neste grupo de doenças os sintomas são causados por deficiência na obtenção ou utilização de energia. Incluem-se as doenças de depósito de glicogênio, defeitos de gliconeogênese, acidemias lácticas congênitas, defeitos de oxidação dos ácidos graxos e doenças mitocondriais de cadeia respiratória.

A incidência isolada de cada uma das doenças metabólicas é pequena, visto que, de forma geral, são de herança autossômica recessiva. No entanto, se forem contabilizados coletivamente os dados de cerca de mais de 500 distúrbios conhecidos, a frequência se torna mais expressiva, chegando a aproximadamente 1:1000 nascidos vivos (Campeau *et al.*, 2008; El-Hattab, 2015). Além disso, deve-se levar em consideração que os números baixos podem representar não só a raridade dos distúrbios, como também a subestimativa de seu diagnóstico e, no que diz respeito a isto, vale destacar o papel fundamental da triagem neonatal, conhecido como "teste do pezinho". Esta triagem possibilitou grande avanço no conhecimento e tratamento dessas doenças a partir de sua detecção em fase pré-clínica, prevenindo o dano neurológico ou mesmo a morte dos pacientes (Jardim e Ashton-Prolla, 1996; Souza *et al.*, 2002).

1.2 Lisossomos e doenças lisossômicas de depósito

Os lisossomos foram descobertos há mais de 60 anos por Christian de Duve durante um estudo de distribuição de enzimas utilizando fracionamento subcelular por centrífuga (De Duve *et al.*, 1955). Estudos subsequentes mostraram que os lisossomos representam cerca de 5% do volume intracelular e possuem morfologia e tamanho heterogêneos (Luzio *et al.*, 2007). Estas organelas recebem substratos através de endocitose, fagocitose ou por autofagia (Saftig e Klumperman, 2009). Os lisossomos estão envolvidos em uma gama de processos fisiológicos como a homeostase do colesterol, reparo da membrana plasmática, remodelamento de ossos e tecidos, defesa contra patógenos, morte e sinalização celular. Estas funções complexas fazem com que o lisossomo seja uma organela dinâmica e importante e não simplesmente o compartimento final da via endocítica (Saftig e Klumperman, 2009).

O pH interno dos lisossomos é mantido entre 4,6-5,0 através de ATPases vacuolares próton-translocadoras. Dentro desta organela estão localizadas enzimas hidrolíticas (incluindo proteases, glicosidases, nucleases, fosfatases e lipases) necessárias para a degradação de macromoléculas como os glicosaminoglicanos, oligossacarídeos e esfingolipídios; também são encontradas permeases de efluxo, que facilitam a translocação de pequenas moléculas geradas durante o catabolismo (Luzio *et al.*, 2007; Heese, 2008).

As doenças lisossômicas de depósito (DLDs) são erros hereditários (inatos) do metabolismo que afetam a função do lisossomo. As DLDs compreendem um grupo de 70 desordens monogênicas do catabolismo lisossomal, a maioria das quais são herdadas como características autossômicas recessivas, excetuando-se três que são ligadas ao cromossomo

X (Platt *et al.*, 2018). Apesar de serem consideradas raras quando isoladas, as DLDs afetam coletivamente 1 a cada 5000 nascidos vivos, tornando-as significativas doenças metabólicas da infância (Thomas e Kermode, 2018). Estes distúrbios são causados por mutações em genes que codificam proteínas lisossomais, tais como glicosidases, proteases, proteínas integrais de membrana, transportadores, modificadores ou ativadores enzimáticos. As mutações afetam a função da proteína codificada, gerando acúmulo gradual de macromoléculas não-metabolizadas no interior do lisossomo e consequente mau funcionamento desta organela e da célula como um todo (Ballabio e Gieselmann, 2009). Existem cerca de 1300 genes envolvidos na função lisossômica e, entre os distúrbios monogênicos, encontram-se 50 deficiências enzimáticas, que podem ser subclassificadas de acordo com o tipo bioquímico de material armazenado (por exemplo, as esfingolipidoses, mucopolissacaridoses e glicoproteinoses) (Platt *et al.*, 2018). Cabe salientar que as DLDs são desordens genética e clinicamente heterogêneas. Os genes que codificam proteínas lisossômicas estão presentes em todas as células. No entanto, devido a exigências metabólicas únicas de diferentes tipos de células, um defeito em uma enzima lisossomal pode ter um impacto significativamente maior em um determinado tecido em comparação com outros tecidos (Heese, 2008). Contudo, o acúmulo de macromoléculas na maioria das DLDs inicia-se na vida fetal e frequentemente elas apresentam-se como doenças neurodegenerativas pediátricas, muitas vezes acompanhadas de visceromegalia (aumento de órgãos abdominais, como o fígado e o baço) (Scriver *et al.*, 2000).

A terapia de reposição enzimática (TRE) continua sendo a principal classe de terapia aprovada para as DLDs. A TRE consiste na reposição, por via intravenosa, de uma forma ativa e recombinante da enzima deficiente com o intuito de diminuição do montante de substrato acumulado nos lisossomos, levando a uma provável melhora clínica do paciente (Platt *et al.*, 2018). A infusão da TRE precisa ocorrer sob supervisão médica. Como as enzimas lisossomais não estão naturalmente localizadas na circulação sanguínea, podem desencadear como consequência uma resposta imune no paciente. Além disso, a produção de anticorpos neutralizantes contra a enzima administrada é uma das principais preocupações relacionadas à segurança e à eficácia das TRE (Lachmann, 2011; Martin-Banderas *et al.*, 2016). Além disso, as TRE originais foram desenvolvidas para distúrbios que não incluíam envolvimento do sistema nervoso central (SNC) e, portanto, não precisavam acessar o cérebro para demonstrar sua eficácia. Contudo, como a maioria das DLDs tem comprometimento neurológico e periférico, o desenvolvimento de medicamentos deve agora incluir fármacos que atravessem a BHE.

1.3 Doença de Niemann-Pick tipo C

A doença de Niemann-Pick tipo C (NPC) é uma desordem genética de herança autossômica recessiva, enquadrada nas DLDs e com incidência aproximada de 1 a cada 89000 nascidos vivos (Wassif *et al.*, 2016). A NPC resulta da mutação em um dos dois genes de transporte de colesterol, o *NPC1* (95% dos casos) ou *NPC2*. O gene *NPC1* codifica uma glicoproteína transmembrana endossomal e o gene *NPC2* codifica uma pequena proteína

lisossomal que se liga ao colesterol com alta afinidade. A ausência das proteínas codificadas por estes genes resulta em acúmulo de colesterol não esterificado, juntamente com glicoesfingolipídios, dentro do compartimento endossomal/lisossomal de todas as células. Esse acúmulo leva a um verdadeiro "engarrafamento intracelular" que, por conseguinte, leva à ativação de outras rotas celulares culminando na destruição da própria célula. O resultado final é uma doença significativa que atinge tanto múltiplos órgãos periféricos, incluindo o fígado, baço e pulmões, quanto o SNC, levando à neurodegeneração e morte precoce (Vanier, 2010; 2015).

O colesterol não-esterificado, principal metabólito acumulado na NPC, por ser componente essencial das membranas plasmáticas, apresenta altas taxas de "turnover" diário. Em ratos, por exemplo, a taxa diária de "turnover" do colesterol em células dos órgãos periféricos é de 8% e chega a 20% em células do SNC (Dietschy e Turley, 2004). Os tecidos periféricos apresentam altas taxas de síntese e captação do colesterol não-esterificado e de ésteres de colesterol, que chegam em lipoproteínas de baixa densidade (LDL), quilomícrons e lipoproteínas de muito baixa densidade (VLDL) (Dietschy *et al.*, 1993). As lipoproteínas são processadas no compartimento endossomal/lisossomal das células e o colesterol resultante se junta ao esterol recém-sintetizado em um *pool* metabolicamente ativo do compartimento citosólico, o qual suporta continuamente o "turnover" de colesterol para a membrana plasmática (figura 1a).

Enquanto os neurônios apresentam altas taxas de "turnover" de colesterol, eles não possuem acesso ao colesterol não-esterificado ou aos ésteres de colesterol das lipoproteínas plasmáticas (Cavender *et al.*, 1995;

Quan *et al.*, 2003) e também apresentam baixas taxas de síntese destes metabólitos (Nieweg *et al.*, 2009). Algumas observações *in vitro* fornecem prováveis explicações para este enigma. O crescimento do axônio em neurônios requer uma fonte extracelular de esterol, provavelmente proveniente do colesterol não-esterificado ligado à apolipoproteína E (apoE) (De Chaves *et al.*, 2000; Hayashi *et al.*, 2004). Além disso, a sinaptogênese *in vitro* também requer uma fonte externa de colesterol não-esterificado e, novamente, este é um complexo apoE-colesterol (apoE-C) derivado das células gliais (Mauch *et al.*, 2001). Tais observações levaram ao modelo ilustrado na figura 1 (Aqul *et al.*, 2011), onde se propõe que a taxa de síntese de esterol nos neurônios é insuficiente para promover o crescimento do axônio e a formação de sinapses. O colesterol não-esterificado e a apoE são sintetizados em astrócitos e o complexo é entregue aos neurônios através do fluido intersticial, absorvido por endocitose mediada por receptor e processado através do compartimento endossomal/lisossomal. A secreção do complexo apoE-C dos astrócitos não é dependente da proteína lisossomal NPC1, diferentemente da movimentação do colesterol não-esterificado através do compartimento endossomal/lisossomal dos neurônios (Karten *et al.*, 2002; Karten *et al.*, 2005). Se este modelo é aplicável ao cérebro *in vivo* e se o processamento desordenado do colesterol não-esterificado através desta via pode levar a algumas formas de neurodegeneração, como a observada na doença de NPC, continua sendo uma questão a ser esclarecida.
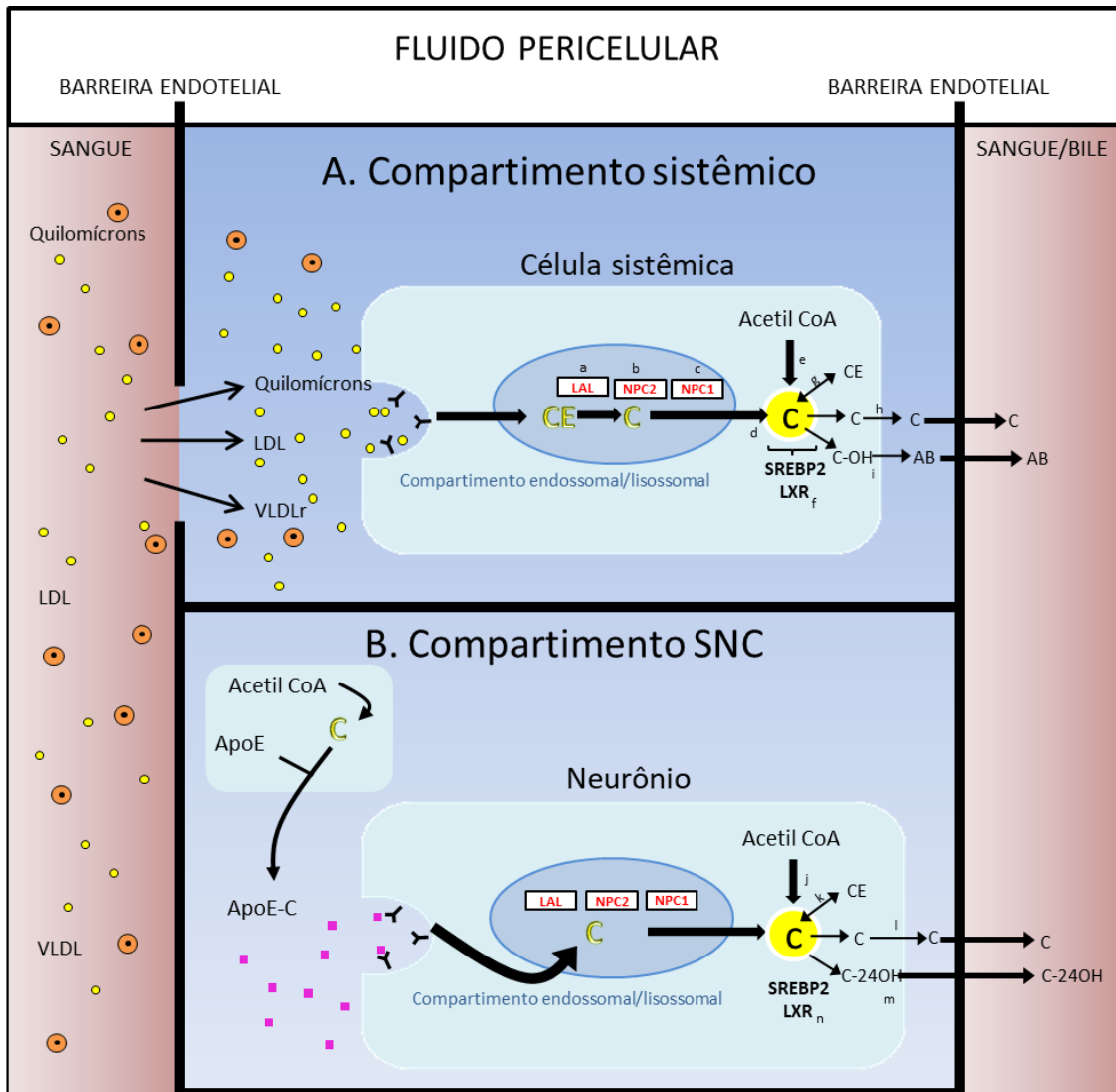
Figura 1. Comparação do tráfego do colesterol em células dos tecidos sistêmicos (representado pelo fígado), e neurônios do SNC. **A.** O fluido pericelular circunjacente às células dos órgãos sistêmicos pode conter várias lipoproteínas, incluindo LDL, e quilomícrons e VLDL remanescentes. Estas partículas são reconhecidas e internalizadas nas células através de endocitose mediada por receptor e então encaminhadas para dentro do compartimento endossomal/lisossomal tardio das células. Neste último, o colesterol esterificado (CE) é metabolizado a colesterol não-esterificado (C) através da Lipase ácida lisossomal (LAL) (a). O C então interage sequencialmente com as proteínas NPC2 (b) e NPC1 (c) atingindo a membrana limitante e deixando o compartimento endossomal/lisossomal (d) para se juntar ao C recém-sintetizado (e) em um *pool* metabolicamente ativo no citoplasma da célula. O tamanho deste *pool* é finamente regulado pelos fatores de transcrição sensíveis a esteróis, SREBP2 e LXR (f).Dependendo do tipo celular, este C pode ser re-esterificado (g), utilizado no "turnover'" remodelando a membrana plasmática (h), hidroxilado a oxiesterol (i) ou, no fígado, a ácido biliar (AB). **B.** A situação do SNC é bastante diferente, visto que a barreira endotelial, neste caso, é impermeável às lipoproteínas plasmáticas. Neste compartimento, postula-se que o C seja sintetizado pela glia, particularmente pelos astrócitos, e carreado como um complexo com a apoE aos neurônios. A captação deste C presumivelmente ignora a necessidade da LAL, interagindo diretamente com as proteínas NPC2 e NPC1 movimentando-se para o *pool* metabolicamente ativo (j). Este C pode ser re-esterificado (k), utilizado no remodelamento da membrana e na formação/manutenção dos dendritos e sinapses (l), ou metabolizado a 24(*S*)-hidroxicolesterol para a excreção (m). Deve-se notar que tanto nas células sistêmicas quanto

nos neurônios, a expansão súbita do *pool* metabolicamente ativo de C no compartimento citosólico está associada com a supressão da síntese de colesterol, um aumento na concentração de CE, supressão de vários genes alvo SREBP2 (n) e ativação de alguns genes controlados por LXR (n).

Por ser considerada uma doença neurovisceral, as manifestações clínicas da NPC podem incluir: hepatoesplenomegalia, icterícia, sintomas neurológicos como disartria, disfagia, paralisia supranuclear vertical, crises convulsivas e também sintomas psiquiátricos como transtorno bipolar, esquizofrenia e déficit cognitivo (Patterson, 2003). A apresentação clínica da doença NPC é extremamente heterogênea, sendo que os primeiros sintomas podem aparecer desde o período perinatal até a idade adulta. Similarmente, o tempo de vida dos pacientes varia desde alguns dias até cerca de 60 anos, sendo que na maioria dos casos os pacientes vêm a óbito entre 10 e 25 anos. Excetuando-se o pequeno subgrupo de pacientes que morrem no parto ou nos primeiros seis meses de vida, devido a complicações hepáticas ou respiratórias, e os casos raros em adultos, todos os pacientes desenvolvem doença neurodegenerativa progressiva e fatal. A doença sistêmica, quando presente, sempre precede o aparecimento dos sintomas neurológicos. Contudo, o componente sistêmico pode não ocorrer ou ser mínimo em aproximadamente 15% do total dos pacientes e, quando se trata de pacientes com início dos sintomas na idade adulta, este valor passa para 50% (Vanier, 2010).

O diagnóstico da NPC é realizado pela coloração de Filipin, o qual é um antibiótico polieno fluorescente que se liga ao colesterol não-esterificado. O acúmulo de colesterol não-esterificado no compartimento endossomal/lisossomal de fibroblastos cultivados é observado após a

coloração com Filipin através de microscopia de fluorescência (Vanier e Latour, 2015). Entretanto, a existência de perfis variantes em termos de fluorescência pode causar dúvidas na interpretação do teste de Filipin, além de ser invasivo, caro e requerer um centro especializado para a sua realização (Vanier e Latour, 2015).

Nas células NPC deficientes existe uma associação entre o estresse oxidativo e o colesterol acumulado devido ao aumento da produção de espécies reativas de oxigênio (ERO) (Ribas *et al.*, 2012). Os produtos da oxidação não-enzimática do colesterol, como o colestano-$3\beta,5\alpha,6\beta$-triol ($3\beta,5\alpha,6\beta$-triol) e o 7-cetocolesterol (7-KC), estão significativamente aumentados no plasma dos pacientes com NPC e também em modelos animais, enquanto permanecem normais em outras DLDs (Jiang *et al.*, 2011; Ribas *et al.*, 2016; Hammerschmidt *et al.*, 2018). Estes achados indicam que o $3\beta,5\alpha,6\beta$-triol e o 7-KC podem ser marcadores bioquímicos específicos da doença de NPC e sugerem uma possível utilidade dos mesmos no diagnóstico e avaliação terapêutica da doença (Jiang *et al.*, 2011; Ribas *et al.*, 2016; Hammerschmidt *et al.*, 2018). A análise de oxisteróis em plasma pode ser realizada por cromatografia líquida ou gasosa acoplada à espectrometria de massas em tandem (LC-MS/MS ou CG-MS/MS, respectivamente). Entretanto, o diagnóstico definitivo ainda é realizado através da análise molecular dos genes *NPC1* e *NPC2 (Vanier, 2010).*

1.4 Tratamento para a doença de Niemann-Pick tipo C

Atualmente não há cura para NPC e até recentemente os tratamentos consistiam somente no controle dos sintomas. A terapia de redução do substrato é uma opção recente de tratamento que pode estabilizar ou desacelerar a progressão da doença. O Miglustat (N-butil-desoxinojirimicina - ZAVESCA®), inibidor da glicosilceramida-sintase (responsável pela síntese de glicoesfingolipídios) é utilizado com o intuito de diminuir o engarrafamento do tráfego pela diminuição da formação do substrato acumulado nas células. O Miglustat foi aprovado para o tratamento das manifestações neurológicas progressivas em adultos e crianças, baseado em resultados que mostraram a melhora ou estabilização de alguns marcadores clínicos de NPC, como movimentos oculares sacádicos, cognição, acuidade auditiva e ambulação. Contudo, a dose utilizada de Miglustat constantemente causa efeitos adversos nos pacientes, como por exemplo, tremores, problemas gastrointestinais como diarréia, diminuição do número de plaquetas, neuropatia periférica e, em populações infantis, diminuição de crescimento (Vanier, 2010). Além disso, o Miglustat não atua na diminuição do colesterol (considerado o principal metabólito acumulado responsável pelos sintomas característicos da doença) e não estão bem elucidados os mecanismos pelos quais ele melhora os sintomas clínicos, uma vez que já foi visto que a redução dos gangliosídeos nos lisossomos e nos endossomos tardios de modelo animal de NPC não parece ser benéfica (Liu *et al.*, 2000; Li *et al.*, 2008; Liu *et al.*, 2008).

Uma ampla gama de moléculas vem sendo estudada como potencial terapia para a NPC. Entre elas, destaca-se a β-ciclodextrina (β-CD) (figura 2), um oligossacarídeo cíclico contendo sete resíduos de glicose, comumente utilizado para aumentar a solubilidade de fármacos lipofílicos em soluções

aquosas (Van Vught e De Jong, 2001). A β-CD apresenta grupamentos hidroxila livres provenientes dos resíduos de glicose que se localizam nas bordas da estrutura em formato de toróide na qual ela se organiza, tornando a molécula solúvel em água. Os grupamentos hidroxila secundários, ligados aos C-2 e C-3 das unidades de glicose, são todos situados na borda maior da molécula, onde formam uma rede de ligações de hidrogênio intramoleculares, fornecendo rigidez à estrutura. A característica mais marcante das ciclodextrinas é a presença de uma cavidade central relativamente apolar, moldada pelos átomos de carbono das unidades de glicose. Sua característica apolar permite a inclusão, na cavidade, de uma grande variedade de moléculas orgânicas em solução aquosa (Van Vught e De Jong, 2001). Devido a essa propriedade de formar complexos com substâncias lipofílicas, foi descoberto o potencial da β-CD em diminuir os níveis de colesterol acumulados nos lisossomos em modelo animal da doença de NPC (Abi-Mosleh *et al.*, 2009; Davidson *et al.*, 2009; Vance e Karten, 2014).
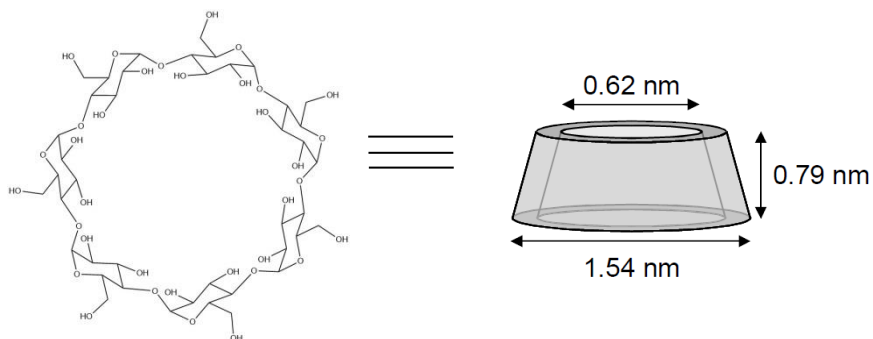

Figura 2. Estrutura da β-ciclodextrina [adaptado de Van Vught e De Jong (2001)].

Em estudos pré-clínicos, o tratamento com a β-CD e seus derivados resultou em redistribuição do colesterol dos compartimentos subcelulares para a circulação e aumento da longevidade dos ratos. Entretanto, as bases para a melhoria neurológica observada ainda permanecem pouco conhecidas (Abi-Mosleh *et al.*, 2009; Davidson *et al.*, 2009; Lopez *et al.*, 2014). Uma combinação de β-CD, alopregnanolona e Miglustat mostrou-se eficaz quanto aos problemas motores, mas não influenciou o déficit cognitivo em modelo animal de NPC. Contudo, foi observado que as inclusões autofagossômicas das células de Purkinje diminuíram, sugerindo que as áreas do cérebro apresentam resposta desigual para o tratamento (Hovakimyan *et al.*, 2013). Utilizando um modelo de células-tronco neurais de pacientes NPC, pôde-se determinar que o tratamento conjunto de β-CD e δ-tocoferol apresentou efeito sinérgico em diminuir os níveis de colesterol acumulado nos lisossomos (Yu *et al.*, 2014).

Em trabalho publicado em 2009, demonstrou-se que apenas uma pequena porcentagem de β-CD é capaz de alcançar o SNC, todavia a passagem demonstrada neste estudo pode ter ocorrido em decorrência de terem sido utilizados camundongos de sete dias, nos quais a barreira hematoencefálica (BHE) parece não estar completamente formada (Davidson *et al.*, 2009). Pontikis e colaboradores (2013) verificaram que a hidroxipropil-β-CD, quando aplicada intraperitonealmente na dose usual de 4000 mg/kg, não atravessa a BHE de ratos adultos ou neonatais. Entretanto, os resultados demonstraram que provavelmente esta ciclodextrina é capaz de se ligar à superfície celular do endotélio vascular cerebral e assim mobililzar e diminuir o colesterol acumulado no SNC.

Embora os resultados da literatura venham se mostrando promissores, ainda permanece incerto o modo pelo qual a β-CD causa diminuição do colesterol nas células NPC, principalmente no tecido cerebral. Alguns estudos apontam indícios de que as ciclodextrinas causam a perda da integridade da BHE através da retirada de componentes das membranas das células endoteliais dos capilares cerebrais. No caso da β-CD, estes componentes seriam os fosfolipídios e o colesterol (Monnaert *et al.*, 2004). Entretanto, Binkowski-Machut e colaboradores (2006) demonstraram que a β-CD monossubstituída com n-alquildimetilamonio (cadeia de 12 carbonos) parece ser não tóxica para a BHE. Os autores levantaram a hipótese de que a cavidade da β-CD estaria preenchida pela cadeia alquílica, ficando assim incapaz de extrair os fosfolipídios ou colesterol das membranas celulares, preservando sua integridade. Além disso, apesar de não lesar a BHE, cerca de 30% da β-CD monossubstituída conseguiu passar pelas células endoteliais (Binkowski-Machut *et al.*, 2006). Cabe mencionar que, apesar de promissora, essa ciclodextrina possui um alto custo de síntese.

Considerando os problemas de permeabilidade cerebral apresentados pela β-CD, se propôs que a hidroxipropil-β-CD fosse administrada diretamente no SNC, através de injeção intracerebroventricular, juntamente com a continuidade das injeções subcutâneas. Esse tratamento resultou em melhora significativa do dano neurológico em modelo animal de NPC, com desaparecimento do acúmulo de lipídios nos neurônios e das evidências histológicas de neurodegeneração, particularmente no cerebelo. Além disso, a presença da a hidroxipropil-β-CD restaurou o fluxo normal de colesterol através das células do SNC em ratos $Npc1^{-/-}$. Este resultado foi reforçado pela

expressão normalizada do RNA_m da apoE e CYP46A1, proteínas que provavelmente participam do transporte do colesterol para fora do SNC e no plasma (Aqul *et al.*, 2011). Administração intracisternal de hidroxipropil-β-CD também já foi testada em felinos pré-sintomaticos com a doença de NPC, sendo capaz de adiar o aparecimento da disfunção cerebelar por mais de um ano, além de diminuir a perda de células de Purkinje e resultar em valores de colesterol e esfingolipídios muito próximos do normal (Vite *et al.*, 2015). Além disso, em felinos que apresentavam disfunção cerebelar, a administração intracisternal de hidroxipropil-β-CD desacelerou a progressão da doença, aumentou a longevidade e diminuiu o acúmulo de colesterol e gangliosíodeos no cérebro. Como efeito adverso, os felinos apresentaram um aumento do limiar auditivo (Vite *et al.*, 2015), problema que já vem sendo relatado em modelo animal de NPC durante o tratamento com β-CD na dose usual de 4000 mg/kg (Ward *et al.*, 2010). Além disso, cabe salientar que as vias de administração utilizadas acima em modelos animais para a chegada da β-CD no SNC são inviáveis para a utilização em humanos. E, por vias de administração usuais, devido ao fato da β-CD ser uma molécula altamente hidrofílica e de peso molecular relativamente baixo (~1414 g mol^{-1}), torna-se nececessária a administração contínua de altas doses, pois cerca de 90% das moléculas são removidas da circulação sistêmica de ratos e humanos dentro de 24 horas. Contudo, baseando-se nos excelentes resultados obtidos em modelos animais de NPC através das injeções de β-CD diretamente no SNC, um ensaio clínico fase I/II foi publicado em 2017 (Ory *et al.*, 2017). No ensaio clínico, a hidroxipropil-β-CD foi administrada mensalmente através de infusão intratecal e os resultados demonstraram uma desaceleração da doença

neurológica e uma melhora da homeostase do colesterol em todos os 14 pacientes com NPC testados. Como efeito adverso esperado, relatou-se a diminuição da acuidade auditiva, mas a molécula demonstrou perfil de segurança aceitável. Contudo, os autores destacam que um aumento na frequência e na concentração de β-CD usada poderia ser benéfica, o que será testado nas próximas etapas do estudo (Ory *et al.*, 2017). Cabe salientar que a administração intratecal, apesar de evitar que o fármaco tenha que atravessar a BHE, é uma via utilizada somente caso não haja outras vias disponíveis, por causar dor, risco de infecção, risco de lesão medular e necessidade de pessoal adequadamente treinado (Golan *et al.*, 2009).

Sendo assim, o desenvolvimento de um sistema nanoparticulado biocompatível, de fácil administração, com baixa depuração plasmática, capaz de atravessar a BHE e carrear β-CD para o compartimento endossomal/lisossomal das células poderia melhorar a depuração do colesterol, atuando como uma terapia altamente vantajosa para a NPC. Além disso, nanopartículas vêm sendo propostas como uma estratégia de carrear moléculas ao cérebro em concentrações terapêuticas (Georgieva *et al.*, 2014), o que permitiria aumentar consideravelmente a concentração de β-CD no tecido cerebral.

1.5 Administração de fármacos incorporados a nanopartículas

A via enteral é sempre a melhor alternativa no que se refere à administração de fármacos em humanos pela sua conveniência. No entanto, isso implica em uma administração sistêmica de fármacos, que resulta na sua

biodistribuição a todo o organismo, de forma que altas doses são necessárias para que concentrações terapêuticas sejam atingidas no local de ação. Isso pode levar à toxicidade não-específica e outros efeitos adversos (Torchilin, 2000).

Nos últimos anos, a procura por novos sistemas de liberação de fármacos tem sido muito relevante no sentido de se estabelecer alternativas terapêuticas mais eficientes, que possibilitem administrar os fármacos com maior segurança e com efeitos colaterais minimizados. Nesse sentido, nanopartículas constituídas por lipídios são excelentes candidatas ao carreamento de fármacos e enzimas pela sua biocompatibilidade. Dentre o arsenal de nanoestruturas de lipídios, destacam-se aquelas com estruturas bicontínuas desordenadas, em particular a fase esponja (L_3) e a microemulsão bicontínua (figura 3) (Kogan *et al.*, 2009; Valldeperas *et al.*, 2016), em virtude de sua capacidade de acomodar compostos hidrofílicos e hidrofóbicos de diferentes massas molares. Geralmente, os lipídios empregados para preparar esses sistemas apresentam caráter anfifílico.

A fase esponja consiste em dois canais aquosos interconectados e separados por uma bicamada lipídica contínua (figura 3). Ela pode ser considerada equivalente a uma fase líquido-cristalina cúbica bicontínua reversa, porém sem ordem de longo alcance e com canais aquosos relativamente mais largos (Anderson *et al.*, 1989). Para a formação de fase esponja, pode-se recorrer à mistura de lipídios visto que na natureza dificilmente são encontradas moléculas anfifílicas capazes de formar esta mesofase em excesso de água e sob condições fisiológicas de temperatura (Valldeperas *et al.*, 2016). A monoleína (monooleato de glicerila – figura 4a) é

um lipídio biodegradável e biocompatível que, em presença de água, forma uma fase cúbica bicontínua reversa (Lutton, 1965; Hyde e Andersson, 1984). Entretanto, a transição da fase cúbica para a fase esponja pode ser induzida através da mistura de diglicerídeos com a monoleína sem a utilização de solventes orgânicos (Valldeperas *et al.*, 2016).

As microemulsões, por sua vez, podem ser definidas como sistemas termodinamicamente estáveis, isotrópicos, compostos por dois líquidos imiscíveis, usualmente água e óleo, estabilizados por tensoativos localizados na interface óleo/água (Formariz *et al.*, 2005) (figura 3). Entretanto, a possibilidade de formar microemulsões depende do balanço entre as propriedades hidrofílicas e lipofílicas do tensoativo, determinadas não somente pela sua estrutura química, mas por fatores como temperatura, força iônica e a presença de co-tensoativo. As microemulsões são superiores às soluções micelares em termos de potencial de solubilização de substâncias e também de estabilidade termodinâmica (Formariz *et al.*, 2005). A microemulsão bicontínua em particular contém domínios de óleo e água que estão entrelaçados de maneira caótica, mas são estabilizados por monocamadas de surfactante nas zonas de fronteira entre os domínios. Estas monocamadas são formadas devido à tendência do agente tensoativo se localizar entre as regiões ricas em água e ricas em óleo. Semelhantemente à fase esponja, a microemulsão bicontínua não apresenta ordem de longo alcance.
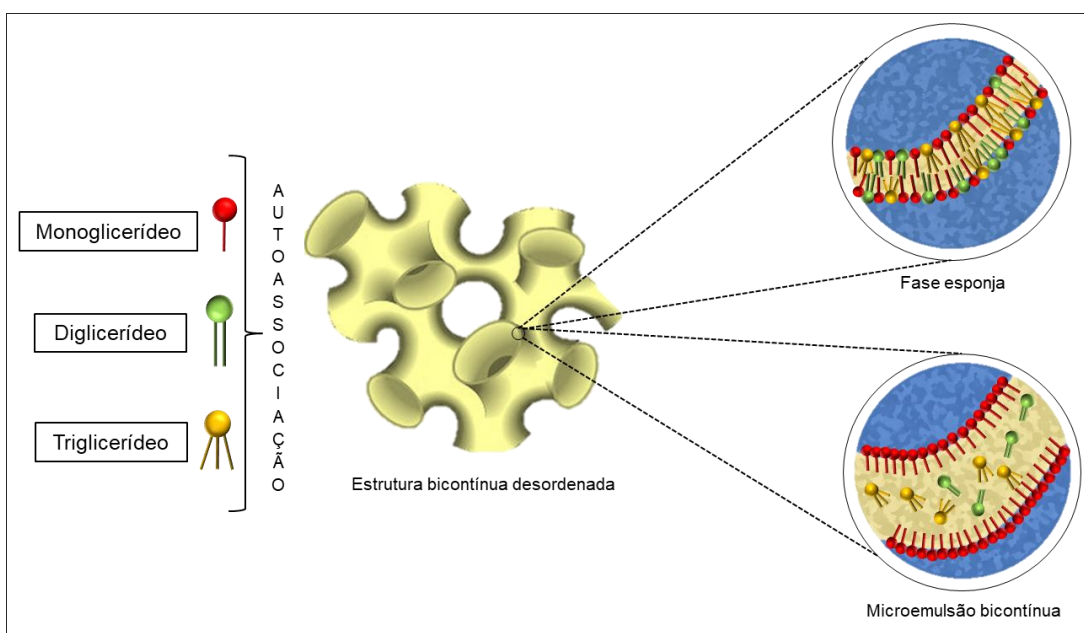
Figura 3. Representação esquemática da formação de estruturas bicontínuas desordenadas a partir da mistura de mono, di e triglicerídeos. Em destaque a diferença entre a estruturação da fase esponja e da microemulsão bicontínua no nível molecular.

Estruturas lipídicas bicontínuas desordenadas são capazes de acomodar macromoléculas sem comprometer sua estrutura (Angelov *et al.*, 2011). Apesar das vantagens dos sistemas lipídicos com estruturas bicontínuas desordenadas como carreadores de macromoléculas, sua utilização na modificação do curso de doenças neurodegenerativas é limitado pela BHE. Estudos prévios demonstraram que a administração de nanopartículas revestidas pelo tensoativo hidrofílico polissorbato 80 (figura 4b) leva ao aumento da concentração de fármacos no tecido cerebral, em comparação com a solução do fármaco livre ou mesmo com nanopartículas revestidas por outros estabilizantes (Kreuter, 2001; Kreuter *et al.*, 2002; Kreuter *et al.*, 2003; Bernardi *et al.*, 2009; Frozza *et al.*, 2010; Gelperina *et al.*, 2010).
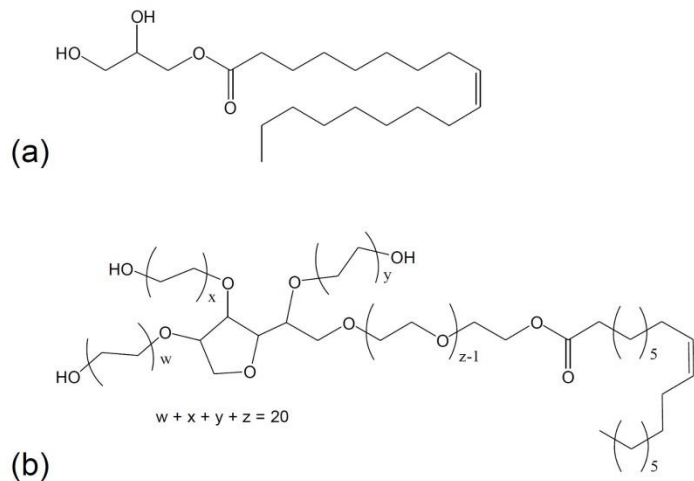
Figura 4. Estrutura química da monoleína (a) e do polissorbato 80 (b).

O revestimento com polissorbato 80 supostamente propicia a adsorção de apolipoproteínas B e E, que estão relacionadas a processos de endocitose mediada por receptor. Essa adsorção levaria tais partículas a atuar como *Cavalos-de-Troia* (Pardridge, 2006). Nesse processo, elas são internalizadas para o tecido cerebral através da BHE, tal qual as LDLs, que também apresentam apolipoproteínas B e E em sua composição (Kreuter et al., 2002). O polissorbato 80 é um tensoativo não-iônico amplamente utilizado em produtos farmacêuticos como estabilizante por ser um produto de baixo custo, acessível, biodegradável e não-tóxico para as células em baixas concentrações (Alyaudtin *et al.,* 2001). Além disso, comparado a outros surfactantes, o polissorbato 80 foi mais efetivo em diminuir a captura das nanopartículas pelo fígado, aumentando o tempo de circulação das mesmas em ratos (Storm *et al.,* 1995).

Durante o desenvolvimento de nanopartículas para utilização biomédica, faz-se necessária a análise toxicológica das formulações, uma vez que os materiais não-prejudiciais em sua forma natural podem se tornar tóxicos na escala nanométrica (Chatterjee *et al.*, 2017). Existem vários parâmetros físico-químicos para determinar a toxicidade das formulações como: tamanho de partícula, forma, carga superficial, composição, degradabilidade, biocompatibilidade e estabilidade cinética e química da nanopartícula. Além disso, fatores relacionados às partículas como dose, via de administração e distribuição tecidual parecem ser importantes parâmetros para a nanotoxicidade. Ainda, outros prováveis mecanismos envolvidos na nanotoxicidade parecem ser o estresse oxidativo e a ativação de genes proinflamatórios. Portanto, uma série de testes de triagem é utilizada para a avaliação de risco dos nanomateriais e da formulação como um todo (Chatterjee *et al.*, 2017). Os ensaios *in vitro* que são rotineiramente utilizados para a avaliação da toxicidade de nanopartículas são os ensaios de viabilidade celular, ensaio de estresse oxidativo e ensaio inflamatório (Chatterjee *et al.*, 2017). Além disso, quando se desenvolvem nanopartículas para aplicação parenteral, um pré-requisito importante a ser investigado é a atividade hemolítica, que deve ser nula ou negligenciável (Barauskas *et al.*, 2010).

Considerando os problemas apresentados pelas atuais terapias para as DLDs, foi proposto neste estudo de doutorado o desenvolvimento de uma nanopartícula lipídica como plataforma inteligente para a entrega de enzimas/fármacos diretamente no compartimento endossomal/lisossomal das células. Além disso, levantou-se a hipótese de que, devido ao recobrimento da partícula com polissorbato 80, esta seria capaz de atingir o tecido cerebral,

demonstrando vantagem tecnólogica frente aos tratamentos utilizados hoje para as DLDs. Utilizando a β-CD nesta plataforma, propôs-se a atuação da nanopartícula na redução de colesterol em lisossomos de pacientes NPC.

2. OBJETIVOS

2.1 Objetivo geral

Este estudo de doutorado teve como objetivo desenvolver uma plataforma nanotecnológica biocompatível contendo β-CD, com capacidade de vetorização ao SNC e redução do teor de colesterol acumulado em lisossomos de células de pacientes com a doença de NPC visando potencial redução de danos neurológicos.

2.2 Objetivos específicos

a) Desenvolver nanopartículas de monoleína revestidas por polissorbato 80 como plataforma para entrega de fármacos no sistema nervoso central e tratamento de doenças lisossômicas de depósito.

b) Desenvolver uma estratégia de incorporação de β-ciclodextrina às nanopartículas de monoleína, empregando-se princípios da química supramolecular.

c) Avaliar a biodistribuição das nanopartículas de monoleína revestidas por polissorbato 80 com e sem β-ciclodextrina (e marcadas com cumarina-6) em camundongos.

d) Avaliar o o potencial terapêutico das nanopartículas de monoleína revestidas por polissorbato 80 com β-ciclodextrina em fibroblastos de pacientes com a doença de Niemann-Pick C.

e) Avaliar as propriedades toxicológicas das nanopartículas de monoleína revestidas por polissorbato 80 contendo ou não β-ciclodextrina.

3. RESULTADOS

Os resultados desta tese de doutorado serão apresentados na forma de capítulos, referentes a artigos científicos. O primeiro capítulo de resultados trata do desenvolvimento de nanopartículas de monoleína como plataforma para vetorização de fármacos ao sistema nervoso central e tratamento de doenças lisossômicas de depósito. O capítulo seguinte discorre sobre a estratégia de incorporação de β-ciclodextrina às nanopartículas de monoleína e seu potencial terapêutico para tratamento da doença de NPC visando potencial redução de danos neurológicos. O último capítulo de resultados versa sobre os aspectos toxicológicos das nanopartículas desenvolvidas e discutidas nos capítulos anteriores.

3.1 Artigo 1: Monoolein-based nanoparticles for drug delivery to the central nervous system: A platform for Lysosomal Storage Disorder treatment

Este artigo científico foi publicado no periódico *European Journal of Pharmaceutics and Biopharmaceutics (JCR: 4,491).*

Research paper

Monoolein-based nanoparticles for drug delivery to the central nervous system: A platform for lysosomal storage disorder treatment

Bruna Donida[a], Bárbara Tauffner[b], Marco Raabe[c], Maira F. Immich[b], Marcelo A. de Farias[d], Diego de Sá Coutinho[e], Andryele Zaffari Machado[f], Rejane Gus Kessler[f], Rodrigo V. Portugal[d], Andressa Bernardi[e], Rudimar Frozza[e], Dinara J. Moura[c], Fernanda Poletto[a,b,*], Carmen Regla Vargas[a,f,*]

[a] Programa de Pós-Graduação em Ciências Biológicas, Bioquímica, Universidade Federal do Rio Grande do Sul, Zip Code 90035-003, Porto Alegre, RS, Brazil
[b] Programa de Pós Graduação em Química, Universidade Federal do Rio Grande do Sul, Zip Code 91501-970, Porto Alegre, Brazil
[c] Universidade Federal de Ciências de Saúde de Porto Alegre, Zip Code 90050170, Porto Alegre, RS, Brazil
[d] Brazilian Nanotechnology National Laboratory (LNNano), Brazilian Center for Research in Energy and Materials (CNPEM), Zip Code 13083-970, Campinas, Sao Paulo, Brazil
[e] Instituto Oswaldo Cruz (IOC), Fundação Oswaldo Cruz (FIOCRUZ), Zip Code 21040-360, Rio de Janeiro, RJ, Brazil
[f] Serviço de Genética Médica, Hospital de Clínicas de Porto Alegre, Zip Code 90035-003, Porto Alegre, RS, Brazil

ARTICLE INFO

ABSTRACT

Lysosomal Storage Disorders (LSDs) are characterized by an abnormal accumulation of substrates within the lysosome and comprise more than 50 genetic disorders with a frequency of 1:5000 live births. Nanotechnology may be a promising way to circumvent the drawbacks of the current therapies for lysosomal diseases. The blood circulation time and bioavailability of the enzymes or drugs could be improved by inserting them in nano-carriers, which could decrease and/or avoid the need of frequent intravenous infusions along with the mini-mization or elimination of associated immunogenic responses. Considering the exposed, we aimed to build monoolein-based nanoparticles stabilized by polysorbate 80 as a smart platform able to reach the central nervous system (CNS) to deliver drugs or enzymes inside lysosomes. We developed and characterized the nanoparticles by dynamic light scattering (DLS), small-angle X-ray scattering (SAXS) and cryogenic transmission electron microscopy (Cryo-TEM). The nanoparticles showed a diameter of 115 nm, which is compatible with *in vivo* application. The SAXS patterns of the formulations displayed a single broad correlation peak that was fitted to the Teubner-Strey model confirming that disordered bicontinuous structures were obtained. Cryo-TEM images corroborated this finding and showed nanoparticles with size values that are similar to those determined by DLS. Furthermore, the nanoparticles did not present cytotoxicity when they were incubated with human fibroblasts, and demonstrated hemolytic activity proportional to the negative control, proving to be safe for parenteral administration. Through the use of a fluorescent dye to track the nanoparticles inside the cell, we demonstrated that they reached lysosomes after 1 h of treatment. More interestingly, the fluorescent dye was detected in the CNS of mice just after 3 h of treatment. The nanoparticles show great potential to improve the treatment of LSDs with brain impairment, acting as a smart platform to targeted delivery of drugs or enzymes.

1. Introduction

Lysosomes are membrane-bound organelles involved in several physiological processes, such as cholesterol homeostasis, plasma membrane repair, bone and tissue remodeling, pathogen defense, cell death and cell signaling [1,2]. These complex functions make the ly-sosome a central and dynamic organelle and not simply the dead end of the endocytic pathway. Two classes of proteins are essential for the

40

function of lysosomes: soluble lysosomal hydrolases and integral lysosomal membrane proteins [2]. Mutations in genes that encode any of these proteins could cause Lysosomal Storage Disorders (LSDs), which are characterized by an abnormal accumulation of substrates within the lysosome [1]. Taken together, LSDs comprise more than 50 genetic disorders with a frequency of 1:5000 live births [3]. Some LSDs are characterized by a broad spectrum phenotype, with progressive cellular impairment and dysfunction of numerous organs and systems [1,4]. Clinical hallmarks, which may manifest from early childhood until adulthood, include neurocognitive decline, dysmorphia, hydrops fetalis, hepatosplenomegaly and musculoskeletal abnormalities [5].

The past two decades have been characterized by remarkable progress in LSDs treatment, including drugs that aim to reduce accumulated substrate inside the lysosomes, and strategies that aim to increase the missing enzyme activity, like enzyme replacement therapy (ERT), hematopoietic stem cell transplantation, pharmacological chaperones and gene therapy [6]. These therapies are based on the property of lysosomal enzymes to be secreted and taken up by neighboring cells on the mannose-6-phosphate pathway. After endocytic internalization, the enzyme is transported by endosomes to the lysosome, resulting in the breakdown of accumulated storage material [7].

The ERT is considered the standard of care for several LSDs and has served as a stimulus for less common diseases; however, ERT still presents important limitations to overcome in terms of efficacy. This therapy is based on the administration of a recombinant enzyme by intravenous infusion and needs to occur under medical supervision because the lysosomal enzymes are not naturally located in the blood circulation and, as a consequence, they can trigger an immune response during the infusion. Also, the production of neutralizing antibodies against the administered enzyme is one of the main concerns about the safety and efficacy of ERT [8]. Furthermore, recombinant enzymes are large molecules that do not freely diffuse across membranes and are unable to reach therapeutic concentrations in some tissues, particularly in the brain. Whereas approximately two-thirds of LSDs cause neurodegeneration, the major therapeutic goals in treating many LSDs are focused on correcting enzyme levels or decreasing the accumulated substrate inside the brain lysosomes to treat the pathology in the CNS [9].

Nanotechnology may be a promising way to circumvent the drawbacks of the current ERT and also could be used for other therapies. The blood circulation time and bioavailability of the enzymes and/or drugs could be improved by inserting them in nanocarriers, which could decrease and/or avoid the need of frequent intravenous infusions along with the minimization or elimination of associated immunogenic responses [8]. Furthermore, nanoparticles can be tuned to target the cargo directly to the active site in the organism [10].

A wide range of nanoparticle systems, based on lipids and polymers, have been proposed for delivery of smaller bioactive molecules to the site of action. However, it is still challenging to load enzymes into nanocarriers without facing a change in the protein structure, such as unfolding, that may cause the loss of enzyme activity. In this sense, the flexible three-dimensional nanostructure make lipid-based nanocarriers with disordered bicontinuous structures, such as bicontinuous microemulsion and sponge phase, excellent candidates for enzyme and drug loading. The sponge phase (L$_3$) consists of two interpenetrating aqueous domains separated by a continuous lipid bilayer. L$_3$-based structures with relatively large aqueous channels are particularly favorable for the entrapment of macromolecules [11]. Bicontinuous microemulsion, in its turn, consists of aqueous and lipid domains separated by a monolayer of oriented surfactant molecules [12].

Lipids that self-assemble as the L$_3$ phase in physiological conditions are not easily found in the nature. In this sense, mixtures of lipids can be used to obtain L$_3$ structures [11]. Monoolein (Fig. 1a) is a biodegradable and biocompatible lipid that commonly shows a reverse bicontinuous cubic phase in the presence of water [13,14]. However, a transition to the L$_3$ phase can be induced mixing diglycerides to

monoolein without additional organic solvents [11].

Despite the advantages of lipid-based systems with disordered bicontinuous structure for macromolecular loading, its use to modify the course of neurodegenerative diseases is limited by the blood-brain barrier (BBB). Previous studies demonstrated that drugs incorporated in polymeric nanoparticles stabilized by polysorbate 80 (Fig. 1b) showed increased BBB permeability and subsequent uptake into the brain [15–22]. This non-ionic surfactant has been widely used in pharmaceutical products as a surface stabilizer because it is a low-cost product, easily available, biodegradable and it is also non-toxic to the cells at low concentrations [23]. Moreover, polysorbate 80 decreased the liver uptake and increased the circulation time of nanocarriers in mice more effectively than other surfactants [24]. Interestingly, polymeric nanocapsules stabilized by polysorbate 80 are shown to be capable of being internalized by endocytic organelles, which could suggest that this surfactant can also target nanocarriers to lysosomes [25].

Considering the exposed, we aimed to build monoolein-based nanoparticles with inner disordered bicontinuous structure (NS) stabilized by polysorbate 80 as a smart platform. We hypothesized that NS could be able to reach the brain tissue and could be internalized by lysosomes, opening a perspective of their potential application in the therapy of LSDs. In this way, we firstly developed and characterized the nanoparticles and also labeled the system (NS^F) with the fluorescent dye coumarin-6 (Fig. 1c). We evaluated the cytotoxicity and uptake of the monoolein-based nanoparticles by lysosomes in a human dermal fibroblasts culture and their potential of drug delivery to the CNS in animal model. Notably, drug delivery to CNS has never been demonstrated before *in vivo* for monoolein-based nanoparticles with inner disordered bicontinuous structure stabilized by polysorbate 80.

2. Experimental

2.1. Materials

Monoolein technical grade (1-oleoyl-*rac*-glycerol 40% mixed with di- and triglycerides), coumarin-6 [3-(2-Benzothiazolyl)-7-(diethylamino)coumarin], polysorbate 80 and Neutral Red dye were purchased from Sigma-Aldrich (St. Louis, USA) and used as received. LysoTracker Red dye L-7528 (Life Technologies), Dulbecco's Modified Eagle Medium (DMEM), fetal bovine serum (FBS), trypsin–EDTA, L-glutamine, penicillin/streptomycin, fungizone and phosphate buffered saline (PBS) were purchased from Thermo Fisher Scientific. Ultrapure water (Milli-Q, Millipore Corp., Bedford, MA) was used to prepare all the formulations.

2.2. Nanoparticle preparation and characterization

2.2.1. Preparation of the nanoparticles

The NS were prepared by adding 10 mL of polysorbate 80 aqueous solution (5 mg mL^{-1}) into a flask containing 0.200 g of monoolein. The mixture was sealed and left for 24 h on a mechanical shaking table at 350 rpm and 35 °C. After this time period, the formulation was stirred with a T10 Basic Ultra-Turrax equipment (IKA™-Werke GmbH & Co. KG, Germany) at 24,000 rpm for 15 min. The coumarin-6 loaded-nanoparticles (NS^F) were prepared by adding 0.1 mg of coumarin-6 to the flask containing monoolein before the mixture with the aqueous phase.

2.2.2. Dynamic light scattering (DLS)

The mean particle size of the formulations was determined using a dynamic light scattering instrument (Malvern™ Zetasizer 3600, UK) at an angle of 173° at 25 °C (Brazilian Nanotechnology National Laboratory – LNNano, Campinas/Brazil). The formulations were previously diluted in MilliQ™ water to avoid multiple scattering. The autocorrelation functions were analyzed by the cumulant method and the inverse Laplace transform-based CONTIN algorithm.

41
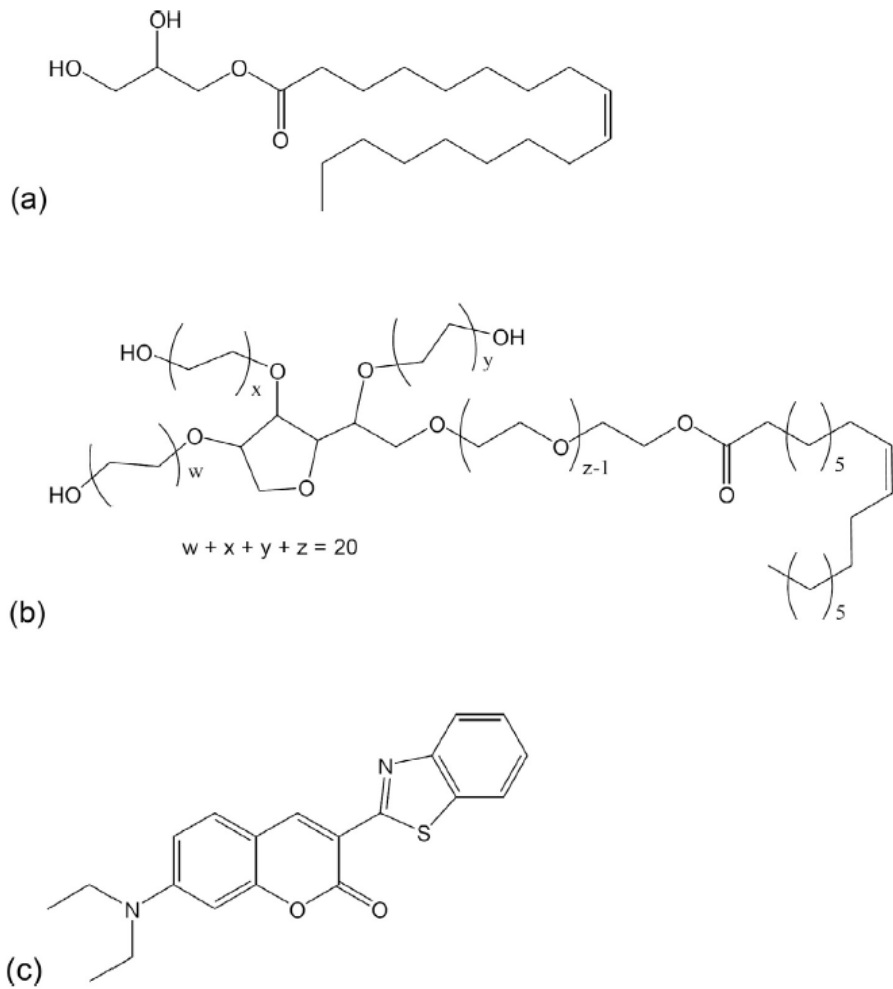
Fig. 1. Chemical structures of (a) monoolein, (b) polysorbate 80, and (c) coumarin-6.

2.2.3. Small-angle X-ray scattering (SAXS)

The SAXS measurements were performed using the SAXS1 beam line at the Brazilian Synchrotron Laboratory (LNLS, Campinas/Brazil). The samples were injected into a sample holder closed by two mica windows with temperature control (37 °C). The X-ray wavelength was 1.544 Å and the calibration was carried out with a silver behenate standard. The scattered intensity $I(q)$ was obtained from the scattering vector q ranging from 0.1 to 4.0 nm^{-1}. The intensities were corrected for the detector response and the dark current signal. Pure water was subtracted from the formulation scattering data. Fit2D™ software was used for data reduction from 2D SAXS images to 1D curves. Data fitting was carried out using the SASFit™ software.

2.2.4. Cryogenic transmission electron microscopy (Cryo-TEM)

Samples were prepared as described before [26] and analyzed in low dose condition, using a TALOS F200C (Thermo Fischer Scientific, USA) electron microscope operating at 200 kV (Brazilian Nano-technology National Laboratory – LNNano, Campinas/Brazil). Images were acquired using a CMOS camera Ceta 16 M 4 k × 4 k pixels (Thermo Fisher Scientific, USA).

2.2.5. Fluorescence measurements

The fluorescence measurements of formulations were obtained using a Shimadzu™ RF5301PC equipment and a triangular cuvette (Hellma, Quartz, Suprasil™, 10 nm). The fluorescence emission was recorded at 508 nm (λ_{em}). The excitation wavelength (λ_{ex}) was 458 nm.

The λ_{ex} value corresponds to the maximum absorption of coumarin-6 in ethanolic solution (4 µg mL^{-1}), which was measured using a Shimadzu™ UV-2450 spectrophotometer. All the spectra were recorded at room temperature.

2.3. In vitro assays

2.3.1. Cell culture

The target cells used in this experiment were human dermal fibro-blasts isolated from healthy subjects [27] and used to carry out the cytotoxicity assay (Neutral red uptake assay) and cell localization (LysoTracker red staining). The cells were maintained at 37 °C under 5% CO$_2$ in DMEM and supplement with 10% FBS (fetal bovine serum), antibiotics (200 µg mL^{-1} penicillin G, 200 µg mL^{-1} streptomycin) and fungizone (2 µg mL^{-1}). After sufficient growth for experimentation, cells (1 × 10^4 cells/well) were seeded in complete media in 96-well-culture plates and grown for one day prior to treatment with the na-noparticles. The nanoparticles NS and NS^F at three different con-centrations (28.3 µg mL^{-1}, 58.2 µg mL^{-1} and 117.9 µg mL^{-1}) [28,29] were added to DMEM complete media (125 µL) in 96-well-culture plate and the cells were treated for 24 h under standard conditions. The treatments were repeated three times at least.

2.3.2. Neutral red uptake assay (NRU)

Following a 24 h incubation period the cell viability of the plate was assessed. The nanoparticle solution was removed from each well and
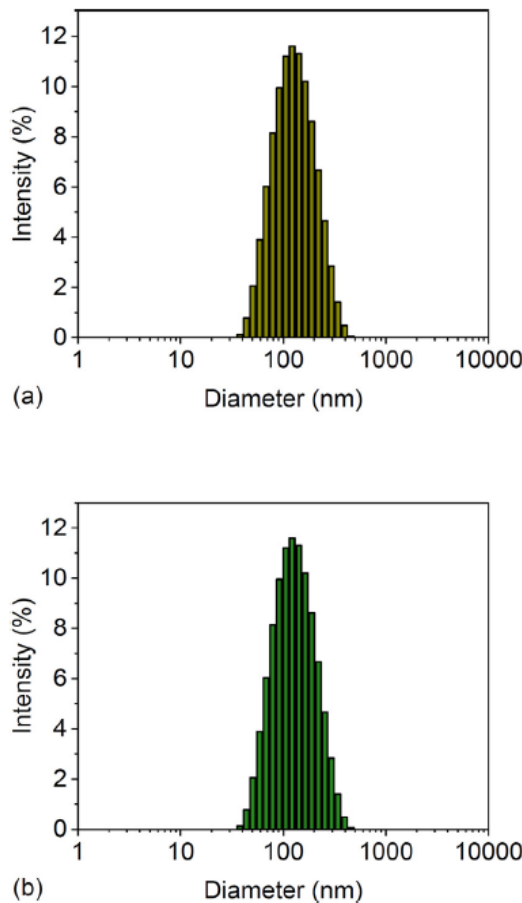
Fig. 2. Particle size distribution according to intensity of (a) NS, and (b) NS^F (DLS measurements carried out at a detection angle of 173°, 25 °C).

cells were washed with PBS. After, 150 µL of neutral red dye (100 µg mL^{-1}) dissolved in the serum-free medium (pH 6.4) were added to the culture and incubated for 3 h at 37 °C. Cells were washed again with PBS, and then 150 µL of elution medium (water:-ethanol:acetate, 50:49:1, v/v/v) were added and followed by a 20 min gentle shaking for complete dissolution. Absorbance was recorded at 540 nm using a microtiter plate reader. The absorbance of negative control (DMEM) cells was set as 100% viability, and the values for treated cells were calculated as a percentage of the control.

2.3.3. Hemolysis assay

Fresh whole blood (100 µL, heparinized) from healthy subject was mixed with 100 µL of formulation (117.9 µg mL^{-1}, which refers to the lipid concentration in the formulation) for 1 h at 37 °C. Then, the erythrocytes were separated by centrifugation (2,000 rpm for 10 min) and the supernatant (100 µL) was collected. The amount of released hemoglobin was determined by reading the absorbance at 540 nm using a microtiter plate reader. To determine the absorbance of 100% hemolysis, erythrocytes were lysed with 0.1% Triton X-100 (Sigma-Aldrich). The negative control was PBS. The hemolytic activities were calculated relative to the 0.1% Triton X-100-treated samples. The experiments were made in triplicate.

2.3.4. LysoTracker red staining

LysoTracker dye stains cellular acidic compartments and visualizes enlarged lysosomes at the proper dye concentration in patient cells [30]. Briefly, 1.2 10^5 cells/well were seeded in Chamber Slide™. Following a 24 h incubation period at 37 °C under 5% CO$_2$, cells were

washed with PBS and incubated with 1000 µL/well of NS^F in DMEM (117.9 µg mL^{-1} refer to lipid in the formulation) at 37 °C for 1 h. Subsequently, cells were washed with PBS and incubated with LysoTracker 1000 µL/well (50 nM LysoTracker Red dye L-7528, Life Technologies) at 37 °C for 1 h. Cells were then fixed with 4% paraformaldehyde solution in PBS for 30 min and mounted with DAPI Vectashield. Cells were analyzed by confocal microscopy (Olympus – FV100).

2.4. In vivo assay

2.4.1. Animals

Male A/J mice (18–20 g) were obtained from the *Instituto de Ciência e Tecnologia em Biomodelos* (FIOCRUZ, Rio de Janeiro, Brazil). They were kept in the animal-housing facilities with 5 animals per cage under controlled temperature (22 °C–25 °C), with a 12-hour light–dark cycle (6 am–6 pm) and food and water *ad libitum*. This study and the procedures were performed in accordance with the guidelines of the Guide for the Care and Use of Laboratory Animals and the recommendations of the Animal Ethics Committee of the *Instituto Oswaldo Cruz* (Protocol L006/2016), which also approved this research.

2.4.2. Animals treatment and fluorescence measurements

To determine whether NS^F was able to reach the CNS, the fluorescence of coumarin-6 in the brain tissue was measured. Briefly, 300 µL of NS^F were intraperitoneally administered. After 3, 6 or 24 h the animals were killed by anesthetic overdose (sodium pentobarbital, 500 mg kg^{-1}, intraperitoneal) perfused with saline, and the brain and liver tissues were rapidly removed and weighed. Then, 3 mL (brain) or 5 mL (liver) of acetonitrile were added to extract the coumarin-6. The mixtures were centrifuged at 4,000 × g for 10 min and 200 µL of supernatant were taken and added to 96-well special optics microplate. The fluorescence measurements were obtained using a microplate reader Spectramax M5 (Molecular Devices). The fluorescence emission was recorded at 495 nm (λ_{em}) and the excitation wavelength (λ_{ex}) was 310 nm. All the spectra were recorded at room temperature. The fluorescence intensity values were normalized by expressing them relative to the organ weight.

3. Results and discussion

The formulations were prepared using monoolein technical grade, which is composed of 40% (w/w) 1-oleoyl-*rac*-glycerol and 60% (w/w) of impurities that are the corresponding diglyceride and triglyceride compounds. Several proportions of monoolein and polysorbate 80 were tested to obtain an efficient nanoparticle steric stabilization. The lowest concentration of polysorbate 80 that gave bluish-white liquids without macroscopic agglomerates was 5.0 mg mL^{-1} using 20 mg mL^{-1} monoolein. This formulation (NS) was measured by DLS and showed a monomodal particle size distribution (Fig. 2a). The Z-average diameter of NS corresponded to 115 ± 3 nm with a low polydispersity index (PDI = 0.22). In order to visualize the nanoparticles *in vitro* and *in vivo*, the fluorophore coumarin-6 was loaded to the nanoparticles. This strategy was previously used to label polymeric nanoparticles because of the high biocompatibility and good fluorescence quantum yield of coumarin-6 [31,32]. The nanoparticles labeled with coumarin-6 (NS^F) were also measured by DLS to verify the effect of the fluorescent dye in the mean particle size. The results (Fig. 2b) showed that coumarin-6 loading did not affect the particle size distribution of the nanoparticles (NS^F), which presented a Z-average diameter of 117 ± 4 nm and a PDI of 0.24. All the measurements were carried out in triplicate. The Z-average sizes are closely related to those observed for other lipid-based liquid crystalline dispersions prepared by solvent displacement using polysorbate 80 as stabilizer [33].

Nanocarriers composed of pure monoolein usually present a lyotropic liquid crystalline inner structure with a reverse bicontinuous cubic phase (Q$_2$) [11]. Based on previous reports [34] we hypothesized
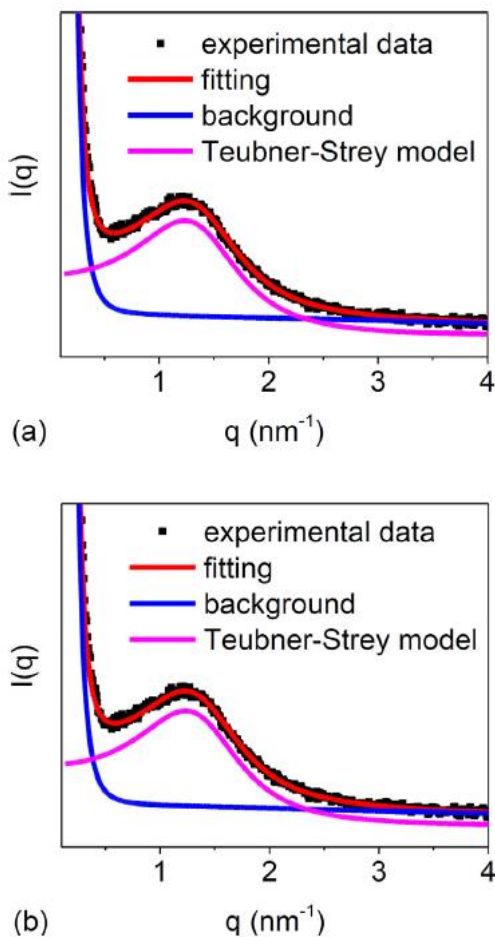
Fig. 3. SAXS profiles of (a) NS, and (b) NS^F formulations. The data (black dots) were fitted (red line) to the Teubner-Strey model (magenta line) with a background (blue line). (For interpretation of the references to colour in this figure legend, the reader is referred to the web version of this article.)
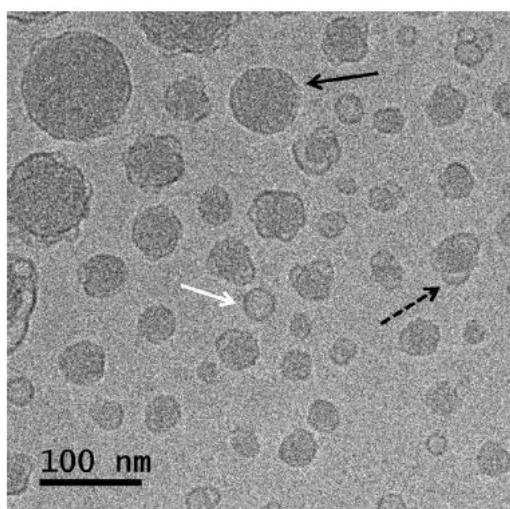

Fig. 4. Cryo-TEM image from the NS formulation showing disordered bicontinuous structures (black arrow), vesicles (white arrow) and disordered bicontinuous-vesicle mixed particles (dashed arrow).
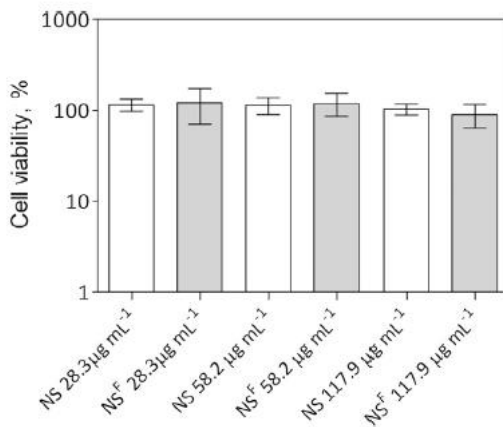

Fig. 5. Cell viability of NS and NS^F (human dermal fibroblasts). The values 28.3, 58.2 and 117.9 μg mL^{-1} refer to the concentration of lipid in the formulation. The experiments were made in triplicate. Data = mean $\pm$ SD.
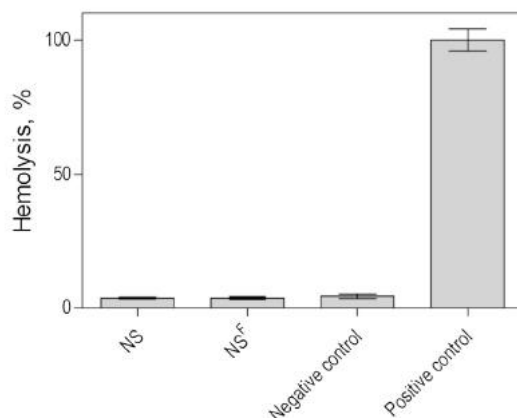

Fig. 6. Hemoglobin release due to the interaction of NS and NS^F with the human erythrocytes. The data were normalized to the hemoglobin release level of the Triton X-100 control. The experiments were made in triplicate. Data = mean $\pm$ SD.

that the diglyceride and triglyceride compounds that are impurities of the monoolein technical grade could decrease the interfacial curvature of the monoolein bilayer. The SAXS patterns of the NS and NS^F formulations displayed a single broad correlation peak (Fig. 3) that was successfully fitted to the Teubner-Strey model (Eq. (1)) superimposed on a decaying background,

$$I(q) = \frac{8\pi \langle \eta^2 \rangle / \xi}{a^2 - 2bq^2 + q^4} \tag{1}$$

where η^2 is the squared scattering length density contrast, ξ is the correlation length, and a and b are parameters related to ξ and the characteristic domain size $d = 2\pi/q_{max}$ (q_{max} is the peak position). Teubner and Strey [35] introduced this model to describe density fluctuations in microemulsion. Later, it was successfully applied to describe the L$_3$ phase [36].

The background function is described as (Equation (2)):

$$I(q) = c_0 + c_1 q + c_4 q^{-\alpha} \tag{2}$$

Initially, the background parameters were found by fitting Eq. (2) to the SAXS curve. The values found corresponded to $c_0 = 57212$, $c_1 = 0$, $c_4 = 2300$, and $\alpha = 4.6$. These values were fixed to carry out the fitting of the SAXS data to the Teubner-Strey model.

The satisfactory fitting of the SAXS curves to the Teubner-Strey model suggested a disordered bicontinuous inner structure of the

44
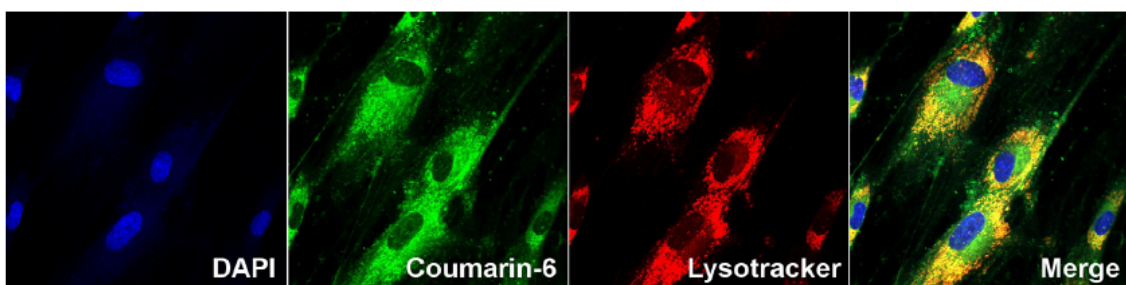
Fig. 7. Confocal microscopy images showing the internalization of fluorescent nanoparticles in dermal human fibroblast cells (1 h incubation). Column 1:DAPI channels showing the blue fluorescence from 40,6-diamidino-2-phenylindole (DAPI) stained nuclei; Column 2: Coumarin-6 channels showing the green fluorescence from coumarin-6 loaded nanoparticles (NS^F); Column 3: Lysotracker channels showing the red fluorescence from Lysotracker labeled acidic organelles; and Column 4: Merged channels DAPI, Coumarin-6 and Lysotracker. (For interpretation of the references to colour in this figure legend, the reader is referred to the web version of this article.)

monoolein-based nanoparticles. Monoolein technical grade used to prepare them is composed of 1-oleoyl-rac-glycerol 40% blended with 60% of the corresponding diglyceride and triglyceride compounds. In this way, the system could be structured as a sponge phase (L$_3$) with two interpenetrating aqueous channels and a disordered bilayer formed by the lipids. However, the assembly of pure monoolein (1-oleoyl-rac-glycerol) as a monolayer film separating lipid-rich (diglyceride and triglyceride compounds) and water-rich domains of a bicontinuous microemulsion cannot be ignored as another valid description of the system.

The extracted fit parameters using the Teubner-Strey model are related to the average length of a single lipid-water periodicity (d) and the length scale in which the quasi-periodical order is lost (ξ). Correlation lengths ξ of the systems were 1.7 nm (NS) and 1.6 nm (NS^F). The parameter ξ can be interpreted as a measure of the dispersion of d [35]. The characteristic domain size d was calculated as 4.6 nm and 4.5 nm for NS and NS^F, respectively. These values correspond to the average diameter comprised by the water-rich and lipid-rich pseudo-phase domains. A lamellar bilayer thickness of 3.2 nm was previously calculated for pure monoolein using molecular dynamics simulation [37]. The comparison between this theoretical value and those obtained for the characteristic domain size d in the monoolein-based nanoparticles suggests a low hydration level of the bicontinuous structure.

The amphiphilicity factor f_a [38,39] was obtained from ξ and d (Eq. (3)) to compare the NS and NS^F formulations.

$$f_a = \frac{1-(2\pi\xi/d)^2}{1+(2\pi\xi/d)^2} \qquad (3)$$

This value is typically close to -1 for very strong amphiphiles in a given solution (lamellar phase). Slightly less negative values of f_a were obtained for NS and NS^F (-0.69 and -0.67, respectively), which are consistent with disordered bicontinuous systems. Both formulations showed almost identical amphiphilicities and can be considered structurally equivalent.

The fluorescent dye did not affect the bicontinuous structure of the system and the size of the domains in a significant way probably because of the low dye concentration that was loaded into the nanoparticles. Despite this, intense fluorescence emission (λ_{em}) was detected at 508 nm for the NS^F formulation using the maximum absorption wavelength of coumarin-6 ethanolic solution (λ_{abs} = 458 nm) as the excitation wavelength (λ_{exc}). Therefore, the NS^F formulation was considered suitable to probe the nanoparticle tracking in animal model and the lysosome uptake in cell culture.

The NS formulation was visualized by cryo-TEM (Fig. 4) and the particle sizes were compatible with the DLS results. Typical disordered structures were observed in the images, corroborating the SAXS results. Additionally, vesicles with similar size values were also observed. Moreover, there is a third phase of particles combining vesicles and a disordered structure. The coexistence of these structures in the

formulation could be explained by the proximity of the sponge-to-lamellar phase transition [11]. Lamellar phase may also be in equilibrium with a microemulsion phase at higher surfactant concentrations.

The application of the monoolein-based nanoparticles as a platform for biomedical purposes involves the investigation of their potential toxicity. Neutral red is a weak cationic dye that can cross the plasma membrane by diffusion and tends to accumulate in lysosomes within the cell. If the cell membrane is altered, the uptake of neutral red is decreased and can leak out, allowing for discernment between live and dead cells. Cytotoxicity can be quantified from molecular absorption spectroscopy measurements of the neutral red under varying exposure conditions [40]. In this context, we exposed a culture of dermal human fibroblasts to NS and NS^F during 24 h and the results obtained by neutral red assay showed that NS and NS^F in all tested concentrations did not present cytotoxicity, showing viability values close to 100% (Fig. 5). In recent years, understanding the inherent cytotoxicity of drug nanocarriers with a lyotropic liquid crystalline inner structure has become an important research issue. The induced cytotoxicity of these nanocarriers may be dependent on several factors, including cell line, incubation time, the inner phase structure, and nanoparticle composition and concentration [28,41].

A pre-requisite for a parenteral delivery system is low or negligible hemolytic activity. Although the phase behavior and structural features of some non-lamellar lipid dispersions are rather well investigated, a good understanding of interaction aspects between such delivery vehicles and blood cell or model membranes is still lacking. Nevertheless, a previous study of monoolein-based nanosponges showed a small degree of hemolytic activity, in order of 1–2% [42]. On the other hand, the same study showed that monoolein-based cubosomes can cause a hemolysis degree incompatible with the parenteral administration [42]. According to the authors, the hemolytic activity was strongly dependent on both the lipid nature and the overall composition. In the present study, the highest concentration of nanoparticles used in the cytotoxicity assay was chosen for the hemolytic activity test. The NS and NS^F formulations showed no hemolytic activity (Fig. 6), proving to be safe for parenteral administration.

After validating the nontoxic effect of NS and NS^F, a cell uptake study was performed to examine the targeting ability of the NS^F (117.9 µg mL^{-1} of lipid, which is equivalent to 0.18 µM of coumarin-6) in a cell culture of human dermal fibroblasts. The dyes DAPI, coumarin-6 and Lysotracker were used to label nuclei, nanoparticles, and acidic organelle, respectively, as shown in Fig. 7. After 1 h of treatment with the nanoparticles, a high level of co-localization (yellow) of NS^F (green) and lysosomes (red) was exhibited indicating that the NS^F was confined in acidic compartments. Therefore, NS^F could be used for drug transmembrane transport and accumulation in lysosomes. The green fluorescence observed out of the lysosomes is probably related to an excess of formulation that overloaded the capacity of lysosomal uptake in healthy fibroblasts. It should be noted that fibroblasts from LSD patients

45
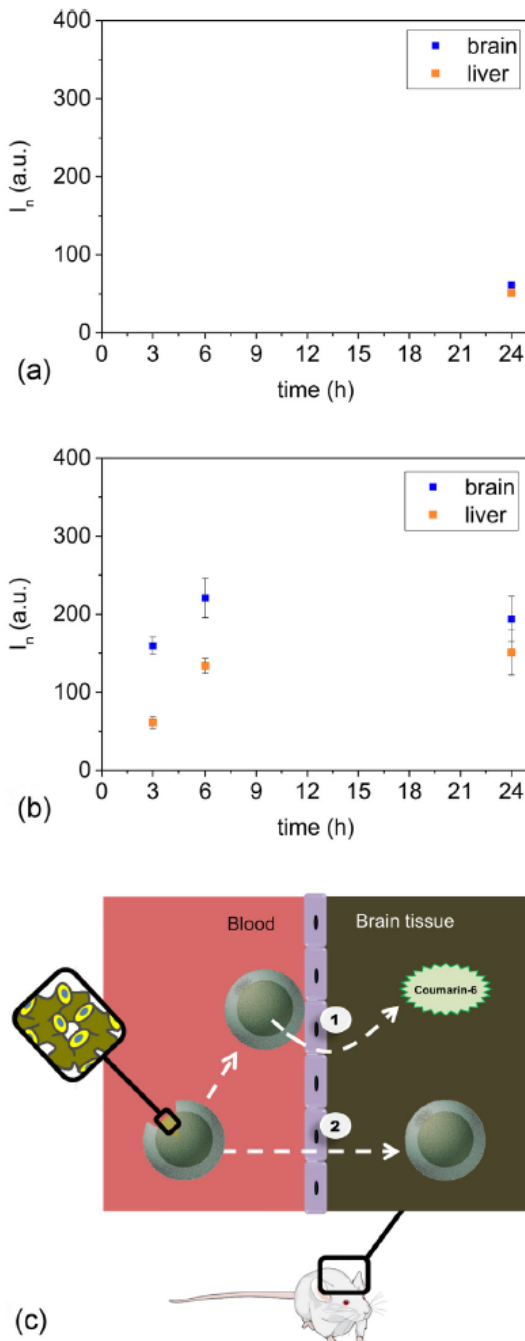
Fig. 8. Normalized fluorescence intensity of liver and brain homogenates of (a) untreated animals and (b) animals treated with NS^F as a function of time. A schematic representation (c) of possible mechanisms for the fluorescent dye delivery is also depicted (the blood-brain barrier is simplified for clarity): 1 - translocation of the fluorescent dye coumarin-6 from blood to the brain tissue; and 2 - translocation of the nanoparticle containing coumarin-6 from blood to the brain tissue.

present higher cellular mass of lysosomes, which could considerably increase the total lysosomal uptake capacity compared to healthy cells. These findings open the perspective to target drugs or enzymes safely to lysosomes, improving the treatment of LSDs.

The ability of the nanoparticles to reach the CNS was monitored in mice using the fluorescent labeled NS^F formulation. The liver was also analyzed, since this is the major site of xenobiotics metabolism. The formulations were administered to the animals and the fluorescence

was followed after 3, 6, and 24 h. As expected, coumarin-6 was detected at the liver. The normalized fluorescence intensity increased from 6 to 24 h evidencing the detoxification role of the liver and the time period necessary to the nanoparticles reach this organ. In the same way, the fluorescent dye was detected in the CNS just after 3 h and the normalized fluorescence intensity increased after 6 h. A plateau was then observed from 6 to 24 h (Fig. 8). The untreated animal (negative control) presented significantly lower basal fluorescence signal.

4. Conclusion

In summary, we obtained lipid-based nanoparticles with inner disordered bicontinuous structure using a low-cost product and a scalable technique. The *in vitro* studies showed that the nanoparticles were not toxic for human fibroblasts, were safe to parenteral administration, and were internalized by lysosomes after 1 h of treatment. Decorating the nanoparticles with polysorbate 80 gave them the ability to deliver a fluorescent dye in CNS just after 3 h of treatment. Taking the results into account, the nanoparticles show a great potential as a platform for delivery of drugs or enzymes into lysosomes improving the treatment of lysosomal diseases with brain impairment in a significant way.

Conflict of interest

The authors declare that they have no conflict of interest.

Acknowledgements

Ethical statement

The *in vitro* assays were conducted in compliance with the Council for International Organizations of Medical Sciences/World Health Organization (CIOMS/WHO 1993) and the Resolution number 466/2012 of the Brazilian Health Council Regulating Guidelines and Standards of Research that Involves Human Beings ("Conselho Nacional de Saúde - Diretrizes e Normas Regulamentadoras de Pesquisas Envolvendo Seres Humanos"). Written informed consent was obtained from all participants. The study was approved (number 15-0468) by the Research Ethics Committee of the Hospital de Clínicas de Porto Alegre (CEP/HCPA).

The *in vivo* assay with animals was performed in accordance with the guidelines of the Guide for the Care and Use of Laboratory Animals and the recommendations of the Animal Ethics Committee of the Instituto Oswaldo Cruz (number L006/2016), which also approved this research.

References

[1] A.H. Futerman, G. Van Meer, The cell biology of lysosomal storage disorders, Nat. Rev. Mol. Cell Biol. 5 (7) (2004) 554.

[2] P. Saftig, J. Klumperman, Lysosome biogenesis and lysosomal membrane proteins: trafficking meets function, Nat. Rev. Mol. Cell Biol. 10 (9) (2009) 623.

[3] E.B. Vitner, F.M. Platt, A.H. Futerman, Common and uncommon pathogenic cascades in lysosomal storage diseases, J. Biol. Chem. 285 (27) (2010) 20423–20427.

[4] B.A. Heese, Current strategies in the management of lysosomal storage diseases. Seminars in Pediatric Neurology, 2008, pp. 119–126.

[5] S.D. Kingma, O.A. Bodamer, F.A. Wijburg, Epidemiology and diagnosis of lysosomal storage disorders; challenges of screening, Best Practice Res. Clin. Endocrinol. Metabolism 29 (2) (2015) 145–157.

[6] B. Donida, C.E.D. Jacques, C.P. Mescka, D.G.B. Rodrigues, D.P. Marchetti, G. Ribas, R. Giugliani, C.R. Vargas, Oxidative damage and redox in lysosomal storage disorders: biochemical markers, Clinica Chimica Acta 466 (2017) 46–53.

[7] W.S. Sly, H.D. Fischer, A. Gonzalez-Noriega, J.H. Grubb, M. Natowicz, Role of the 6-phosphomannosyl-enzyme receptor in intracellular transport and adsorptive pinocytosis of lysosomal enzymes. Methods in Cell Biology, Elsevier, 1981, pp. 191–214.

[8] L. Martin-Banderas, M.A. Holgado, M. Duran-Lobato, J.J. Infante, J. Álvarez-Fuentes, M. Fernández-Arévalo, Role of nanotechnology for enzyme replacement therapy in lysosomal diseases. a focus on gaucher's disease, Curr. Med. Chem. 23 (9) (2016) 929–952.

[9] G. Parenti, G. Andria, A. Ballabio, Lysosomal storage diseases: from pathophysiology to therapy, Annu. Rev. Med. 66 (2015) 471–486.

[10] E.C. Wang, A.Z. Wang, Nanoparticles and their applications in cell and molecular biology, Integr. Biol. 6 (1) (2014) 9–26.

[11] M. Valldeperas, M. Wisniewska, M. Ram-On, E. Kesselman, D. Danino, T. Nylander, J. Barauskas, Sponge phases and nanoparticle dispersions in aqueous mixtures of mono-and diglycerides, Langmuir 32 (34) (2016) 8650–8659.

[12] A. Kogan, D.E. Shalev, U. Raviv, A. Aserin, N. Garti, Formation and characterization of ordered bicontinuous microemulsions, J. Phys. Chem. B 113 (31) (2009) 10669–10678.

[13] E.S. Lutton, Phase behavior of aqueous systems of monoglycerides, J. Am. Oil Chem. Soc. 42 (12) (1965) 1068–1070.

[14] S.T. Hyde, S. Andersson, A cubic structure consisting of a lipid bilayer forming an infinite periodic minimum surface of the gyroid type in the glycerolmonooleat-water system, Zeitschrift für Kristallographie - Crystalline Mater. 168 (1–4) (1984) 213–220.

[15] J. Kreuter, R.N. Alyautdin, D.A. Kharkevich, A.A. Ivanov, Passage of peptides through the blood-brain barrier with colloidal polymer particles (nanoparticles), Brain Res. 674 (1) (1995) 171–174.

[16] J. Kreuter, D. Shamenkov, V. Petrov, P. Ramge, K. Cychutek, C. Koch-Brandt, R. Alyautdin, Apolipoprotein-mediated transport of nanoparticle-bound drugs across the blood-brain barrier, J. Drug Target. 10 (4) (2002) 317–325.

[17] J. Kreuter, P. Ramge, V. Petrov, S. Hamm, S.E. Gelperina, B. Engelhardt, R. Alyautdin, H. Von Briesen, D.J. Begley, Direct evidence that polysorbate-80-coated poly (butylcyanoacrylate) nanoparticles deliver drugs to the CNS via specific mechanisms requiring prior binding of drug to the nanoparticles, Pharm. Res. 20 (3) (2003) 409–416.

[18] A. Bernardi, E. Braganhol, E. Jäger, F. Figueiró, M.I. Edelweiss, A.R. Pohlmann, S.S. Guterres, A.M. Battastini, Indomethacin-loaded nanocapsules treatment reduces in vivo glioblastoma growth in a rat glioma model, Cancer Lett. 281 (1) (2009) 53–63.

[19] R.L. Frozza, A. Bernardi, K. Paese, J.B. Hoppe, T.D. Silva, A.M. Battastini, A.R. Pohlmann, S.S. Guterres, C. Salbego, Characterization of trans-resveratrol-loaded lipid-core nanocapsules and tissue distribution studies in rats, J. Biomed. Nanotechnol. 6 (6) (2010) 694–703.

[20] G. Mittal, H. Carswell, R. Brett, S. Currie, M.R. Kumar, Development and evaluation of polymer nanoparticles for oral delivery of estradiol to rat brain in a model of Alzheimer's pathology, J. Control. Release 150 (2) (2011) 220–228.

[21] A. Bernardi, R.L. Frozza, A. Meneghetti, J.B. Hoppe, A.M. Battastini, A.R. Pohlmann, S.S. Guterres, C.G. Salbego, Indomethacin-loaded lipid-core nanocapsules reduce the damage triggered by Aβ1-42 in Alzheimer's disease models, Int. J. Nanomed. 7 (2012) 4927.

[22] D. Jain, A. Bajaj, R. Athawale, S. Shrikhande, P.N. Goel, Y. Nikam, R. Gude, S. Patil, P. Prashant Raut, Surface-coated PLA nanoparticles loaded with temozolomide for improved brain deposition and potential treatment of gliomas: development, characterization and in vivo studies, Drug Delivery 23 (3) (2016) 989–1006.

[23] R.N. Alyaudtin, A. Reichel, R. Löbenberg, P. Ramge, J. Kreuter, D.J. Begley, Interaction of poly (butylcyanoacrylate) nanoparticles with the blood-brain barrier in vivo and in vitro, J. Drug Target. 9 (3) (2001) 209–221.

[24] G. Storm, S.O. Belliot, T. Daemen, D.D. Lasic, Surface modification of nanoparticles to oppose uptake by the mononuclear phagocyte system, Adv. Drug Deliv. Rev. 17 (1) (1995) 31–48.

[25] F.S. Poletto, L.A. Fiel, M.V. Lopes, G. Schaab, A.M. Gomes, S.S. Guterres, B. Rossi-Bergmann, A.R. Pohlmann, Fluorescent-labeled poly (ε-caprolactone) lipid-core nanocapsules: synthesis, physicochemical properties and macrophage uptake, J. Coll. Sci. Biotechnol. 1 (1) (2012) 89–98.

[26] M.J. Altube, S.M. Selzer, M.A. de Farias, R.V. Portugal, M.J. Morilla, E.L. Romero, Surviving nebulization-induced stress: dexamethasone in pH-sensitive archaeosomes, Nanomedicine 11 (16) (2016) 2103–2117.

[27] J.C. Coelho, R. Giugliani, Fibroblasts of skin fragments as a tool for the investigation of genetic diseases: technical recommendations, Genetics and Mol. Biology 23 (2) (2000) 269–271.

[28] S. Murgia, A.M. Falchi, M. Mano, S. Lampis, R. Angius, A.M. Carnerup, J. Schmidt, G. Diaz, M. Giacca, Y. Talmon, M. Monduzzi, Nanoparticles from lipid-based liquid crystals: emulsifier influence on morphology and cytotoxicity, J. Phys. Chem. B 114 (10) (2010) 3518–3525.

[29] T.M. Hinton, F. Grusche, D. Acharya, R. Shukla, V. Bansal, L.J. Waddington, P. Monaghana, B.W. Muir, Bicontinuous cubic phase nanoparticle lipid chemistry affects toxicity in cultured cells, Toxicol. Res. 3 (1) (2014) 11–22.

[30] D. Yu, M. Swaroop, M. Wang, U. Baxa, R. Yang, Y. Yan, T. Coksaygan, L. DeTolla, J.J. Marugan, C.P. Austin, J.C. McKew, D.W. Gong, W. Zheng, Niemann–pick disease type c: Induced pluripotent stem cell–derived neuronal cells for modeling neural disease and evaluating drug efficacy, J. Biomol. Screen. 19 (8) (2014) 1164–1173.

[31] Y. Hu, J. Xie, Y.W. Tong, C.H. Wang, Effect of PEG conformation and particle size on the cellular uptake efficiency of nanoparticles with the HepG2 cells, J. Control. Release 118 (1) (2007) 7–17.

[32] B. Sun, B. Ranganathan, S.S. Feng, Multifunctional poly (D, L-lactide-co-glycolide)/montmorillonite (PLGA/MMT) nanoparticles decorated by Trastuzumab for targeted chemotherapy of breast cancer, Biomaterials 29 (4) (2008) 475–486.

[33] F.S. Poletto, F.S. Lima, D. Lundberg, T. Nylander, W. Loh, Tailoring the internal structure of liquid crystalline nanoparticles responsive to fungal lipases: A potential platform for sustained drug release, Colloids Surf. B: Biointerf. 147 (2016) 210–216.

[34] B. Angelov, A. Angelova, R. Mutafchieva, S. Lesieur, U. Vainio, V.M. Garamus, G.V. Jensen, J.S. Pedersen, SAXS investigation of a cubic to a sponge (L 3) phase transition in self-assembled lipid nanocarriers, PCCP 13 (8) (2011) 3073–3081.

[35] M. Teubner, R. Strey, Origin of the scattering peak in microemulsions, J. Chem. Phys. 87 (5) (1987) 3195–3200.

[36] A. Angelova, B. Angelov, R. Mutafchieva, V.M. Garamus, S. Lesieur, S.S. Funari, R. Willumeit, P. Couvreur, Swelling of a sponge lipid phase via incorporation of a nonionic amphiphile: SANS and SAXS studies, Trends in Colloid and Interface Science XXIV, Springer, Berlin, Heidelberg, 2011, pp. 1–6.

[37] S.J. Marrink, D.P. Tieleman, Molecular dynamics simulation of a lipid diamond cubic phase, J. Am. Chem. Soc. 123 (49) (2001) 12383–12391.

[38] K.V. Schubert, R. Strey, S.R. Kline, E.W. Kaler, Small angle neutron scattering near Lifshitz lines: transition from weakly structured mixtures to microemulsions, J. Chem. Phys. 101 (6) (1994) 5343–5355.

[39] H. Leitão, M.M. Telo da Gama, R. Strey, Scaling of the interfacial tension of microemulsions: a Landau theory approach, J. Chem. Phys. 108 (10) (1998) 4189–4198.

[40] N. Lewinski, V. Colvin, R. Drezek, Cytotoxicity of nanoparticles, Small 4 (1) (2008) 26–49.

[41] J. Zhai, R. Suryadinata, B. Luan, N. Tran, T.M. Hinton, J. Ratcliffe, X. Hao, C.J. Drummond, Amphiphilic brush polymers produced using the RAFT polymerisation method stabilise and reduce the cell cytotoxicity of lipid lyotropic liquid crystalline nanoparticles, Faraday Discuss. 191 (2016) 545–563.

[42] J. Barauskas, C. Cervin, M. Jankunec, M. Špandyreva, K. Ribokaitė, F. Tiberg, M. Johnsson, Interactions of lipid-based liquid crystalline nanoparticles with model and cell membranes, Int. J. Pharm. 391 (1–2) (2010) 284–291.

47

3.2 Artigo 2: A promising nanodevice to deliver β-cyclodextrin in the central nervous system and treat Niemann-Pick C disease.

Manuscrito a ser submetido.

A promising nanodevice to deliver β-cyclodextrin in the central nervous system and treat Niemann-Pick C disease.

Bruna Donida[a*] MSc, Marco Raabe[b] BS, Bárbara Tauffner[c] BS, Marcelo A. de Farias[d] DSc, Andryele Zaffari Machado[e] BS, Fernanda Timm[e] DSc, Rejane Gus Kessler[e] DSc, Rodrigo V. Portugal[d] DSc, Andressa Bernardi[f] DSc, Rudimar Frozza[f] DSc, Dinara J. Moura[b] DSC, Fernanda Poletto[a,c] DSc, Carmen Regla Vargas[a,e*] DSc

[a] Programa de Pós-Graduação em Ciências Biológicas, Bioquímica, Universidade Federal do Rio Grande do Sul, Zip Code 90035-003, Porto Alegre, RS, Brazil.

[b] Universidade Federal de Ciências de Saúde de Porto Alegre, Zip Code 90050170 Porto Alegre, RS, Brazil.

[c] Programa de Pós Graduação em Química, Universidade Federal do Rio Grande do Sul, Zip Code 91501-970, Porto Alegre, Brazil.

[d] Brazilian Nanotechnology National Laboratory (LNNano), Brazilian Center for Research in Energy and Materials (CNPEM), Zip Code 13083-970, Campinas, Sao Paulo, Brazil.

[e] Serviço de Genética Médica, Hospital de Clínicas de Porto Alegre, Zip Code 90035-003, Porto Alegre, RS, Brazil.

[f] Instituto Oswaldo Cruz (IOC), Fundação Oswaldo Cruz (FIOCRUZ), Zip Code 21040-360, Rio de Janeiro, RJ, Brazil.

* to whom correspondence should be addressed:

MSc Bruna Donida

E-mail: donida.bruna@gmail.com, Phone: +55 51 33598011.

DSc Carmen Regla Vargas

E-mail: crvargas@hcpa.edu.br, Phone: +55 51 33598011.

Manuscript word count: 4979

Abstract word count: 150

Number of references: 32

Number of figures: 8

ABSTRACT

Recently, β-cyclodextrin has been identified as a promising therapy for Niemann-Pick C disease (NPC), because it can mobilize the entrapped cholesterol from lysosomes to blood circulation. Unfortunately, β-cyclodextrin does not act on neurological impairment, because it cannot cross the blood-brain barrier. In order to circumvent this drawback, we aimed to build nanoparticles able to deliver β-cyclodextrin into the brain. We developed and characterized the nanoparticles by dynamic light scattering, small-angle X-ray scattering, and cryogenic transmission electron microscopy. The nanoparticles showed a diameter around 120 nm, with a disordered bicontinuous inner structure, which did not cause cytotoxicity in NPC fibroblasts, and were safe for parenteral administration. Nanoparticles were taken up by lysosomes and were able to reduce the cholesterol accumulated in NPC fibroblasts. During the *in vivo* assay, nanoparticles reached the brain of mice more intensely than the other organs, showing great potential to improve the treatment of NPC brain impairment.

Keywords: Niemann-Pick C, β-cyclodextrin, nanoparticle.

Abbreviations: β-CD – β-ciclodextrin**;** BBB - Blood-brain barrier; CNS – Central nervous system; Cryo-TEM – Cryogenic transmission electron microscopy; DLS- Dynamic light scattering; DMA-C_{12}-CD- Monosubstituted n-alkyldimethylammonium-β-cyclodextrin; LE/LY – late endosomal/lysosomal; LSD - Lysosomal Storage Disorders; NPC – Niemann Pick type C; NRU – Neutral red uptake; NS - Nanoparticles; $NS_{β-CD}$ – Nanoparticles with β-cyclodextrin; $NS^{F}_{β-CD}$ – Nanoparticles with β-cyclodextrin and labeled with coumarin-6; P80 – Polysorbate 80; P80@2β-CD – complex of polysorbate 80 and β-cyclodextrin (1:2); PDI – Polydispersity index; SAXS - Small-angle X-ray scattering

1. Background

Niemman-Pick C (NPC) is an autosomal recessive lysosomal storage disorder (LSD) with an estimated incidence around 1/89,000 live births [1]. The mutation in the cholesterol transport genes, *NPC1* (95% of cases) or *NPC2,* causes impairment in intracellular lipid trafficking, which consequently affects the entire cell machinery. The *NPC1* gene encodes an endosomal transmembrane glycoprotein, and the *NPC2* gene encodes a small lysosomal protein. The absence of proteins encoded by *NPC1* or *NPC2* genes results in accumulation of non-esterified cholesterol and glycosphingolipids within the late endosomal/lysosomal (LE/LY) compartment of cells. NPC has an important visceral involvement, and about 90 % of patients showed a progressive neurodegeneration as dominant feature. The age of onset and initial severity may vary among affected individuals; however, the disease is usually fatal before adolescence. Unfortunately, an effective cure has yet to be discovered [2].

Several drugs are being tested as potential therapies for NPC, including β-cyclodextrin (β-CD), which is a cyclic oligosaccharide commonly used to increase the solubility of lipophilic drugs in aqueous solution [3-5]. β-CD can form a supramolecular inclusion complex with cholesterol, increasing the apparent solubility of this compound in water. Davidson *et al*. [4] showed that 2-hydroxypropyl-β-CD administration delayed clinical disease onset, reduced intraneuronal storage of cholesterol, and significantly increased the lifespan of NPC mouse model. However, high doses or continuous administration of β-CD (or its derivatives) are required to obtain therapeutic effects, since 90% of this compound is cleared from the bloodstream within 24 h. It has been reported that high doses of cyclodextrin can cause hearing problems in NPC animal model [6].

Although the strategies proposed in the literature helped to remove cholesterol from peripheral organs and tissues affected by NPC disease, obtaining neurological benefits in humans remains a challenging issue to overcome. Access of therapeutic agents to the central nervous system (CNS) is often problematic because the blood-brain barrier (BBB) is impermeable to many molecules. Pontikis *et al.* [7] demonstrated that hydroxypropyl-β-CD was not taken up by cerebral tissue when an usual dose of 4000 mg kg^{-1} was injected intraperitoneally in NPC mouse. Similarly, neurological symptoms were not considerably improved by cyclodextrin in the NPC mouse model, as reported by Camargo *et al.* [8], which may be partially due to apparent non-permeation of cyclodextrin through BBB. Another study showed that a treatment using cyclodextrin, allopregnanolone, and miglustat has demonstrated to be effective for motor problems, but did not influence the cognitive deficit in the NPC animal model [9]. Therefore, the development of a long circulating biocompatible system to deliver β-CD within the LE/LY compartment of NPC cells that is able to cross the BBB could improve the cholesterol clearance in the brain of NPC patients.

Recently [10], we proposed a new monoolein-based nanoparticle as an innovative platform to incorporate drugs aiming treatment of LSD with brain impairment. Monoolein is a biodegradable and biocompatible lipid that commonly shows a reverse bicontinuous cubic phase in the presence of water [11, 12]. However, a disordered bicontinuous structure was obtained using monoolein technical grade, which is composed of 1-oleoyl-rac-glycerol mixed with di- and triglycerides. Disordered bicontinuous structures are flexible, which makes them able to incorporate high amounts of macromolecules [13]. The nanoparticles showed a potential to reach the CNS in an animal model and also were internalized by LE/LY compartment in cell culture, showing a great potential to be applied as drug delivery systems for LSD with brain

impairment [10]. Brain targeting was obtained decorating the nanoparticles with the non-ionic surfactant polysorbate 80 (P80). Several studies demonstrated that drugs incorporated in polymeric nanoparticles stabilized by P80 showed increased BBB permeability and subsequent uptake into the brain [14-19].

In light of the advantages of disordered bicontinuous structures to incorporate macromolecules, and the efficient brain-targeting of nanoparticles promoted by the P80 surface coating, we propose that nanoparticles stabilized with P80 can be used for targeted delivery of β-CD to the brain. The formation of an inclusion complex between β-CD and P80 was used as strategy for β-CD loading to the nanoparticles.

2. Methods

2.1 Materials

Monoolein technical grade (39.9 % of 1-oleoyl-rac-glycerol mixed with 22.5% of diglycerides and 34.7% of triglycerides; batch number BCBQ8354V), coumarin-6, β-cyclodextrin, polysorbate 80, Filipin III from *Streptomyces filipinensis*, and neutral red dye were purchased from Sigma-Aldrich (St. Louis, USA) and used as received. LysoTracker Red dye L-7528 (Life Technologies), Dulbecco's Modified Eagle Medium (DMEM), fetal bovine serum (FBS), trypsin–EDTA, L-glutamine, penicillin/streptomycin, fungizone, and phosphate buffered saline (PBS) were purchased from Thermo Fisher Scientific. Ultrapure water (Milli-Q™, Millipore Corp., Bedford, MA) was used to prepare all the formulations.

2.2 Samples

Skin biopsy [20] and blood samples (EDTA tube) were obtained from NPC patients ($n = 3$) and healthy subjects ($n = 3$). An aliquot of whole blood was centrifuged at 1000 $\times g$ for 10 min and plasma was removed by aspiration, aliquoted and frozen at −80 °C until biochemical determination. Diagnosis of NPC patients was confirmed by the filipin staining test, performed on cultured fibroblasts [21].

2.3 Nanoparticle preparation and characterization

2.3.1 Inclusion complex

The P80@2β-CD inclusion complex was prepared mixing β-CD, P80, and water at a β-CD/P80 molar ratio of 2:1 and β-CD concentration of 7.5 mM. The solution was maintained under magnetic stirring at 35 °C for 24 h to allow self-assembly of the inclusion complex [22].

2.3.2 Preparation of the nanoparticles

The nanoparticle formulation containing β-CD ($NS_{β-CD}$) was prepared by adding 10 mL of P80@2β-CD (7.5 mM of β-CD) into a flask containing 0.200 g of monoolein. The mixture was sealed and left for 24 h on a mechanical shaking table at 350 rpm and 35ºC. After this time period, the formulation was stirred with a T10 Basic Ultra-Turrax equipment (IKA[TM]-Werke GmbH & Co. KG, Germany) at 24,000 rpm for 15 min. The coumarin-6 loaded-nanoparticles ($NS^F_{β-CD}$) were prepared by adding 0.1 mg of coumarin-6 to the flask containing monoolein before the mixture with P80@2β-CD.

2.3.2 Dynamic light scattering (DLS)

The mean particle size of the formulations was determined using a dynamic light scattering instrument (Malvern[TM] Zetasizer 3600, UK) at an angle of 173° at 25ºC (Brazilian Nanotechnology National Laboratory, Campinas/Brazil). The formulations were previously diluted in MilliQ[TM] water to avoid multiple light scattering. The autocorrelation functions were analyzed by the cumulant method and the inverse Laplace transform-based CONTIN algorithm.

2.3.3 Small-angle X-ray scattering (SAXS)

The SAXS measurements were performed as described before [10] at the SAXS1 beam line at the Brazilian Synchrotron Laboratory (LNLS, Campinas/Brazil). Fit2D™ software was used for data reduction from 2D SAXS images to 1D curves. Data fitting was carried out using the SASFit™ software.

2.3.4 Cryogenic transmission electron microscopy (Cryo-TEM)

Samples were prepared as described before [23] and analyzed in low dose condition, using a TALOS F200C (Thermo Fischer Scientific, USA) electron microscope operating at 200 kV. Images were acquired using a CMOS camera Ceta 16M 4k × 4k pixels (Thermo Fisher Scientific, USA).

2.4. Cholestane-3β,5α,6β-triol analysis

Levels of triol were determined by liquid chromatography/tandem mass spectrometry (LC-MS/MS) in EDTA-plasma, using cholestane-3β,5α,6β-triol D7 as internal standard and derivatization with dimethylglycine esters, according to a previous report [24] with some modifications. The optimized MS/MS conditions were described by Ribas, et al. [25] and quantification was based on standard curve ranging from 2 to 400 ng/mL for the triol [25].

2.5 Hemolysis assay

Fresh whole blood (100 µL, heparinized) from healthy subject was mixed with 100 µL of treatment (all treatments presented a β-CD final concentration of 45 µM) for 1 h at 37ºC. Then, the erythrocytes were separated by centrifugation (2,000 rpm for 10 min) and the supernatant (100 µL) was collected. The amount of released hemoglobin was determined by reading the absorbance at 540 nm using a microtiter plate reader. To determine the absorbance of 100 % hemolysis, erythrocytes were lysed with 0.1 % Triton X-100 (Sigma-Aldrich). The negative control was PBS. The hemolytic activities were calculated relative to the 0.1 % Triton X-100-treated samples. The experiments were made in triplicate.

2.6 Cell culture

The target cells used in this experiment were human dermal fibroblasts isolated from healthy subjects (n = 3) and from NPC patients (n = 3) [20]. The cells were maintained at 37ºC under 5% CO_2 in DMEM supplemented with 10% FBS, antibiotics (200 µg mL^{-1} penicillin G, 200 µg mL^{-1} streptomycin), and 2 µg mL^{-1} of fungizone.

2.6.1 Neutral red uptake assay (NRU)

After sufficient growth for experimentation, fibroblasts from healthy subjects (1 × 10^4 cells/well) were seeded in complete media in the 96-well-culture plates and grown for one day prior to treatment with the nanoparticles. Free β-CD, $NS_{β-CD}$, $NS^F_{β-CD}$, and P80@2β-CD at three different concentrations of β-CD (11.25, 22.5 and 45 µM), were added to DMEM complete media (125 µL) in 96-well-culture plate and the cells were treated for 48 h under standard conditions. The treatments were repeated three times at

least. After the incubation time, the treatment solution was removed from each well and cells were washed with PBS. In sequence, 150 µL of neutral red dye (100 µg mL^{-1}) dissolved in the serum-free medium (pH 6.4) were added to the culture and incubated for 3 h at 37ºC. Cells were washed with PBS, and then 150 µL of elution medium (water:ethanol:acetate, 50:49:1, v/v/v) were added and followed by a 20 min gentle shaking for complete dissolution. Absorbance was recorded at 540 nm using a microtiter plate reader. The absorbance of negative control (DMEM) cells was set as 100% of viability and the values for treated cells were calculated as a percentage of the control. The experiment was repeated in NPC patient-derived dermal fibroblasts using the highest dose of β-CD for all treatments.

2.6.2 LysoTracker red staining

LysoTracker dye stains cellular acidic compartments and visualizes enlarged lysosomes at the proper dye concentration in patient cells [26]. Briefly, 1.2×10^5 cells/well were seeded in Chamber Slide™. Following a 24 h incubation period at 37ºC under 5 % CO_2, cells were washed with PBS and incubated with 1000 µL/well of $NS^F_{β-CD}$ in DMEM (equivalent to 45 µM of β-cyclodextrin) at 37ºC for 1 and 3 h. Subsequently, cells were washed with PBS and incubated with LysoTracker 1000 µL/well (50 nM LysoTracker Red dye - L-7528) at 37ºC for 15 min. Cells were analyzed by confocal microscopy (Olympus – FV100).

2.6.3 Filipin assay

The sequestration and resulting accumulation of unesterified cholesterol in the LE/L compartment can be visualized in cells by fluorescence microscopy after staining with filipin reagent [21]. To determine cholesterol depletion using the nanoparticles, 1.2×10^5 cells/well were seeded in Chamber Slide™. Following a 24 h incubation period at 37ºC under 5 % CO_2, cells were washed with PBS and incubated with 1000 µL/well of DMEM, $NS_{\beta\text{-CD}}$, P80@2β-CD, and free β-CD in DMEM (45 µM of β-cyclodextrin) at 37 ºC for 48 h. Subsequently, cells were washed with PBS, fixed with paraformaldehyde (3.6 %) for 30 min and incubated with filipin reagent (1 h) for histological examination in a fluorescent microscope (Olympus Optical, BX41TF).

2.7 In vivo assay

2.7.1 Animals

Male *Swiss* mice (40-50 g) were obtained from the *Instituto de Ciência e Tecnologia em Biomodelos* (FIOCRUZ, Rio de Janeiro, Brazil). They were kept in the animal-housing facilities with 4 animals per cage under controlled temperature (22°C–25°C), with a 12-hour light-dark cycle (6 am–6 pm) and food and water *ad libitum*.

2.7.2 Fluorescence measurements

$NS^F_{\beta\text{-CD}}$ or $NS_{\beta\text{-CD}}$ were intraperitoneally injected (300 µL) and mice were killed by anesthetic overdose (sodium pentobarbital, 500 mg kg^{-1}, intraperitoneal) after 15 min, 1 h, and 24 h of treatment with the nanoparticles. The organs were rapidly dissected and *ex vivo* fluorescence images were acquired on an IVIS Lumina System

live animal biophotonic imaging system (Xenogen Corp, CA, USA). Signals were collected from a determined region of interest (ROI) using the contour ROI tool and total flux intensities (photons/s) analyzed using Living Image Software 4.5. Experiments were repeated 2 times (3 animals/group) with different batches of formulations.

2.8 Statistical analysis

All results were expressed as mean ± standard error of the mean (SEM). Comparisons between means were analyzed by unpaired *t* test (for 3β,5α,6β-triol analysis) or by one-way ANOVA, followed by Tukey's multiple range test (for all other assays).

3. Results

A previous study from our group [10] has demonstrated that monoolein-based nanoparticles stabilized by P80 are a versatile platform for brain targeting. In order to incorporate β-CD into the nanoparticles, we proposed to add to the formulation an inclusion complex of β-CD with P80 as guest (P80@2β-CD). The inclusion complex was prepared maintaining an aqueous solution of P80 and β-CD under magnetic stirring at 35°C. After 24 h, the appearance of this solution was pearlescent indicating self-assembly of the system. The mixture of P80@2β-CD and monoolein technical grade generated a milky pearlescent formulation ($NS_{\beta-CD}$) without macroscopic aggregates.

The particle size distribution of $NS_{\beta-CD}$ was determined by dynamic light scattering. A monomodal distribution was observed (Figure 1a) with Z-average diameter (calculated by the cumulant method) of 121 ± 1 nm and polydispersity index lower than 0.2. The system was labeled with the fluorescent dye coumarin-6 ($NS^F_{\beta-CD}$) aiming *in vivo* tracking. The formulation showed green fluorescence as expected. The particle size distribution (Figure 1b) was similar to that obtained without the fluorescent dye, with a Z-average diameter of 122 ± 4 nm and polydispersity index lower than 0.2.

[Insert Figure 1]

The $NS_{\beta-CD}$ formulation was visualized by cryo-TEM (Figure 2) and three different structures were observed. Most of the structures present in the formulation were round particles (white arrow, Figure 2). The size of these particles is compatible with the Z-average diameter obtained by dynamic light scattering. As expected [10], some vesicles (dashed white arrow) coexisted with the nanoparticles. Interestingly, the image also shows micrometric flat plate structures (black arrow), which probably caused the pearlescent appearance of the formulation.

[Insert Figure 2]

The SAXS curve of the $NS_{\beta-CD}$ formulation displayed a single broad correlation peak between $q = 1.0$ and 2.5 nm^{-1} (Figure 3). This region of the curve was fitted to the Teubner-Strey model (Equation 1),

$$I_{TS}(q) = \frac{8\pi(\eta^2)/\xi}{a^2 - 2bq^2 + q^4} \qquad (1)$$

where η^2 is the squared scattering length density contrast, ξ is the correlation length, and a and b are parameters related to ξ and the characteristic domain size $d = 2\pi/q_{max}$ (q_{max} is the peak position). The Teubner-Strey model describes density fluctuations in disordered bicontinuous systems [27]. The adequate fitting to this model (Figure 3) suggested that the monoolein-based nanoparticles present a disordered bicontinuous inner structure, similarly to the nanoparticles without β-CD [10]. The fitting of the SAXS data to the Teubner-Strey model gives the average length of a single lipid-water periodicity (d) and the length scale in which the quasi-periodical order is lost (ξ). The correlation length ξ of the bicontinuous structure was 1.5 nm and the characteristic domain size d was 4.6 nm. These values were similar to those obtained for the nanoparticles without β-CD [10], suggesting that the hydration level of the system was not affected by the inclusion complex. In this way, the inclusion complex is probably decorating the surface of the nanoparticles.

[insert Figure 3]

We measured the concentration of 3β,5α,6β-triol in the plasma of NPC patients and healthy subjects by LC-MS/MS. NPC patients had 3β,5α,6β-triol levels of 208 ± 32.8 ng mL^{-1} (mean ± SEM), while healthy subjects had significantly lower levels (9.7

$\pm$ 3.2 ng mL^{-1}). The results demonstrated that LC-MS/MS can be considered as a non-invasive technique, compared to filipin test, to confirm the diagnosis of NPC disease.

The fibroblasts were cultivated to test the cytotoxicity of the formulations by NRU (figure 4). P80@2β-CD and pure β-CD were also evaluated for comparison. Initially, samples with three different concentrations of β-CD were tested in healthy human dermal fibroblasts (figure 4a). As all samples presented non-toxic effects, the samples with the highest concentration of β-CD (45 μM) were used in NPC patient-derived dermal fibroblasts (figure 4b). In agreement with the results obtained in healthy fibroblasts, the formulations, P80@2β-CD, and free β-CD did not show toxic effects in NPC patient-derived dermal fibroblasts.

[Insert Figure 4]

Since formulations have demonstrated safety under tested conditions, the lysosomal uptake of the dye-labeled formulation NS$^F_{\beta\text{-CD}}$ (green fluorescence) was evaluated in NPC patient-derived dermal fibroblasts by confocal microscopy (Figure 5). The lysosomes were labeled with LysoTracker red fluorescent dye. The images were evaluated by ImageJ in order to calculate the Pearson's coefficient, which determines the efficiency of two fluorophores co-localization (LysoTracker and cumarin-6). After 1 h of incubation, NS$^F_{\beta\text{-CD}}$ presented high co-localization with lysosomes (yellow fluorescence-Pearson's coefficient of 0.80 $\pm$ 0.03). Even after 3 h, the nanoparticles remained highly co-localized with lysosomes (Pearson's coefficient of 0.78 $\pm$ 0.06).

[Insert Figure 5]

In order to evaluate the potential of NS$_{\beta\text{-CD}}$ to decrease the concentration of unesterified cholesterol accumulated inside the LE/LY compartment of NPC cells, NPC patient-derived dermal fibroblasts were exposed to free β-CD, pure P80@2β-CD, and NS$_{\beta\text{-CD}}$ for 48 h. The cholesterol depletion induced by these samples was investigated

using filipin as a histochemical marker for cholesterol, and cells were observed using a fluorescence microscope (Figure 6a). The images were treated with ImageJ software in order to compare the intensity of fluorescence among the treatments (Figure 6b). The fluorescence intensity decreased by about 50 % after all treatments, demonstrating the ability of the samples to capture the accumulated cholesterol inside the cells. Considering the results obtained by cryo-TEM, which showed a presence of flat plate micrometric structures in the $NS_{\beta-CD}$ formulation, we also evaluated the cholesterol depletion by the filtered (0.45 µm or 0.22 µm) formulation. Both filtered aliquots caused cholesterol depletion similar to that observed for the $NS_{\beta-CD}$. This result suggests that the flat plate structures in the formulation were not the main responsible for cholesterol depletion in the cells.

[Insert Figure 6]

The *in vitro* hemolytic activity was tested to verify the risk of the formulations for parenteral administration (figure 7). Free hemoglobin was not detected in the blood samples after adding the formulations. This result suggests that the formulations are potentially safe for injectable use.

[Insert Figure 7]

The biodistribution of nanoparticles was monitored in mice using the fluorescent labeled nanoparticles ($NS^F_{\beta-CD}$). The $NS_{\beta-CD}$ was also tested for comparison. The formulations were administered to the animals and the fluorescence was followed after 15 min, 1 h, and 24 h with IVIS Lumina System live animal biophotonic imaging system (Xenogen Corp, CA, USA). The main organs affected by NPC were isolated after administration of nanoparticles (figure 8). The images obtained after treatment with $NS_{\beta-CD}$ showed no significant fluorescence in any analyzed organ, as expected. On the other hand, the images obtained after treatment with $NS^F_{\beta-CD}$ demonstrated high

fluorescence intensity in the brain and low fluorescence intensity in the kidney, spleen, and liver just after 15 min of injection. The fluorescence intensity decayed in all organs after 1 h or 24 h of treatment.

[Insert Figure 8]

4. Discussion

NPC is a lysosomal disease currently conceived as a lipid trafficking disorder. Impaired egress of cholesterol from the LE/LY compartment is a specific key element of the pathogenesis [28]. The reduction of lipid storage in brain tissues can be linked with neurological improvements, but it is also particularly challenging because the drug must cross the BBB. Recently, some studies have proposed β-CD as a potential treatment to the NPC disease. This macromolecule can contribute to decreasing the cholesterol accumulation in the LE/LY of animal models and in cells of NPC patients. However, the cytotoxicity of β-CD cannot be ignored, because of its ability to release lipid compounds from cell membranes [29]. In addition, free β-CD is not capable to cross the BBB [7, 30]. Brain targeting could circumvent the cytotoxicity drawback of β-CD and also improve the neurological response to the treatment.

In this study, an inclusion complex of β-CD and P80 was incorporated into monoolein-based nanoparticles aiming brain targeting. The DLS and SAXS results suggest that the inclusion complex acted as a supramolecular stabilizer decorating the nanoparticle surface. It seems that we used an excess of the inclusion complex to obtain the formulations, because flat plate micrometric structures coexisting with the nanoparticles were observed by cryo-TEM. These structures gave a pearlescent appearance to the formulations.

We exposed a culture of healthy human dermal fibroblasts to free β-CD, P80@2β-CD, and to the nanoparticle formulation loaded ($NS^F_{β\text{-}CD}$) or unloaded ($NS_{β\text{-}CD}$) with coumarin-6, during 48 h to evaluate the cytotoxicity of the samples using the NRU. Neutral red is a weak cationic dye that can cross the plasma membrane by diffusion and tends to accumulate in lysosomes within the cell. If the cell membrane is

altered, the uptake of neutral red is decreased and can leak out, allowing for discernment between live and dead cells [31]. Results showed negligible cytotoxic effects for all systems in the three tested concentrations of β-CD (11.25, 22.5, and 45 µM) with viability values close to 100% (Figure 4a). The protocol was repeated in NPC patient-derived dermal fibroblasts using the highest β-CD concentration (45 µM) for all samples. The results corroborated with those obtained in healthy fibroblasts, showing that the tested systems were non-toxic to NPC patient-derived dermal fibroblasts.

A cell uptake study was performed to examine the targeting ability of the nanoparticle in the cell culture of NPC patient-derived dermal fibroblasts. The dyes coumarin-6 and LysoTracker were used to label nanoparticles and acidic organelles, respectively, as shown in Figure 5. After 1 h of treatment with the nanoparticles, a high level of co-localization (yellow) of $NS^F_{\beta-CD}$ (green) and lysosomes (red) was exhibited, indicating that the $NS^F_{\beta-CD}$ was confined in acidic compartments. This retention level remained even after 3 h of treatment with high co-localization. Also, during 48 h of incubation with NPC patient-derived dermal fibroblasts, the $NS_{\beta-CD}$ was able to reduce and promote the release of accumulated cholesterol from LE/LY demonstrating *in vitro* efficacy, without damaging cell membranes. This is a consequence of the targeted internalization of β-CD into the lysosomes mediated by the nanoparticles.

A pre-requisite for a parenteral delivery system is low or negligible hemolytic activity. Although the structural features of some non-lamellar lipid dispersions are rather well investigated, good understanding of interaction aspects between such delivery vehicles and blood cells or model membranes is still lacking. Nevertheless, a previous study of our group with monoolein-based nanoparticles showed a negligible hemolytic activity, with values similar to those of the negative control [10]. On the other hand, another study developed by Barauskas *et al.*[32] showed that monoolein-based

cubosomes can cause a hemolysis degree incompatible with parenteral administration. According to the authors, the hemolytic activity was strongly dependent on both the lipid nature and the overall composition. In the present study, the nanoparticle with the highest β-CD concentration was chosen for the hemolytic activity test. For comparison, pure P80@2β-CD and free β-CD were also tested. The hemolytic values caused by all tested systems were similar to those caused by the DMEM media, which means that the nanoparticles were potentially safe for parenteral administration. The result was opposite to that observed by Barauskas and coworkers, even though both systems were made of monoolein. This divergence is probably because we obtained a disordered bicontinuous structure instead of a liquid crystalline phase. The absence of hemolytic activity presented by $NS_{\beta\text{-CD}}$ was corroborated with the non-toxic effects observed in cultured fibroblasts.

The most severe consequence of NPC is neurodegeneration, which contributes to the reduced weight gain, cognitive decline, and premature death [5]. Cholesterol metabolism in the brain is compartmentalized from that in the periphery by the BBB. Essentially all cholesterol in the brain is synthesized within this organ rather than being delivered from plasma lipoproteins. The most striking consequence of NPC1 deficiency in the brains of mice and humans is a profound loss of Purkinje neurons in the cerebellum. This is not repaired by free β-CD because this macromolecule is not capable to cross the BBB [7, 30]. Despite this, the results obtained in the present study demonstrated that the $NS^{F}_{\beta\text{-CD}}$ formulation reached the brain tissue of the animal more intensely than the other tissues investigated, even just after 15 min of injection. In this way, the ability of P80 to target monoolein-based nanoparticles to the brain [10] was not affected by the formation of an inclusion complex with β-CD. Therefore, the

nanoparticles loaded with β-CD may be a technological advantage in the treatment of the NPC disease with brain impairment.

The $NS^F_{\beta-CD}$ formulation reached the liver after 15 min, remaining there at least for 1 h. This is an important result for NPC treatment because severe liver damage is prevalent in many NPC patients [5]. The $NS^F_{\beta-CD}$ also reached the kidney and spleen of animals, probably due to processes related to detoxification of the nanoparticles from the body. The localization of nanoparticles in these organs (even less intensely than in brain tissue) is an important finding, as these organs are also affected by cholesterol accumulation [28].

Concluding, the results showed that the formulation with β-CD was able to be retained inside the lysosomes for at least 3 h and demonstrated the capacity to decrease accumulated cholesterol in NPC patient-derived dermal fibroblasts. In addition, the biodistribution profile of the formulation with β-CD was favorable to treat NPC mainly affected organs. It is important to emphasize the infiltration of the nanoparticles in the brain tissue, which is poorly reached by free β-CD according to the literature. Also, the use of nanoparticles to deliver β-CD would probably decrease the toxic effects caused by this macromolecule. Although the therapeutic effect of the formulation with β-CD was not evaluated in different organs, the results of biodistribution in the animal model combined with the cholesterol reduction observed in NPC patient-derived dermal fibroblasts reveal a great potential of $NS_{\beta-CD}$ for the treatment of neurological impairments caused by NPC.

Conflict of interest

The authors declare that they have no conflict of interest.

Ethical statement

The *in vitro* assays were conducted in compliance with the Council for International Organizations of Medical Sciences/World Health Organization (CIOMS/WHO 1993) and the Resolution number 466/2012 of the Brazilian Health Council Regulating Guidelines and Standards of Research that Involves Human Beings ("Conselho Nacional de Saúde - Diretrizes e Normas Regulamentadoras de Pesquisas Envolvendo

Seres Humanos"). Written informed consent was obtained from all participants. The study was approved (number 15-0468) by the Research Ethics Committee of the *Hospital de Clínicas de Porto Alegre* (CEP/HCPA).

The *in vivo* assay with animals was performed in accordance with the guidelines of the Guide for the Care and Use of Laboratory Animals and the recommendations of the Animal Ethics Committee of the *Instituto Oswaldo Cruz* (number L008/2018), which also approved this research. All efforts were made to minimize the number of animals and their suffering.

4. References

1.   Wassif, C. A.; Cross, J. L.; Iben, J.; Sanchez-Pulido, L.; Cougnoux, A.; Platt, F. M.; Ory, D. S.; Ponting, C. P.; Bailey-Wilson, J. E.; Biesecker, L. G., High incidence of unrecognized visceral/neurological late-onset Niemann-Pick disease, type C1, predicted by analysis of massively parallel sequencing data sets. *Genetics in Medicine* **2016,** 18, (1), 41.

2.   Vanier, M. T., Niemann-Pick disease type C. *Orphanet journal of rare diseases* **2010,** 5, (1), 16.

3.   Abi-Mosleh, L.; Infante, R. E.; Radhakrishnan, A.; Goldstein, J. L.; Brown, M. S., Cyclodextrin overcomes deficient lysosome-to-endoplasmic reticulum transport of cholesterol in Niemann-Pick type C cells. *Proceedings of the National Academy of Sciences* **2009,** 106, (46), 19316-19321.

4.   Davidson, C. D.; Ali, N. F.; Micsenyi, M. C.; Stephney, G.; Renault, S.; Dobrenis, K.; Ory, D. S.; Vanier, M. T.; Walkley, S. U., Chronic cyclodextrin treatment of murine Niemann-Pick C disease ameliorates neuronal cholesterol and glycosphingolipid storage and disease progression. *PLoS ONE* **2009,** 4, (9), e6951.

5.   Vance, J. E.; Karten, B., Niemann-Pick C disease and mobilization of lysosomal cholesterol by cyclodextrin. *Journal of lipid research* **2014**, jlr. R047837.

6.   Ward, S.; O'donnell, P.; Fernandez, S.; Vite, C. H., 2-hydroxypropyl-β-cyclodextrin raises hearing threshold in normal cats and in cats with Niemann-Pick type C disease. *Pediatric research* **2010,** 68, (1), 52.

7.   Pontikis, C. C.; Davidson, C. D.; Walkley, S. U.; Platt, F. M.; Begley, D. J., Cyclodextrin alleviates neuronal storage of cholesterol in Niemann-Pick C disease without evidence of detectable blood–brain barrier permeability. *Journal of inherited metabolic disease* **2013,** 36, (3), 491-498.

8.   Camargo, F.; Erickson, R. P.; Garver, W. S.; Hossain, G. S.; Carbone, P. N.; Heidenreich, R. A.; Blanchard, J., Cyclodextrins in the treatment of a mouse model of Niemann-Pick C disease. *Life sciences* **2001,** 70, (2), 131-142.

9.   Hovakimyan, M.; Maass, F.; Petersen, J.; Holzmann, C.; Witt, M.; Lukas, J.; Frech, M.; Hübner, R.; Rolfs, A.; Wree, A., Combined therapy with cyclodextrin/allopregnanolone and miglustat improves motor but not cognitive functions in Niemann–Pick Type C1 mice. *Neuroscience* **2013,** 252, 201-211.

10.   Donida, B.; Tauffner, B.; Raabe, M.; Immich, M. F.; de Farias, M. A.; de Sá Coutinho, D.; Machado, A. Z.; Kessler, R. G.; Portugal, R. V.; Bernardi, A., Monoolein-based nanoparticles for drug delivery to the central nervous system: A platform for lysosomal storage disorder treatment. *European Journal of Pharmaceutics and Biopharmaceutics* **2018,** 133, 96-103.

11.   Lutton, E., Phase behavior of aqueous systems of monoglycerides. *Journal of the American Oil Chemists Society* **1965,** 42, (12), 1068-1070.

12.   Hyde, S.; Andersson, S., A cubic structure consisting of a lipid bilayer forming an infinite periodic minimum surface of the gyroid type in the glycerolmonooleat-water system. *Zeitschrift für Kristallographie-Crystalline Materials* **1984,** 168, (1-4), 213-220.

13.   Valldeperas, M.; Wiśniewska, M.; Ram-On, M.; Kesselman, E.; Danino, D.; Nylander, T.; Barauskas, J., Sponge phases and nanoparticle dispersions in aqueous mixtures of mono-and diglycerides. *Langmuir* **2016,** 32, (34), 8650-8659.

14.   Kreuter, J., Nanoparticulate systems for brain delivery of drugs. *Advanced drug delivery reviews* **2001,** 47, (1), 65-81.

15.   Kreuter, J., Mechanism of polymeric nanoparticle-based drug transport across the blood-brain barrier (BBB). *Journal of microencapsulation* **2013,** 30, (1), 49-54.

16.   Kreuter, J.; Ramge, P.; Petrov, V.; Hamm, S.; Gelperina, S. E.; Engelhardt, B.; Alyautdin, R.; Von Briesen, H.; Begley, D. J., Direct evidence that polysorbate-80-coated poly (butylcyanoacrylate) nanoparticles deliver drugs to the CNS via specific mechanisms requiring prior binding of drug to the nanoparticles. *Pharmaceutical research* **2003,** 20, (3), 409-416.

17.   Kreuter, J.; Shamenkov, D.; Petrov, V.; Ramge, P.; Cychutek, K.; Koch-Brandt, C.; Alyautdin, R., Apolipoprotein-mediated transport of nanoparticle-bound drugs across the blood-brain barrier. *Journal of drug targeting* **2002,** 10, (4), 317-325.

18.   Wagner, S.; Zensi, A.; Wien, S. L.; Tschickardt, S. E.; Maier, W.; Vogel, T.; Worek, F.; Pietrzik, C. U.; Kreuter, J.; Von Briesen, H., Uptake mechanism of ApoE-modified nanoparticles on brain capillary endothelial cells as a blood-brain barrier model. *PLoS ONE* **2012,** 7, (3), e32568.

19.   Frozza, R. L.; Bernardi, A.; Paese, K.; Hoppe, J. B.; Silva, T. d.; Battastini, A. M.; Pohlmann, A. R.; Guterres, S. S.; Salbego, C., Characterization of trans-resveratrol-

loaded lipid-core nanocapsules and tissue distribution studies in rats. *Journal of biomedical nanotechnology* **2010,** 6, (6), 694-703.

20.   Coelho, J. C.; Giugliani, R., Fibroblasts of skin fragments as a tool for the investigation of genetic diseases: technical recommendations. *Genetics and Molecular Biology* **2000,** 23, (2), 269-271.

21.   Vanier, M. T.; Latour, P., Laboratory diagnosis of Niemann–Pick disease type C: The filipin staining test. In *Methods in cell biology*, Elsevier: 2015; Vol. 126, pp 357-375.

22.   Zhou, C.; Cheng, X.; Zhao, Q.; Yan, Y.; Wang, J.; Huang, J., Self-assembly of nonionic surfactant tween 20@ 2β-CD inclusion complexes in dilute solution. *Langmuir* **2013,** 29, (43), 13175-13182.

23.   Altube, M. J.; Selzer, S. M.; de Farias, M. A.; Portugal, R. V.; Morilla, M. J.; Romero, E. L., Surviving nebulization-induced stress: dexamethasone in pH-sensitive archaeosomes. *Nanomedicine (Lond)* **2016,** 11, (16), 2103-17.

24.   Jiang, X.; Sidhu, R.; Porter, F. D.; Yanjanin, N. M.; Speak, A. O.; te Vruchte, D. T.; Platt, F. M.; Fujiwara, H.; Scherrer, D. E.; Zhang, J., A sensitive and specific LC-MS/MS method for rapid diagnosis of Niemann-Pick C1 disease from human plasma. *Journal of lipid research* **2011**, jlr. D015735.

25.   Ribas, G.; Souza, H.; de Mari, J.; Deon, M.; Mescka, C.; Saraiva-Pereira, M.; Kessler, R.; Trapp, F.; Michelin, K.; Burin, M., Selective screening of Niemann–Pick type C Brazilian patients by cholestane-3β, 5α, 6β-triol and chitotriosidase

measurements followed by filipin staining and NPC1/NPC2 gene analysis. *Clinica Chimica Acta* **2016,** 459, 57-62.

26. Yu, D.; Swaroop, M.; Wang, M.; Baxa, U.; Yang, R.; Yan, Y.; Coksaygan, T.; DeTolla, L.; Marugan, J. J.; Austin, C. P., Niemann–Pick Disease Type C: Induced Pluripotent Stem Cell–Derived Neuronal Cells for Modeling Neural Disease and Evaluating Drug Efficacy. *Journal of biomolecular screening* **2014,** 19, (8), 1164-1173.

27. Teubner, M.; Strey, R., Origin of the scattering peak in microemulsions. *The Journal of Chemical Physics* **1987,** 87, (5), 3195-3200.

28. Vanier, M. T., Complex lipid trafficking in Niemann-Pick disease type C. *Journal of inherited metabolic disease* **2015,** 38, (1), 187-199.

29. Monnaert, V.; Tilloy, S.; Bricout, H.; Fenart, L.; Cecchelli, R.; Monflier, E., Behavior of α-, β-, and γ-cyclodextrins and their derivatives on an in vitro model of blood-brain barrier. *Journal of Pharmacology and Experimental Therapeutics* **2004,** 310, (2), 745-751.

30. Ramirez, C. M.; Liu, B.; Taylor, A. M.; Repa, J. J.; Burns, D. K.; Weinberg, A. G.; Turley, S. D.; Dietschy, J. M., Weekly cyclodextrin administration normalizes cholesterol metabolism in nearly every organ of the Niemann-Pick type C1 mouse and markedly prolongs life. *Pediatric research* **2010,** 68, (4), 309.

31. Repetto, G.; Del Peso, A.; Zurita, J. L., Neutral red uptake assay for the estimation of cell viability/cytotoxicity. *Nature protocols* **2008,** 3, (7), 1125.

32.   Barauskas, J.; Cervin, C.; Jankunec, M.; Spandyreva, M.; Ribokaite, K.; Tiberg, F.; Johnsson, M., Interactions of lipid-based liquid crystalline nanoparticles with model and cell membranes. *Int J Pharm* **2010,** 391, (1-2), 284-91.

FIGURE CAPTIONS

Figure 1. Particle size distribution by intensity for (a) $NS_{\beta\text{-}CD}$, and (b) $NS^F_{\beta\text{-}CD}$ (DLS measurements carried out at a detection angle of 173°, 25 °C).

Figure 2. Cryo-TEM image of the $NS_{\beta\text{-}CD}$ formulation showing disordered bicontinuous structures (white arrow), vesicles (dashed white arrow), and flat plate structures (black arrow).

Figure 3. SAXS curve of the $NS_{\beta\text{-}CD}$ formulation. The data (black dots) were fitted to the Teubner-Strey model (red line).

Figure 4. (a) Cell viability of healthy human dermal fibroblasts incubated with β-CD, P80@2β-CD, $NS_{\beta\text{-}CD}$, and $NS^F_{\beta\text{-}CD}$. The values 11.25, 22.5, and 45 μM refer to the concentration of β-CD in the test; (b) cell viability of NPC patient-derived dermal fibroblasts incubated with β-CD, P80@2β-CD, $NS_{\beta\text{-}CD}$, and $NS^F_{\beta\text{-}CD}$ (the final concentration of β-CD was 45 μM). The experiments were made in triplicate. Data = mean ± SEM (one-way ANOVA, followed by Tukey's multiple range test).

Figure 5. Confocal microscopy images showing the internalization of $NS^F_{\beta\text{-}CD}$ by NPC patient-derived dermal fibroblasts after 1 and 3 h of incubation. Column 1: Coumarin-6 channels showing the green fluorescence from coumarin-6 loaded nanoparticles/complex; Column 2: LysoTracker channels showing the red fluorescence from LysoTracker labeled acidic organelles; and Column 3: Merged channels coumarin-6 and LysoTracker.

Figure 6. (a) Filipin staining of NPC patient-derived dermal fibroblasts. (1) NPC fibroblasts without treatment (WT); (2) NPC fibroblasts treated with 45µM of free β-CD; (3)NPC fibroblasts treated with $NS_{\beta-CD}$ (45µM of β-CD); (4) NPC fibroblasts treated with P80@2β-CD (45µM of β-CD); (5) NPC fibroblasts treated with $NS_{\beta-CD}$ (after passed through 0.45 µm filter); (6) NPC fibroblasts treated with $NS_{\beta-CD}$ (after passed through 0.22 µm filter). (b) Fluorescence quantification of all formulations by ImageJ. Data = mean ± SEM. **$p<0.001$, ***$p<0.0001$ compared to NPC patient-derived dermal fibroblasts without treatment (one-way ANOVA, followed by Tukey's multiple range test).

Figure 7. Hemoglobin release from human blood due to the interaction of β-CD, P80@2β-CD, $NS_{\beta-CD}$, and $NS^F_{\beta-CD}$ with erythrocytes. The data were normalized to the hemoglobin release level of the Triton X-100 positive control. The experiments were made in triplicate. Data = mean ± SEM. ***$p<0.0001$ compared to positive control (one-way ANOVA, followed by Tukey's multiple range test).

Figure 8. Fluorescence in mice organs after intraperitoneal injection of nanoparticles. A/J mice were treated with 300 µL of (A) $NS_{\beta-CD}$ (*n*=3) or (B) $NS^F_{\beta-CD}$ (*n*=6). *Ex vivo* fluorescence images of the brain, lung, kidney, spleen, and liver, respectively, after (a) 15 min, (b) 1 h and (c) 24 h of treatment with nanoparticles.

FIGURES

Figure 1

Fgure 2

Figure 3

Figre 4

Figure 5

1 hour of treatment

coumarin-6   lysotracker   merge

3 hours of treatment

coumarin-6   lysotracker   merge
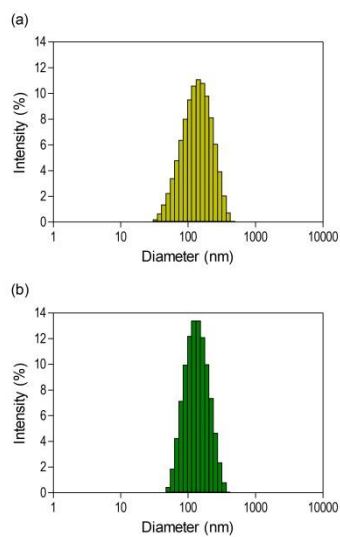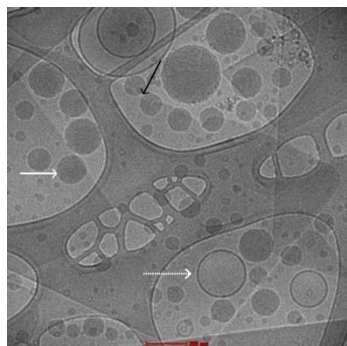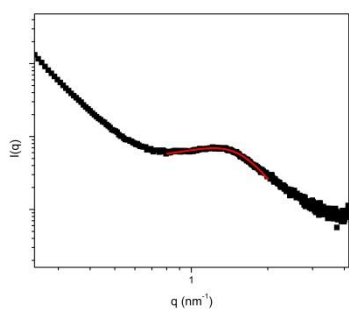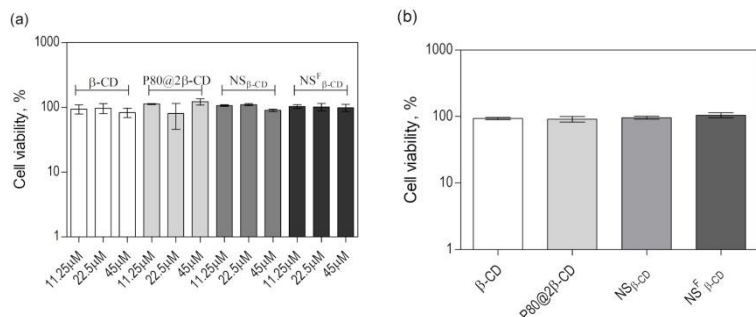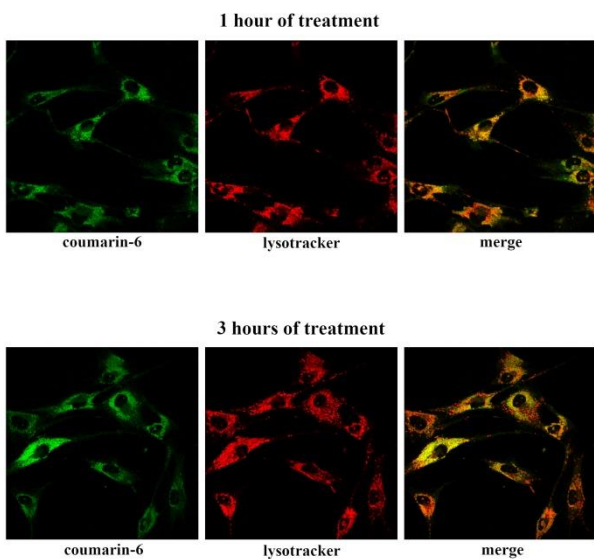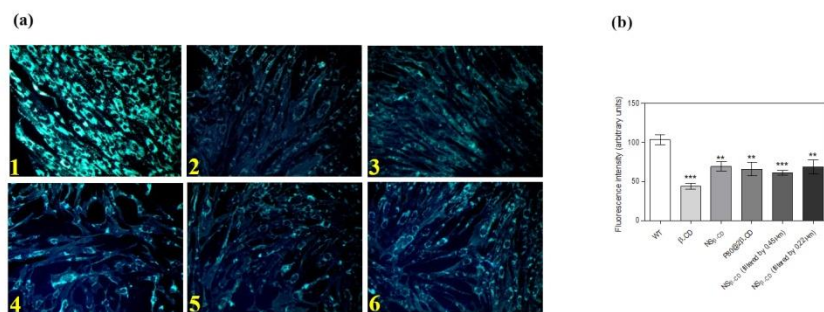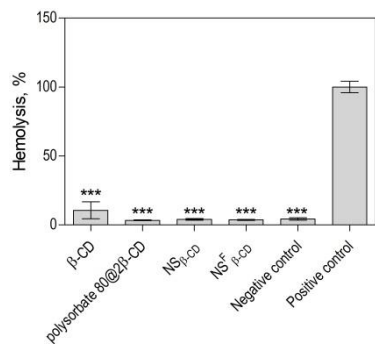
Figure 6

Figure 7

Figure 8
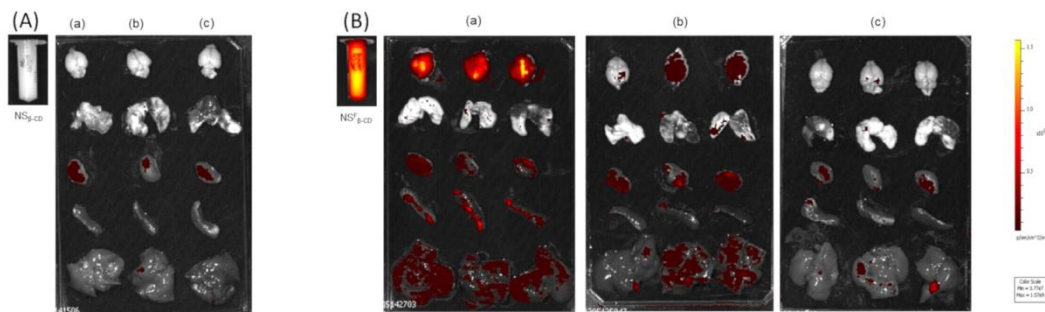
GRAPHICAL ABSTRACT
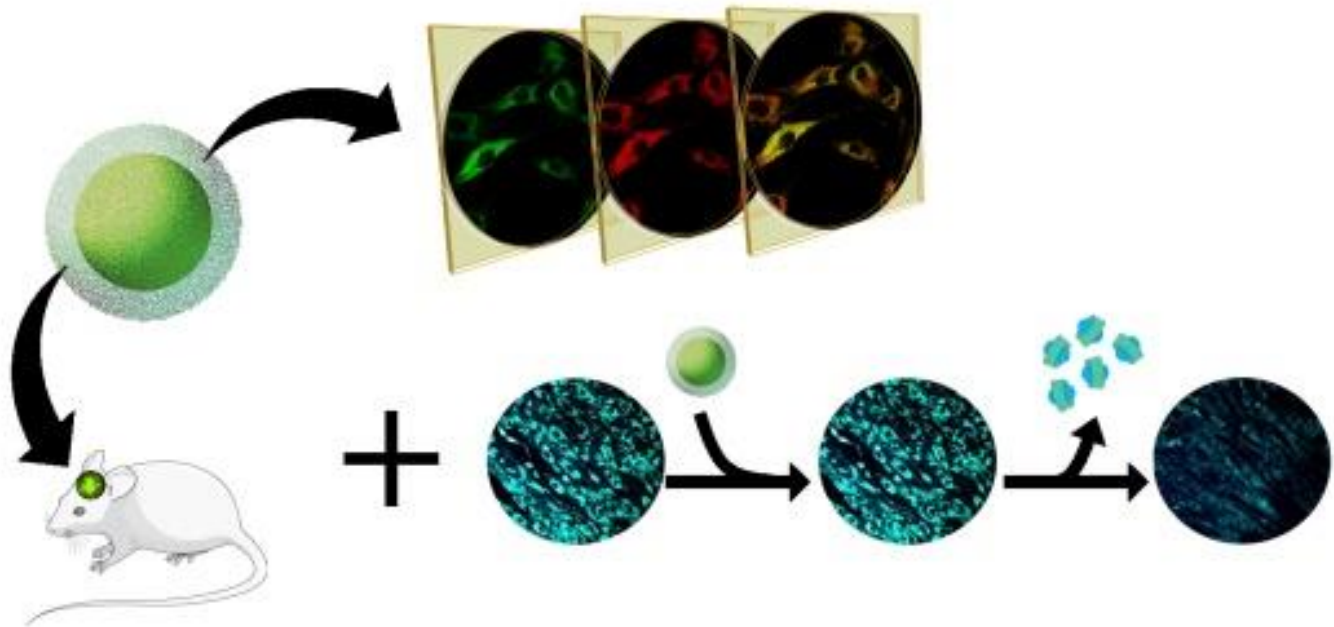
Monoolein-based nanoparticles loaded with an inclusion complex between polysorbate 80 and β-cyclodextrin were developed and presented high lysosomal uptake and non-cytotoxicity in Niemann-Pick C patients-derived dermal fibroblasts. The nanoparticles depleted the accumulated cholesterol in these patient´s cells and showed a desired biodistribution in mice, being more intensely located in the brain tissue. The nanoparticles present a great potential for the treatment of neurological impairments caused by the Niemann-Pick C disease.

3.3 Artigo 3: Preliminary toxicological evaluation of nanoparticles developed to delivery drugs in central nervous system.

Manuscrito a ser submetido.

Preliminary toxicological evaluation of nanoparticles developed to delivery drugs in central nervous system

Bruna Donida[a*], Marco Raabe[b], Verônica Bidinotto Brito[b,c], Desirèe Padilha Marchetti[a], Andryele Zaffari Machado[d], Rejane Gus Kessler[d], Dinara J. Moura[b], Fernanda Poletto[e], Carmen Regla Vargas[a,d*]

[a] Programa de Pós-Graduação em Ciências Biológicas, Bioquímica, Universidade Federal do Rio Grande do Sul, Zip Code 90035-003, Porto Alegre, RS, Brazil.

[b] Laboratório de Genética Toxicológica, Universidade Federal de Ciências da Saúde de Porto Alegre, Zip Code 90050170, Porto Alegre, RS, Brazil.

[c] Departamento de Fisioterapia, Faculdades Integradas de Taquara (FACCAT), Zip Code 95612115, Taquara, RS, Brazil.

[d] Serviço de Genética Médica, Hospital de Clínicas de Porto Alegre, Zip Code 90035-003, Porto Alegre, RS, Brazil.

[e] Programa de Pós Graduação em Química, Universidade Federal do Rio Grande do Sul, Zip Code 91501-970, Porto Alegre, Brazil.

* to whom correspondence should be addressed:

Msc. Bruna Donida

E-mail: donida.bruna@gmail.com, Phone: + 55 51 33598011.

Prof. Carmen Regla Vargas

E-mail: crvargas@hcpa.edu.br, Phone: +55 51 33598011.

ABSTRACT

Understand the properties of nanoparticles and their effect on body is crucial when these systems were developed for biomedical application. Our group developed monoolein-based nanoparticles (NS) with a disordered inner structure able to reach the brain tissue. These nanoparticles were firstly built as a platform to treat lysosomal storage disorders (LSDs) with brain impairment. Using NS as a platform, we incorporate β-cyclodextrin in nanoparticles ($NS_{β-CD}$) and tested them as a therapy for Niemann-Pick type C (NPC) disease, a LSD characterized by cholesterol accumulation in lysosomes. Considering the promising results obtained with nanoparticles, we aimed to evaluate the cytotoxicity potential of NS and $NS_{β-CD}$ in dermal fibroblasts derived from NPC patients. After cell incubation with nanoparticles for 48 hours the cytotoxicity parameters were analyzed. The neutral red uptake assay demonstrated that nanoparticles did not cause decrease in cell viability. Also, the nanoparticles did not cause impairment in oxidative/nitrative stress evaluated in NPC patient-derived dermal fibroblast and they did not induce genotoxicity in healthy fibroblasts. These results have important implications for *in vivo* use of monoolein-based nanoparticles with a disordered inner structure.

Keywords: Nanoparticle, Lysosomal storage disorder, Niemann-Pick C, β-cyclodextrin, toxicological evaluation.

1. Introduction

Since the application of nanotechnology has been increasingly studied in the biomedical field, human contact with nanoparticles becomes inevitable, which makes the study of nanotoxicology increasingly important (Lewinski *et al.*, 2008). Exposure to nanoparticles for medical purposes involves intentional contact or administration; therefore, understanding the properties of nanoparticles and their effect on the body is crucial before clinical use can occur (Lewinski *et al.*, 2008). In this context, nanoparticle toxicity refers to the ability of the particles to adversely affect the normal physiology as well as to directly interrupt the normal structure of organs and tissues of humans and animals. One important feature of nanotoxicology is that materials which are not harmful in their bulk form may be toxic on the nanoscale (Chatterjee *et al.*, 2017).

Considering nanoparticles to biomedical application, a thorough scientific validation is necessary for the risk evaluation of nanomaterials, and screening assays are needed to assess their chemical and physical properties. There are several physiochemical parameters to determine toxicity such as particle size, shape, surface charge and chemistry, composition, degradability, biocompatibility, and subsequent nanoparticle stability (Chatterjee *et al.*, 2017). Further particle-related factors, the administered dose, route of administration, and extent of tissue distribution seem to be important parameters in nanocytotoxicity. A probable nanotoxicity mechanism has been associated to oxidative stress and proinflammatory gene activation (Arora *et al.*, 2008; Hsin *et al.*, 2008).

We developed monoolein-based nanoparticles as a smart platform to delivery drugs/enzymes in the central nervous system (CNS) and treat lysosomal storage

disorders (LSD) with brain impairment (Donida *et al.*, 2018). The lipid-based nanoparticles with inner disordered (NS) were composed by monoolein (technical grade) and polysorbate 80, which are biodegradable and biocompatible products (Lutton, 1965; Alyaudtin *et al.*, 2001). After, using NS as model, we built a nanoparticle containing β-cyclodextrin ($NS_{\beta-CD}$), aiming treat Niemann-Pick C (NPC) disease, a lysosomal storage disorder (LSD) characterized by cholesterol accumulation inside the lysosomes (Donida et al., 2019). The both lipid-based nanoparticles with inner disordered bicontinuous structure were extensively characterized by dynamic light scattering (DLS), small angle X-ray (SAXS) and by cryogenic transmission electron microscopy (cryo-TEM). Also, they were uptake by lysosomes *in vitro*, reached CNS in animal model, in addition the $NS_{\beta-CD}$ was able to decrease accumulated cholesterol in NPC fibroblasts. Taking into account that the nanoparticles were developed for biological application and considering the promising previous results obtained, we intend to study the cytotoxicity related to NS and $NS_{\beta-CD}$ in NPC patient-derived dermal fibroblast; as well as genotoxicity in dermal fibroblasts derived from healthy subjects.

2. Materials and Methods

2.1 Materials

Monoolein technical grade (39.9 % of 1-oleoyl-rac-glycerol mixed with 22.5% of diglycerides and 34.7% of triglycerides; batch number – BCBQ8354V), β-cyclodextrin, polysorbate 80, Filipin III from *Streptomyces filipinensis* and Neutral Red dye were purchased from Sigma-Aldrich (St. Louis, USA). Dulbecco's Modified Eagle Medium (DMEM), fetal bovine serum (FBS), trypsin–EDTA, L-glutamine, penicillin/streptomycin, fungizone and phosphate buffered saline (PBS) were purchased from Thermo Fisher Scientific (Massachusetts, EUA). Ultrapure water (Milli-Q, Millipore Corp., Bedford, MA) was used to prepare all the formulations.

2.2 Nanoparticle preparation

The load-off NS and the NS loading β-CD (NS$_{β-CD}$ – 7.5 mM of β-CD) were prepared and characterized as described by Donida *et al.* (2018) and Donida et al. (2019), respectively.

2.3 Samples and cell culture

Skin biopsy (Coelho and Giugliani, 2000) was obtained from NPC patients (*n*=3) at the moment of diagnosis and from healthy subjects (*n*=3). The clinical features presented by NPC patients include dystonia, dysphagia, seizures, vertical supranuclear palsy and psychiatric disorders. Diagnosis was confirmed by the Filipin test, performed on cultured fibroblasts (Vanier and Latour, 2015).

The skin biopsy fragment was placed in polyethylene sterile vials for culture cells. The target cells used in this experiment were human dermal fibroblasts. The fibroblasts were maintained at 37 °C under 5% CO_2 in DMEM and supplement with

10% FBS (fetal bovine serum), antibiotics (200 µg mL^{-1} penicillin G, 200 µg mL^{-1} streptomycin) and fungizone (2 µg mL^{-1}). After approximately 4 weeks, when cell confluence was achieved, the fibroblasts were harvested with trypsin and seeded in complete media 96-well culture plates (1.6×10^4 cells/mL) or 24-well culture plates (1 x 10^5 cel/mL) and grown for one day prior to treatment with the nanoparticles. The final concentration, related to monoolein, of NS and NS$_{\beta\text{-CD}}$ used in all tests was 117.9 µg mL^{-1}. The final β-CD concentration of NS$_{\beta\text{-CD}}$ was 45 µM, in all tests. The cells were treated for 48 h under standard conditions. To oxidative/nitrative stress analyses cells and supernatants were harvested and frozen at −80 ℃, which were performed in less than 2 weeks (Coelho and Giugliani, 2000). The cytotoxicity and genotoxic assays were performed shortly after 48 hours treatment.

The work was conducted in compliance with the Council for International Organizations of Medical Sciences/World Health Organization (CIOMS/WHO 1993) and the Resolution number 466/2012 of the Brazilian Health Council Regulating Guidelines and Standards of Research that Involves Human Beings. Written informed consent was obtained from all participants. The study was approved (number 15-0468) by the Research Ethics Committee of the *Hospital de Clínicas de Porto Alegre* (CEP/HCPA).

2.4 Neutral red uptake assay (NRU)

The cytotoxicity was evaluated using NRU, in accordance to protocol previously described by Repetto *et al.* (2008). Briefly, after treatment cells were washed with PBS and incubated with 250 µL of neutral red solution (25 µg mL^{-1}) at 37°C for 3 h. Then, cells were washed and incubated for 30 minutes, protected from light, with adsorbent solution (mixture of acetic acid, ethanol and water in ration of 1:50:49) and absorbance

was measured at 540 nm in spectrophotometer microplate reader. The absorbance of cells without treatment (WT) was set as 100% viability, and the values for treated cells were calculated as a percentage of the WT.

2.5 Superoxide Dismutase (SOD) activity

The SOD assay was performed in the cell lysate. The activity of SOD was calculated by the method described by Misra and Fridovich (1972), which estimates the dismutation of the superoxide radical through the inhibition of adrenaline oxidation at 480 nm. Inhibition of adrenaline oxidation occurs by the presence of SOD enzyme in the sample, and the activity was indirectly evaluated by kinetic mode in the microplate reader SpectraMax® M2^{e} (Molecular Devices, MDS Analytical Technologies, Sunnyvale, California). A unit (U) of SOD is defined as the amount of enzyme required to inhibit 50 % of adrenaline oxidation. The SOD activity is expressed as U SOD/mg protein.

2.6 Catalase enzyme activity (CAT)

The CAT activity was determined in cell lysate through the method previously described by Aebi (1984), which is based on the decay of absorbance at 240 nm due to consumption of H_2O_2 by the enzyme present in the sample. The activity was evaluated by kinetic mode in the microplate reader SpectraMax® M2e (Molecular Devices, MDS Analytical Technologies, Sunnyvale, California). One unit (U) of CAT is defined as 1 µmol of H_2O_2 consumed per minute expressed as U CAT/mg protein.

2.7 Dichlorofluorescein diacetate oxidation (H₂DCF-DA) measurement

The generation of Reactive Oxygen Species (ROS) can be estimated by the method described by LeBel *et al.* (1992) in cell lysate. H_2DCF-DA in presence of ROS leads to the production of dichlorofluorescein (DCF), a fluorescent product that can be quantified by fluorimetry. Fluorescence intensity was evaluated in SpectraMax® M2e Microplate Reader (Molecular Devices, MDS Analytical Technologies, Sunnyvale, California) using excitation and emission wavelengths at 480 and 535 nm, respectively. A calibration curve was performed with standard DCF (10 μM) and the ROS level of was expressed as nmol DCF/mg protein.

2.8 Isoprostanes measurement

Isoprostanes, products of arachidonic acid metabolism and biomarkers of lipid peroxidation, were measured by a competitive enzyme-linked immunoassay (ELISA) (Cayman Chemical, Ann Arbor, MI, USA) in cell supernatants, according to the manufacturer's instructions. This assay is based on competition with an 8-isoprostane/acetylcholinesterase conjugate for a limited number of 8-isoprostane-specific rabbit antiserum binding sites. The absorbance (λ = 415 nm) determined spectrophotometrically, was inversely related to the amount of free 8-isoprostane in samples. Results were expressed as pg of isoprostanes / mL.

2.9 Nitrate and Nitrite assay

The quantification of NO equivalents in cell supernatants was performed using the nitrate/nitrite colorimetric assay kit (Cayman Chemical, Ann Arbor, MI) according to the manufacturer's instructions. The NO produced in biological systems rapidly degrades to its stable products NO^{-3} (nitrate) and NO^{-2} (nitrite). The first step is the conversion of NO^{-3} to NO^{-2} using nitrate reductase. Subsequently, the formed NO^{-2} is

quantified using the Griess reaction, which results in a colored product, read at 540 nm. Results were expressed as µM of $NO^{-3} + NO^{-2}$.

2.10 Protein determination

The protein concentration in fibroblasts extracts was determined according to the method described by Bradford (1976), using bovine serum albumin as standard.

2.11 Comet assay

The alkaline comet assay was performed as reported by Singh et al. (1988). Cells were mixed with low melting point agarose solution and spread on agarose-precoated microscope slides. For each treatment, three slides were made. Slides were incubated in ice-cold lysis solution (2.5 mol/L NaCl, 10 mmol/L Tris, 100 mmol/L EDTA, 1% Triton X-100 and 10% DMSO, pH 10.0) at 4 °C for 24 h to remove cell membranes. Then, slides were placed in a horizontal electrophoresis unit and incubated with fresh alkaline buffer solution (300 mmol/L NaOH, 1 mmol/L EDTA, pH 13.0) at 4 °C for 20 min to allow DNA unwinding and the expression of alkali-labile sites. Electrophoresis was conducted for 20 min at 25 V (94 V/cm). All these steps were performed under yellow light or in the dark to prevent additional DNA damage. Slides were stained using silver nitrate. One hundred cells from each treatment were selected and analyzed for DNA migration and the average of the three slides from each treatment group was used to determine the damage index. The damage index is an arbitrary score calculated for cells in different damage classes, which is scored visually according to the tail length of the "comet" into five classes: Class 0, undamaged, without a tail; Class 1, with a tail shorter than the diameter of the head nucleus; Class 2, with a tail length one- to twofold greater than the diameter of the head; Class 3, with a tail longer than

twofold the diameter of the head; and Class 4, comets with no heads. The damage index ranges from 0 (no tail) to 400 (maximum migration).

2.12 Statistical analysis

The results obtained were expressed as mean ± SEM (standard error of the mean). Comparisons between the mean values were made through one-way analysis of variance ANOVA followed by Tukey post roc test. Values of $p < 0.05$ were considered significant. The software used for statistical analysis and graphs was GraphPad Prism (GraphPad Software Inc., San Diego, CA, USA - version 5.0).

3. Results

3.1 Cell viability assay

Fibroblasts viability was verified by NRU assay. The results demonstrate that there is no significant difference between the groups: WT (fibroblasts without treatment), NS and $NS_{\beta\text{-CD}}$ [$F_{(2,6)}$ = 0.1429, p > 0.05]. These results allow us to assert that the nanoparticles NS and $NS_{\beta\text{-CD}}$, at the tested concentrations, were no toxic for NPC patient-derived dermal fibroblast and did not impair cell growth.
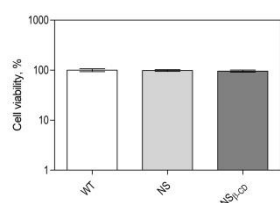
Fig 1. Neutral red viability assay in NPC patient-derived dermal fibroblast without treatment (WT), and incubated with NS and $NS_{\beta\text{-CD}}$ during 48h. Results represent mean ± SEM (standard error of the mean). One-way analysis of variance ANOVA followed by Tukey post roc test.

3.2 Markers of oxidative and nitrative stress

Both NS and $NS_{\beta\text{-CD}}$ were not able to alter the enzymatic activity of SOD [$F_{(2,6)}$ = 5.864, p > 0.05] and CAT [$F_{(2,6)}$ = 1.841, p > 0.05] presented in NPC patient-derived dermal fibroblast without treatment (WT) (figure 2a and 2b, respectively). The nanoparticles did not increase the ROS generation when compared to WT group [$F_{(2,6)}$ = 4.411, p > 0.05]. The lipid peroxidation was also not alter by nanoparticles [$F_{(2,6)}$ = 0.4737, p > 0.05] and the nanoparticles seems not cause nitrative stress in cells [$F_{(2,6)}$ = 0.2277, p > 0.05].
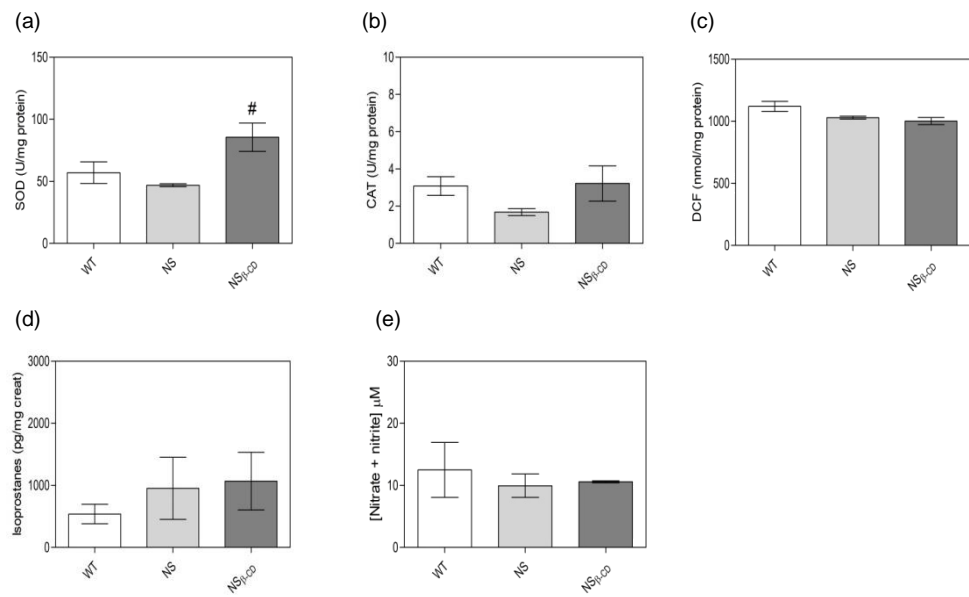
Fig. 2. Evaluation of oxidative and nitrative stress in NPC patient-derived dermal fibroblast without treatment (WT) and treated with NS and $NS_{\beta\text{-}CD}$. (a) Superoxide dismutase (SOD) activity; (b) catalase (CAT) activity; (c) DCF determination; (d) isoprostanes measurement; (e) nitrite/nitrate levels. Results represent mean ± SEM (standard error of the mean). [#] $p < 0.05$ compared NS to $NS_{\beta\text{-}CD}$. One-way analysis of variance ANOVA followed by Tukey post roc test.

3.3 Genotoxicity evaluation

NS and $NS_{\beta\text{-}CD}$ did not cause genotoxicity in human dermal fibroblasts from healthy subjects, evaluated by comet assay [$F_{(2,6)} = 0.1047$, $p > 0.05$].
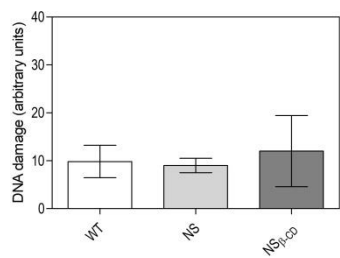
Fig. 3. Evaluation of genotoxicity in human dermal fibroblast from healthy subjects without treatment (WT) and treated with NS and $NS_{\beta\text{-}CD}$.

4. Discussion

In the last two decades, the use of nanoparticles in experimental and clinical fields has risen exponentially due to their wide range of biomedical applications. Therefore, a thorough toxicological evaluation is necessary to assess the risk of the nanocarriers for human exposure (Chatterjee *et al.*, 2017).

The size of the nanoparticles, an important toxicity-determining parameter, plays a crucial role in the accessibility of particles to cells. This could be attributed to the fact that nanoparticles of size >100-1000 nm have access to only a small number of cells, like macrophages, and are less harmful, whereas nanoparticles <100 nm can be internalized by any cell via endocytosis, that can ultimately pose more harm to the biological system (Chatterjee *et al.*, 2017). The nanoparticles developed by our group - NS and $NS_{\beta-CD}$- presented size about 100 nm and a disordered inner structure, which is a less rigid structure achieved by simply mixing the components without the use of any organic solvent (Donida *et al.*, 2018) (Donida et al., 2019). These characteristics added to the fact that they are formed with food ingredients and have high stability makes NS and $NS_{\beta-CD}$ probably non-toxic nanocarries. However, the study of possible damages caused by these nanoparticles in patients' tissues is necessary. The concentration of $NS_{\beta-CD}$ used in all assays was based on the concentration of β-CD that presented pharmacological effect (Donida et al., 2019). Then, we used the volume of NS correspondent.

The first method applied in cytotoxicity evaluation of nanoparticles was the NRU (Repetto *et al.*, 2008). Once the lysosomes were already injured in LSD patients and the NS and $NS_{\beta-CD}$ seems to be uptake by this organelle, the evaluation of nanoparticle effects in this organelle is extremely important. Both nanoparticles studied

did not impair the ability of NPC patient-derived dermal fibroblast to incorporate and bind the supravital dye neutral red (figure 1). Neutral red is a weakly cationic dye that penetrates cell membranes by nonionic passive diffusion and concentrates in the lysosomes, where it binds by electrostatic hydrophobic bonds to anionic and/or phosphate groups of the lysosomal matrix (Repetto *et al.*, 2008). When the cell dies or the pH gradient is reduced, the dye cannot be retained. Consequently, the amount of retained dye is proportional to the number of viable cells. Our previous results using healthy dermal fibroblasts also showed no cytotoxic effects for the NS. We already demonstrated the safety for parenteral administration because nanoparticles did not cause hemoglobin release (Donida *et al.*, 2018) (Donida et al., 2019). Similar results were obtained by Valldeperas *et al.* (2016) when they test nanoparticles built with a mixture of mono e di-glycerides.

ROS play a central role in chemical process involved in nanotoxicology as they may have a direct impact on cell integrity or even lead to secondary processes that can ultimately cause cell damage, pro-inflammatory response and cell death (Gou *et al.*, 2010). Oxidative stress acts by alterations in enzymes like SOD and CAT. An increase or decrease in these responses can be interpreted as evidence for oxidative stress, as the cell either compensates for increased stress by upregulating the production of antioxidants, or the exhaustion of cellular stores of SOD or CAT by oxidation from reactive nitrogen species or ROS (Chatterjee *et al.*, 2017). Analyzing our results we can conclude that nanoparticles not altered oxidation/nitrative status of NPC patient-derived dermal fibroblast, with regard to enzymatic activity of SOD and CAT (figure 2a and 2b, respectively), to ROS release (determined by DCF quantification – figure 2c) and the quantification of nitrite/nitrate levels (figure 2e). These results can be corroborated with the fact that the isoprostanes measurement in cells was not altered after the treatment

with nanoparticles (figure 2d). The isoprostanes are biomarkers of lipid peroxidation, which is the oxidative degradation of cell membranes initiated by the presence of ROS. This assay has been widely used to demonstrate the ability of a variety of nanomaterials to elicit lipid peroxidation in multiple cell types (Chatterjee *et al.*, 2017).

Another important assay to verify the nanoparticle safety is the alkaline comet assay, which was used to determine the genotoxicity of formulations. The alkaline *in vitro* comet assay is a sensitive method for evaluating DNA primary damage, i.e. simple and double-strand breaks as well as alkali-labile sites (Singh *et al.*, 1988). We used fibroblasts from healthy subjects to comet assay, because the NPC patient-derived fibroblast already presented high levels of DNA damage, making it impossible to use the sample of patients to determine the actual effect of nanoparticles on genotoxicity. Our results demonstrated that both NS and $NS_{\beta-CD}$ were not genotoxic in the tested concentrations (figure 3).

Consider the expose we can conclude that the NS and $NS_{\beta-CD}$ did not cause impairment in oxidative/nitrative stress evaluated in NPC patient-derived dermal fibroblast, and also are not cytotoxic and genotoxic in concentration tested. These results have important implications for *in vivo* use of monoolein-based nanoparticles with a disordered inner structure.

5. References

Aebi, H., 1984. Catalase in vitro, Methods in enzymology. Elsevier, pp. 121-126.

Alyaudtin, R.N., Reichel, A., Löbenberg, R., Ramge, P., Kreuter, J., Begley, D.J., 2001. Interaction of poly (butylcyanoacrylate) nanoparticles with the blood-brain barrier in vivo and in vitro. Journal of drug targeting **9**, 209-221.

Arora, S., Jain, J., Rajwade, J., Paknikar, K., 2008. Cellular responses induced by silver nanoparticles: in vitro studies. Toxicology letters **179**, 93-100.

Bradford, M.M., 1976. A rapid and sensitive method for the quantitation of microgram quantities of protein utilizing the principle of protein-dye binding. Analytical biochemistry **72**, 248-254.

Chatterjee, S., Kumari, R.M., Nimesh, S., 2017. Nanotoxicology: Evaluation of toxicity potential of nanoparticles, Advances in Nanomedicine for the Delivery of Therapeutic Nucleic Acids. Elsevier, pp. 187-201.

Coelho, J.C., Giugliani, R., 2000. Fibroblasts of skin fragments as a tool for the investigation of genetic diseases: technical recommendations. Genetics and Molecular Biology **23**, 269-271.

Donida, B., Tauffner, B., Raabe, M., Immich, M.F., de Farias, M.A., de Sá Coutinho, D., Machado, A.Z., Kessler, R.G., Portugal, R.V., Bernardi, A., 2018. Monoolein-based nanoparticles for drug delivery to the central nervous system: A platform for Lysosomal Storage Disorder treatment. European Journal of Pharmaceutics and Biopharmaceutics.

Gou, N., Onnis-Hayden, A., Gu, A.Z., 2010. Mechanistic toxicity assessment of nanomaterials by whole-cell-array stress genes expression analysis. Environmental science & technology **44**, 5964-5970.

Hsin, Y.-H., Chen, C.-F., Huang, S., Shih, T.-S., Lai, P.-S., Chueh, P.J., 2008. The apoptotic effect of nanosilver is mediated by a ROS-and JNK-dependent mechanism involving the mitochondrial pathway in NIH3T3 cells. Toxicology letters **179**, 130-139.

LeBel, C.P., Ischiropoulos, H., Bondy, S.C., 1992. Evaluation of the probe 2', 7'-dichlorofluorescin as an indicator of reactive oxygen species formation and oxidative stress. Chemical research in toxicology **5**, 227-231.

Lewinski, N., Colvin, V., Drezek, R., 2008. Cytotoxicity of nanoparticles. small **4**, 26-49.

Lutton, E., 1965. Phase behavior of aqueous systems of monoglycerides. Journal of the American Oil Chemists Society **42**, 1068-1070.

Misra, H.P., Fridovich, I., 1972. The role of superoxide anion in the autoxidation of epinephrine and a simple assay for superoxide dismutase. Journal of Biological chemistry **247**, 3170-3175.

Repetto, G., Del Peso, A., Zurita, J.L., 2008. Neutral red uptake assay for the estimation of cell viability/cytotoxicity. Nature protocols **3**, 1125.

Singh, N.P., McCoy, M.T., Tice, R.R., Schneider, E.L., 1988. A simple technique for quantitation of low levels of DNA damage in individual cells. Experimental cell research **175**, 184-191.

Valldeperas, M., Wiśniewska, M., Ram-On, M., Kesselman, E., Danino, D., Nylander, T., Barauskas, J., 2016. Sponge phases and nanoparticle dispersions in aqueous mixtures of mono-and diglycerides. Langmuir **32**, 8650-8659.

Vanier, M.T., Latour, P., 2015. Laboratory diagnosis of Niemann–Pick disease type C: The filipin staining test, Methods in cell biology. Elsevier, pp. 357-375.

4. DISCUSSÃO GERAL

Os lisossomos são organelas responsáveis pela decomposição e reciclagem de inúmeras macromoléculas (incluindo carboidratos, lipídios, ácidos nucléicos e proteínas) e estão relacionados com uma ampla gama de processos fisiológicos como a homeostase do colesterol, o reparo de membrana plasmática, o remodelamento ósseo e tecidual, defesa contra patógenos, morte e sinalização celular (Futerman e Van Meer, 2004; Saftig e Klumperman, 2009). Duas classes de proteínas são essenciais para o funcionamento desta organela complexa: hidrolases lisossomais solúveis e proteínas integrais de membrana lisossomal (Saftig e Klumperman, 2009). Mutações em genes que codificam alguma destas proteínas resultam nas DLDs, doenças caracterizadas pelo acúmulo anormal de macromoléculas não metabolizadas no interior dos lisossomos (Futerman e Van Meer, 2004).

As últimas duas décadas foram caracterizadas por notável progresso no tratamento das DLDs, incluindo fármacos que visam reduzir o substrato acumulado dentro dos lisossomos e estratégias que visam aumentar a atividade da enzima em falta, como TRE, transplante de células-tronco hematopoiéticas, chaperonas farmacológicas e terapia gênica (Desnick e Schuchman, 2002; Parenti *et al.*, 2015) Estas terapias baseiam-se na propriedade das enzimas lisossomais de serem secretadas e absorvidas pelas células vizinhas via manose-6-fosfato. Após a internalização endocítica, a enzima é transportada para o lisossomo onde atua na quebra do substrato acumulado (Sly *et al.*, 1981).

Apesar da TRE ser a alternativa mais utilizada no tratamento das DLDs, ela ainda apresenta limitações importantes a serem superadas em termos de eficácia, principalmente no que diz respeito às desordens com comprometimento neurológico (Parenti *et al.*, 2015; Martin-Banderas *et al.*, 2016). Isso porque a TRE induz, comumente, a produção de anticorpos neutralizantes contra a enzima administrada, levando a uma diminuição da eficácia do tratamento e problemas de segurança farmacológica (Martin-Banderas *et al.*, 2016). Além disso, as enzimas recombinantes são moléculas grandes que não se difundem livremente através das membranas e são incapazes de atingir concentrações terapêuticas em alguns tecidos, principalmente no SNC (Parenti *et al.*, 2015).

Considerando os problemas apresentados pelas atuais terapias para as DLDs, propôs-se neste estudo de doutorado desenvolver nanopartículas (NS) que pudessem atuar como uma plataforma inteligente para entrega de enzimas/fármacos nos lisossomos e que fossem capazes de atingir o SNC. Esta plataforma foi utilizada como base para o desenvolvimento de uma nanopartícula contendo β-CD (NS$_{β-CD}$) que fosse potencialmente eficaz para o tratamento da NPC. Também, com a finalidade de melhor compreender o efeito das nanopartículas em células, planejou-se um estudo de toxicidade de ambas as partículas (NS e NS$_{β-CD}$) em fibroblastos de pele derivados de pacientes com a doença de NPC.

Utilizando como base estudos que demonstraram a obtenção de nanoesponjas com a mistura de mono e diglicerídeos (Angelov *et al.*, 2011; Valldeperas *et al.*, 2016), foi escolhida a monoleína de grau técnico (40% de pureza) como lipídio formador da nanoestrutura. Isso porque a monoleína de

grau técnico apresenta em sua constituição, além do monoglicerídeo 1-oleoil-rac-glicerol, impurezas na forma dos di e triglicerídeos correspondentes. A monoleína pura em excesso de água em temperatura fisiológica se auto-associa em uma fase reversa cúbica bicontínua, a qual pode ser dispersa em partículas coloidas na forma de cubossomas (Valldeperas *et al.*, 2016). Entretanto, em termos de toxicidade e carreamento de macromoléculas, os cubossomas parecem ser inferiores às nanoesponjas (Barauskas *et al.*, 2010). Soma-se às vantagens apresentadas pelas nanoesponjas a possibilidade de utilização de um produto grau técnico, com valor cerca de 15 vezes inferior ao produto puro, para a sua formação.

Para o desenvolvimento das nanopartículas, além do lipídio se faz necessária a utilização de um tensoativo, o qual é responsável por manter a estabilidade cinética do sistema. Para isso, escolheu-se o polissorbato 80, baseando-se em trabalhos publicados que demonstram a capacidade desse surfactante, ao revestir nanopartículas, de aumentar a concentração de fármacos no tecido cerebral (Kreuter, 2001; Kreuter *et al.*, 2002; Kreuter *et al.*, 2003; Bernardi *et al.*, 2009; Frozza *et al.*, 2010; Gelperina *et al.*, 2010).

Através da técnica de alto cisalhamento, obteve-se nanopartículas (NS) com diâmetro médio adequado para a aplicação biológica (Blanco *et al.*, 2015), em torno de 115 nm (determinado por espalhamento dinâmico de luz – DLS). O método de alto cisalhamento foi descrito pela primeira vez por Ljusberg-Wahren e colaboradores (1996) e envolve a utilização de um equipamento de agitação do tipo estator-rotor para efetuar o cisalhamento. Através deste método, geralmente obtêm-se partículas com tamanho inferior a 200 nm e baixo índice de polidispersidade (Ljusberg-Wahren *et al.*, 1996).

O espalhamento de raios-X a baixos ângulos (SAXS) é a técnica mais utilizada para identificar a estrutura de fase de nanopartículas líquido-cristalinas e foi utilizada neste trabalho porque fases esponjas podem ser consideradas como fases cúbicas bicontínuas reversas sem ordem de longo alcance (Anderson *et al.*, 1989). O perfil de espalhamento obtido por SAXS ajustou-se ao modelo matemático de Teubner-Strey, o qual foi inicialmente utilizado para descrever flutuações na densidade de microemulsões (Teubner e Strey, 1987) e mais recentemente aplicado com sucesso para descrever fases esponja (Angelova *et al.*, 2011). Cabe salientar que o ajuste dos dados a este modelo não permite diferenciar fase esponja e microemulsão bicontínua. Para isso, um estudo detalhado deveria ser realizado envolvendo a construção de diagrama de fase com os componentes da mistura que compõe a monoleína grau técnico. Como a composição exata dessa mistura não é conhecida, exigindo sua investigação laboriosa com ferramentas da química analítica, este estudo não foi realizado. Portanto, optou-se por descrever a estrutura interna das nanopartículas mais genericamente como sendo uma estrutura bicontínua desordenada. Através do modelo matemático, foi possível determinar o diâmetro médio compreendido pelos domínios das pseudofases ricas em água e ricas em lipídio em cerca de 4,6 nm. A largura da bicamada lipídica para monoleína pura foi previamente calculada em 3,2 nm (Marrink e Tieleman, 2001). Comparando-se este valor àquele igual a 4,6 nm, pôde-se concluir que a estrutura bicontínua desenvolvida apresentou um baixo nível de hidratação. Além disso, o fator de anfifilicidade obtido para a nanoestrutura foi condizente àquele esperado para sistemas bicontínuos desordenados. As imagens de criomicroscopia eletrônica de transmissão (cryo-TEM) foram obtidas com o

intuito de complementar os resultados obtidos por SAXS. Gustafsson *et al.* (1996) foram os primeiros a caracterizar morfologicamente cubossomas utilizando cryo-TEM. Os autores conseguiram identificar uma periodicidade interna consistente com as medidas de espaçamento obtidas a partir de medidas de SAXS. No presente estudo, através da análise das imagens obtidas por cryo-TEM, foram observadas estruturas desordenadas compatíveis com nanoesponjas ou microemulsões bicontínuas e diâmetro médio condizente àquele obtido através da técnica de DLS.

Para determinar a citotoxicidade das nanopartículas, foi utilizado o ensaio de vermelho neutro. O vermelho neutro é um corante catiônico fraco que pode atravessar a membrana plasmática por difusão e tende a se acumular nos lisossomos das células. Se a membrana celular for alterada, a absorção de vermelho neutro é diminuída, pois o corante tende a sair da célula, permitindo o discernimento entre células vivas e mortas (Repetto *et al.*, 2008). A citotoxicidade pode ser então quantificada a partir de medições de espectroscopia de absorção do vermelho neutro sob diferentes condições de exposição. Sabe-se que as nanopartículas podem provocar toxicidade ao romper várias membranas dentro da célula. Quando a integridade da membrana é comprometida, o conteúdo de dentro dos compartimentos circundados por membranas pode extravazar, desencadeando estresse celular e interferindo na função das células e organelas (Wolfram *et al.*, 2015). Nesse contexto, foi possível demonstrar através da técnica de vermelho neutro que diferentes concentrações das nanopartículas, quando incubadas com fibroblastos humanos provenientes de biópsia de pele de indivíduos saudáveis,

não causam citotoxicidade, apresentando valores de viabilidade próximos a 100%.

Outro importante fator que deve ser avaliado ao se desenvolver nanopartículas para administração parenteral é a atividade hemolítica, onde o pré-requisito é uma atividade nula ou negligenciável (Barauskas *et al.*, 2010). Estudos prévios demonstraram que nanoesponjas constituídas por misturas de monoleína e diglicerídeos apresentaram valores de hemólise próximos a 1-2% (Barauskas *et al.*, 2010). Entretanto, os cubossomas preparados somente com a monoleína causaram hemólise incompatível com a administração parenteral. Estes resultados demonstram que a atividade hemolítica não é somente dependente da natureza do lipídio utilizado na fabricação da nanopartícula, mas também da composição de lipídios utilizada (Barauskas *et al.*, 2010). Através da determinação da liberação de hemoglobina pela incubação de sangue total com as nanopartículas, pôde-se comprovar que as NS não causam lise de hemácias, o que é considerado um pré-requisito para administração parenteral de sistemas de liberação.

Verificou-se a capacidade da NS de atingir os lisossomos de fibroblastos humanos saudáveis. Para isso, as nanopartículas foram marcadas com o corante fluorescence verde cumarina-6 (NS^F) e os lisossomos foram corados com "lysotracker red", de fluorescência vermelha. Após 1 h de tratamento das células com as nanopartículas, foi observada colocalização entre os dois corantes, indicando que a NS^F foi confinada no compartimento ácido e pode ser utilizada como transportadora transmembrana de enzimas/fármacos para os lisossomos.

A NS^F também foi utilizada para rastreamento nos tecidos de camundongos. As formulações foram administradas aos animais e a fluorescência foi determinada após 3, 6 e 24 h em homogeneizado de cérebro e de fígado. Como esperado, a cumarina-6 foi detectada no fígado durante todo o tempo de experimento, evidenciando o papel desintoxicante deste órgão. Da mesma forma, o corante fluorescente foi detectado no SNC logo após 3 h, sendo que a intensidade de fluorescência no cérebro aumentou após 6 h e se manteve constante em 24 h. Portanto, os resultados estão de acordo com os encontrados por Kreuter e colaboradores (2002, 2003 e 2013) que sugerem que após a administração parenteral, as lipoproteínas plasmáticas ApoB e ApoE adsorvem-se nas nanopartículas revestidas com polisorbato 80 para formar uma corona de proteína similar àquela vista para LDL, permitindo cruzar a BHE via transcitose mediada por receptores (Kreuter *et al.*, 2002; Kreuter *et al.*, 2003; Kreuter, 2013).

Considerando os resultados promissores obtidos com este trabalho, seguiu-se o estudo das NS, desta vez incorporando a β-CD, que vem sendo estudada como alternativa de tratamento para a doença de NPC. A NPC é uma DLD considerada como um distúrbio no trafego de lipídios, onde a saída prejudicada de colesterol do compartimento endossomal/lisossomal das células é um elemento-chave específico da patogênese (Vanier, 2015). Descobriu-se que a β-CD, anteriormente usada apenas para dissolver a alopregnanolona (neurosteróide estudado para tratar a NPC) (Griffin *et al.*, 2004), foi a responsável por retardar a neurodegeneração e aproximadamente dobrar o tempo de vida de camundongos Npc1$^{-/-}$ de 7 dias de idade (Liu *et al.*, 2008; Davidson *et al.*, 2009; Liu *et al.*, 2010). Então, os efeitos benéficos previamente

reportados à alopregnanolona em camundongos Npc1$^{-/-}$ (Griffin *et al.*, 2004) começaram a ser atribuídos à β-CD. Uma injeção subcutânea de β-CD (4000 mg/kg) em camundongos Npc1$^{-/-}$ uma vez por semana por 7 semanas reduziu o acúmulo de colesterol na maioria dos tecidos, diminuiu acentuadamente a neurodegeneração, melhorou a função hepática e aproximadamente dobrou a expectativa de vida dos camundongos (Ramirez *et al.*, 2010). Além disso, o armazenamento neuronal de colesterol e de gangliosídeos foi reduzido, a neurodegeneração foi retardada e a expectativa de vida foi prolongada, quando a β-CD (4000 mg/kg) foi injetada subcutaneamente em camundongos Npc1$^{-/-}$ em dias alternados, começando no 7º ou no 21º dia após o nascimento (Davidson *et al.*, 2009). Estudos de quantificação do colesterol excretado na bile por camundongos Npc1$^{-/-}$ demonstraram que a β-CD reduziu o armazenamento de colesterol em quase todos os tecidos e promoveu a excreção de colesterol na forma de ácidos biliares (Liu *et al.*, 2010). É importante ressaltar que, embora a injeção de β-CD tenha mobilizado o colesterol do compartimento endossomal/lisossomal e reduzido os parâmetros inflamatórios em camundongos Npc1$^{-/-}$ de 49 dias, sua expectativa de vida não aumentou, provavelmente porque já havia ocorrido dano tecidual extenso nestes animais ou porque a β-CD, provavelmente, não tenha atingido o tecido cerebral (Liu *et al.*, 2010). Além disso, a β-CD é eliminada 6 vezes mais rapidamente do organismo destes camundongos, comparando-se com camundongos de 7 dias de idade, o que poderia contribuir ainda mais para a menor eficácia da molécula em camundongos mais velhos (Liu *et al.*, 2010). Os estudos descritos anteriormente sobre os efeitos notáveis da injeção subcutânea de β-CD em camundongos de 7 dias de idade (Liu *et al.*, 2008;

Davidson *et al.*, 2009; Liu *et al.*, 2009), implicam que pelo menos uma quantidade significativa de β-CD atravessa a BHE e atua no SNC. No entanto, um estudo recente concluiu que a quantidade de β-CD que cruza a BHE em camundongos maduros é muito pequena, e que os benefícios neurológicos da β-CD injetada perifericamente são o resultado da ligação da ciclodextrina ao endotélio vascular cerebral (Pontikis *et al.*, 2013).

Somando-se à impossibilidade de cruzar a BHE o fato de que modelos animais de NPC tratados com a dose de 4000 mg/kg de β-CD vêm apresentando danos auditivos, o desenvolvimento de uma nanopartícula capaz de atingir o tecido cerebral e liberar a β-CD dentro dos lisossomos seria um passo importante no tratamento da doença de NPC. Assim, utilizando como modelo a NS, desenvolveu-se neste estudo de doutorado a $NS_{β-CD}$. A β-CD foi utilizada na forma de um complexo de inclusão com o polissorbato 80, na razão 2:1 (β-CD: polissorbato 80 – P80@2β-CD). As $NS_{β-CD}$ foram caracterizadas da mesma forma que as NS e apresentaram diâmetro médio de cerca de 120 nm, próprio para aplicação biológica. O uso de β-CD não alterou a estrutura interna das partículas, como evidenciado por SAXS, demonstrando que o complexo de inclusão P80@2β-CD esteja, provavelmente, recobrindo a superfície das nanopartículas e atuando como estabilizante.

Para os estudos *in vitro* das nanopartículas, foram escolhidas as doses de 12,25, 22,5 e 45 μM de β-CD. Tais doses estão dentro do intervalo de concentração que sabidamente causa redução do colesterol acumulado em células NPC (Wehrmann *et al.*, 2012). O estudo no qual as doses foram baseadas demonstra uma redução de 46% do colesterol acumulado nas células empregando-se 12,5 μM de β-CD. Essa redução atinge 68%

aumentando-se 24 vezes a concentração de β-CD, o que demonstra uma relação não-linear entre o aumento da dose e a redução de colesterol (Wehrmann *et al.*, 2012). Por esse motivo, optou-se por empregar um intervalo mais baixo de doses. Os experimentos de toxicidade foram realizados utilizando-se as nanopartículas nas 3 doses propostas (11,25, 22,5 e 45 µM de β-CD). Como todas as doses mostraram-se não-tóxicas frente a fibroblastos de pele derivados de pacientes NPC, os experimentos foram realizados somente com a NS$_{β-CD}$ na concentração de 45 µM de β-CD, a qual não causou hemólise quando incubada com sangue total.

Para determinar a eficácia das nanopartículas NS$_{β-CD}$ em reduzir o colesterol acumulado nos lisossomos, estas foram incubadas com os fibroblastos de pacientes NPC e, após 48 horas, as células foram coradas pelo reagente de Filipin. A intensidade de fluorescência conferida por este reagente é proporcional ao colesterol não-esterificado presente no interior dos lisossomos. As NS$_{β-CD}$, na concentração de 45 µM, demostraram a capacidade de reduzir cerca de 50% a intensidade de fluorescência quando comparadas às células NPC sem tratamento, corroborando com os valores encontrados utilizando-se a β-CD livre (Wehrmann *et al.*, 2012). Isto demonstra que a utilização de β-CD na forma de um complexo de inclusão com o polissorbato 80 não alterou sua capacidade de captação de colesterol.

Com o intuito de avaliar a localização das nanopartículas nos compartimentos intracelulares, as NS$_{β-CD}$ foram coradas com o fluoróforo verde cumarina-6 (NS$^F_{β-CD}$) e os lisossomos com fluoróforo vermelho específico para essa organela. Através das imagens sobrepostas obtidas com filtros específicos que evidenciam a fluorescência vermelha ou verde por meio de

microscópio confocal, foi possível confirmar que as nanopartículas ficam confinadas nos lisossomos por pelo menos 3 h após a incubação com as células. Esse resultado pode ser considerando promissor em termos de toxicidade, pois é possível sugerir que ao ficar confinada no compartimento endossomal/lisossomal, a β-CD provavelmente diminui a captação de colesterol de membranas, o que está relacionado com a sua toxicidade *in vivo.*

O rastreamento da $NS^F_{\beta-CD}$ nos tecidos de camundongos foi investigado 15 min, 1 h e 24 h após administração intraperitoneal. A consequência mais grave da NPC é a neurodegeneração, que contribui para a redução do ganho de peso, declínio cognitivo e morte prematura (Vance e Karten, 2014). O metabolismo do colesterol no cérebro é compartimentalizado pela BHE em relação àquele da periferia. Essencialmente, todo o colesterol cerebral é sintetizado no próprio cérebro. A conseqüência mais notável da deficiência de NPC1 no cérebro de camundongos e humanos é uma profunda perda de neurônios de Purkinje no cerebelo, que não é reparada pela captação do excesso de colesterol pela β-CD livre, pois a mesma não é capaz de atravessar a BHE (Ramirez *et al.*, 2010; Pontikis *et al.*, 2013). Cabe salientar que até hoje os melhores resultados obtidos com a β-CD em NPC levaram a um estudo clínico fase I/II nos Estados Unidos (*ClinicalTrials.gov identifier: NCT01747135*). Entretanto, como a β-CD não é capaz de atravessar a BHE, e para que houvesse eficácia na doença neurológica, a administração da molécula teve que ser realizada pela via intratecal. A injeção intratecal é uma via de administração bastante complicada por requerer punção lombar ou colocação cirúrgica de catéter para a implantação de bomba de infusão de fármaco. Durante e após o procedimento de inserção de cateter intratecal, os

pacientes correm grande risco de infeccção, e podem desenvolver cefaleias, confusão; letargia; náuseas, vômitos e até mesmo convulsões. Danos ao tecido neurológico estão entre as complicações mais temidas da terapia intratecal, pela já relatada ocorrência de lesão medular, lesão nervosa e lesão na cauda equina, em pacientes que se submeteram à implantação de catéter no canal raquidiano (Staats, 2008). Os resultados apresentados de forma inédita nesta tese de doutorado são bastante promissores nesse sentido, pois a $NS^F_{\beta\text{-}CD}$ alcançou o tecido cerebral de animais-modelo mais intensamente que os demais tecidos estudados, logo após 15 minutos de injeção intraperitoneal, demonstrando vantagem tecnológica frente à administração da molécula livre e inovação frente aos diversos trabalhos publicados na literatura pela utilização de um sistema nanoestruturado capaz de atingir o SNC.

Além disso, as $NS^F_{\beta\text{-}CD}$ atingem também o fígado após 15 min, permanecendo neste órgão por pelo menos 1 h. Juntamente com a capacidade de atingir o cérebro, a capacidade de atingir o tecido hepático é bastante importante para o tratamento da NPC. A doença hepática grave é prevalente em muitos pacientes, pois a maioria das LDLs circulantes é eliminada pelo fígado via endocitose mediada por receptor, o que leva a um acúmulo de colesterol mais pronunciado no fígado do que em qualquer outro tecido (Vance e Karten, 2014). O rim e o baço, outros órgãos que apresentam acúmulo de colesterol em pacientes, também foram atingidos pelas $NS^F_{\beta\text{-}CD}$. Isso ocorre provavelmente devido a processos relacionados com a detoxificação das nanopartículas pelo organismo dos animais, podendo ter efeito benéfico em reduzir o colesterol acumulado nesses órgãos na doença de NPC.

Cabe salientar que em pacientes NPC, o colesterol acumulado nos ógãos periféricos e no SNC pode ser oxidado por ERO em uma reação não enzimática formando oxiesteróis, principalmente 3β,5α,6β-triol e 7-KC, que podem ser medidos no plasma contribuindo para a investigação da NPC (Jiang *et al.*, 2011). Vários estudos vêm demonstrando a possibilidade da análise de oxiesteróis por LC-MS/MS como um ensaio alternativo e não invasivo para triagem de potenciais pacientes NPC, bem como uma ferramenta para o monitoramento do tratamento (Jiang *et al.*, 2011; Ribas *et al.*, 2016; Hammerschmidt *et al.*, 2018). A validação de um biomarcador de progressão da doença de NPC, que pode ser medido quantitativamente, é um objetivo importante quando novas terapias estão sendo testadas. Neste sentido, demonstrou-se que pacientes com a doença de NPC apresentaram valores plasmáticos de 3β,5α,6β-triol 20 vezes maiores que indivíduos saudáveis, reforçando o uso de LC-MS/MS para análise de oxiesteróis como uma técnica viável e não invasiva para avaliação da doença de NPC.

Quando se planeja nanopartículas para aplicação biológica, um dos pré-requisitos é o entendimento da citotoxicidade desses nanocarreadores. Esta citotoxicidade pode ser dependente de uma série de fatores, incluindo a linhagem celular utilizada nos ensaios, o tempo de incubação da célula com a nanopartícula, a fase da estrutura interna, além da composição e da concentração utilizada da nanopartícula nos testes (Murgia *et al.*, 2010; Zhai *et al.*, 2016). Quanto à composição das nanopartículas desenvolvidas neste trabalho, foram utilizados monoleína grau técnico (apresentando 39,9% de monoglicerídeos, 22,5% de diglicerídeos e 34,7% de triglicerídeos) e polissorbato 80. A monoleína é um material não-tóxico, biodegradável e

biocompatível classificado como *GRAS* (do inglês "*Generally Recognized As Safe*"), e está incluída no guia de ingredientes inativos do *FDA* (órgão americano regulador de alimentos e medicamentos – "Food and Drug Administration") (Ganem-Quintanar *et al.,* 2000). A sua biodegradabilidade vem do fato de que a monoleína está sujeita à hidrólise no organismo, devido a diversos tipos de esterases em diferentes tecidos (Ganem-Quintanar *et al.,* 2000). O polissorbato 80, por sua vez, é um surfactante não-iônico composto de um éster de ácido oleico com sorbitano, no qual as hidroxilas terminais estão subsitutídas com cadeias de poli(oxietileno) (Kerwin, 2008). Esse surfactante tem sido amplamente utilizado em produtos farmacêuticos como estabilizante, pois é um produto de baixo custo, facilmente disponível, biodegradável e também não-tóxico para as células em baixas concentrações (Alyaudtin *et al.,* 2001).

Mesmo utilizando materiais não-tóxicos no desenvolvimento das nanopartículas, cabe salientar que uma importante característica que deve ser considerada na nanotoxicologia é que materiais atóxicos podem se tornar tóxicos quando em escala nanométrica (Chatterjee *et al.,* 2017). Além disso, sabe-se que a β-CD, utilizada na NS$_{β-CD}$, pode causar citotoxicidade devido à sua habilidade de retirar lipídios das membranas celulares (Monnaert *et al.,* 2004). Sendo assim, foi realizado um estudo toxicológico das nanopartículas – NS e NS$_{β-CD}$ – para determinar seus comportamentos frente a fibroblastos derivados de biópsia de pele de pacientes com a doença de NPC.

O primeiro método utilizado para determinar a citotoxicidade das nanopartículas foi o ensaio de vermelho neutro. Uma vez que os lisossomos já estão comprometidos em pacientes com DLDs e as nanopartículas NS e NS$_{β-}$

$_{CD}$ parecem ser capturadas por essa organela, a avaliação dos efeitos das nanopartículas nos lisossomos é extremamente importante. Sendo assim, comprovou-se, ao avaliar as nanopartículas NS e NS$_{β-CD}$ (concentração de β-CD igual a 45 μM) utilizando uma concentração de lipídios de 117,9 μg mL^{-1}, que ambas não causaram prejuízo na capacidade dos fibroblastos de pacientes NPC de incorporar e ligar o corante supravital vermelho neutro, corroborando os resultados anteriores referentes a NS em fibroblastos dérmicos de indivíduos saudáveis.

Um mecanismo que parece ter relação direta com a citotoxicidade gerada por nanopartículas é o estresse oxidativo/nitrativo (Arora *et al.*, 2008; Hsin *et al.*, 2008). O estresse oxidativo/nitrativo é um processo ocasionado pelo desbalanço biológico entre a produção de radicais livres (como as espécies reativas de oxigênio e nitrogênio – ERO e ERN, respectivamente) e a capacidade de reparação do dano pelo sistema antioxidante, que pode levar a diversas alterações celulares, culminando em apoptose. Entre as alterações celulares geradas pelo estresse oxidativo e, que podem ser determinadas por meio de ensaios bioquímicos, destacam-se: lipoperoxidação das membranas celulares, oxidação de proteínas e lesão ao DNA/RNA celular (Halliwell e Gutteridge, 2015). Aumento ou diminuição da resposta das enzimas antioxidantes superóxido dismutase (SOD) ou catalase (CAT) pode também ser interpretado como evidência de estresse oxidativo, pois a célula compensa o aumento do estresse oxidativo, aumentando a produção dessas enzimas antioxidantes, ou há o esgotamento de reservas celulares de SOD ou CAT pela oxidação de ERO ou ERN (Chatterjee *et al.*, 2017). A SOD é uma metaloenzima que catalisa a dismutação do superóxido ($O_2^{\bullet-}$) ao peróxido de

hidrogênio (H_2O_2), o qual é menos reativo e pode ser degradado por outras enzimas, como a CAT. A CAT é uma ferri-hemoenzima, localizada nos peroxissomos, cuja principal função é converter H_2O_2 à água e oxigênio (Halliwell e Gutteridge, 2015). A citotoxicidade de nanopartículas ocasionada através de estresse oxidativo é particularmente importante de ser estudada quando esses sistemas são desenvolvidos com o intuito de tratar DLDs, porque estes pacientes já apresentam dano oxidativo decorrente do acúmulo de macromoléculas não-degradadas nos lisossomos. Essa relação entre o estresse oxidativo e os biomarcadores de DLDs está mais bem detalhada no artigo de revisão adicionado como anexo III desta tese (Donida *et al.*, 2017).

Analisando os resultados, pode-se concluir que as nanopartículas não alteraram o estado oxidativo/nitrativo de fibroblastos dérmicos derivados de pacientes NPC em relação à atividade enzimática da SOD e CAT, à liberação de EROs e quantificação dos níveis de nitrito/nitrato. Estes resultados foram corroborados com o fato de que a determinação de isoprostanos nas células não foi alterada após o tratamento com as nanopartículas. Os isoprostanos são biomarcadores da peroxidação lipídica, que é a degradação oxidativa das membranas celulares iniciada pela presença de EROs. Este ensaio tem sido amplamente utilizado para demonstrar a capacidade de uma variedade de nanomateriais em induzir a peroxidação lipídica de vários tipos de células (Chatterjee *et al.*, 2017).

Outro ensaio importante para verificar a segurança das nanopartículas é o ensaio cometa alcalino, utilizado para determinar a genotoxicidade das formulações. O ensaio cometa alcalino *in vitro* é um método sensível para avaliar danos primários em DNA, isto é, quebras simples e duplas na cadeia,

bem como sítios álcali-lábeis (Singh *et al.*, 1988). Utilizou-se fibroblastos de indivíduos saudáveis para o ensaio cometa, porque os fibroblastos provenientes de pacientes NPC já apresentavam altos níveis de dano ao DNA, tornando impossível usar a amostra de pacientes para determinar o real efeito genótoxico das nanopartículas. Os resultados demonstraram que tanto a NS como a $NS_{\beta\text{-CD}}$ não foram genotóxicas nas concentrações testadas (117,9 μg mL^{-1} de lipídios para ambas formulações e concentração correspondente de β-CD de 45 μM para $NS_{\beta\text{-CD}}$).

Considerando o exposto, conclui-se que as NS e $NS_{\beta\text{-CD}}$ não causaram alterações significativas no estresse oxidativo/nitrativo avaliado em fibroblastos dérmicos derivados de pacientes NPC, e também não foram citotóxicas e genotóxicas nas concentrações testadas. Estes resultados têm importantes implicações para o uso *in vivo* de nanopartículas à base de monoleína com uma estrutura interna desordenada.

5. CONCLUSÕES

A partir do conjunto de resultados apresentados nesta tese de doutorado, demonstrou-se que a incorporação de um complexo de inclusão de β-CD em nanopartículas de monoleína de grau técnico é uma estratégia promissora para tratar pacientes com a doença de NPC visando potencial redução de danos neurológicos. A plataforma nanotecnológica de monoleína e polissorbato 80 apresentou tamanho adequado para aplicação biológica, sendo preparada sem a utilização de solventes orgânicos e através de um método simples e escalonável. A utilização de monoleína grau técnico (produto de baixo custo quando comparado ao produto puro) propiciou a formação de uma estrutura bicontínua desordenada devido à presença de di- e triglicerídeos na mistura. A formação dessa estrutura conferiu baixa toxicidade *in vitro* às nanopartículas frente a células de pacientes NPC; não alterando a viabilidade celular, formação de espécies reativas, enzimas antioxidantes, peroxidação lipídica, parâmetros de estresse nitrativo, além de não causar genotoxicidade. Ainda, as partículas apresentaram um pré-requisito importante para administração parenteral por não causarem hemólise em sangue total.

A nanopartícula desenvolvida foi capturada por lisossomos e mostrou-se capaz de atingir o tecido cerebral em camundongos, sendo altamente promissora para carrear enzimas/fármacos e atuar no tratamento de DLDs com comprometimento neurológico. Essas características conferem grande vantagem tecnológica à partícula frente aos tratamentos recorrentes para DLDs, os quais são ineficientes em alcançar o tecido cerebral e vêm causando

respostas inflamatórias/alérgicas devido às altas doses necessárias para atingir concentrações terapêuticas no local de ação.

A incorporação do complexo de β-CD com polissorbato 80 não modificou a estrutura desordenada bicontínua apresentada pela plataforma, provavelmente por estar atuando no recobrimento da partícula como um estabilizante. A nanopartícula contendo 45 µM β-CD demonstrou eficácia terapêutica *in vitro* em reduzir colesterol acumulado em lisossomos de pacientes NPC. Quando administrada em camundongos, a nanopartícula mostrou-se capaz de atingir órgãos tipicamente comprometidos pelo acúmulo de colesterol em pacientes NPC. Interessantemente, a partícula atingiu de forma mais intensa o tecido cerebral desses animais, mostrando-se bastante promissora no tratamento de pacientes NPC no que se refere ao seu comprometimento neurológico. Sendo assim, a utilização da β-CD na estrutura nanoparticulada apresenta grande vantagem frente à utilização dessa molécula livre, que sabidamente não atravessa a BHE.

Embora mais estudos ainda sejam necessários, a nanopartícula desenvolvida de forma inédita nesta tese pode ser considerada bastante promissora, podendo futuramente, colaborar para o tratamento e melhora da qualidade de vida de pacientes com a doença de NPC. A presente tese e as publicações decorrentes da mesma constituem o primeiro relato de um sistema nanotecnológico, composto por moléculas biodegradáveis e biocompatíveis, capaz de ser internalizado por lisossomos e vetorizado ao SNC, reduzindo a toxicidade previamente relatada para a β-CD livre por outros autores.

6. PERSPECTIVAS

Em virtude do potencial terapêutico da nanopartícula desenvolvida com β-CD para o tratamento da doença de NPC, uma perspectiva importante de continuidade do trabalho reside nos estudos de cinética de liberação da β-CD e eficácia biológica *in vivo*. A investigação dos mecanismos bioquímicos envolvidos na internalização das nanopartículas por outras organelas celulares, principalmente pela mitocôndria (devido ao seu importante envolvimento em doenças neurológicas), também se constitui em interessante objeto de estudo.

7. REFERÊNCIAS

ABI-MOSLEH, L. et al. Cyclodextrin overcomes deficient lysosome-to-endoplasmic reticulum transport of cholesterol in Niemann-Pick type C cells. **Proceedings of the National Academy of Sciences,** v. 106, n. 46, p. 19316-19321, 2009. ISSN 0027-8424.

ALYAUDTIN, R. N. et al. Interaction of poly (butylcyanoacrylate) nanoparticles with the blood-brain barrier in vivo and in vitro. **Journal of drug targeting,** v. 9, n. 3, p. 209-221, 2001. ISSN 1061-186X.

ANDERSON, D.; WENNERSTROEM, H.; OLSSON, U. Isotropic bicontinuous solutions in surfactant-solvent systems: the L3 phase. **The Journal of Physical Chemistry,** v. 93, n. 10, p. 4243-4253, 1989. ISSN 0022-3654.

ANGELOV, B. et al. SAXS investigation of a cubic to a sponge (L3) phase transition in self-assembled lipid nanocarriers. **Phys Chem Chem Phys,** v. 13, n. 8, p. 3073-81, Feb 28 2011. ISSN 1463-9084.

ANGELOVA, A. et al. Swelling of a sponge lipid phase via incorporation of a nonionic amphiphile: SANS and SAXS studies. In: (Ed.) . **Trends in colloid and interface science XXIV**: Springer, 2011. p.1-6.

AQUL, A. et al. Unesterified cholesterol accumulation in late endosomes/lysosomes causes neurodegeneration and is prevented by driving cholesterol export from this compartment. **Journal of Neuroscience,** v. 31, n. 25, p. 9404-9413, 2011. ISSN 0270-6474.

ARORA, S. et al. Cellular responses induced by silver nanoparticles: in vitro studies. **Toxicology letters,** v. 179, n. 2, p. 93-100, 2008. ISSN 0378-4274.

BALLABIO, A.; GIESELMANN, V. Lysosomal disorders: from storage to cellular damage. **Biochimica et Biophysica Acta (BBA) -Molecular Cell Research,** v. 1793, n. 4, p. 684-696, 2009. ISSN 0167-4889.

BARAUSKAS, J. et al. Interactions of lipid-based liquid crystalline nanoparticles with model and cell membranes. **Int J Pharm,** v. 391, n. 1-2, p. 284-91, May 31 2010. ISSN 1873-3476

BERNARDI, A. et al. Indomethacin-loaded nanocapsules treatment reduces in vivo glioblastoma growth in a rat glioma model. **Cancer letters,** v. 281, n. 1, p. 53-63, 2009. ISSN 0304-3835.

BINKOWSKI-MACHUT, C. et al. How cyclodextrins can mask their toxic effect on the blood ' brain barrier. **Bioorganic & medicinal chemistry letters,** v. 16, n. 7, p. 1784-1787, 2006. ISSN 0960-894X.

BLANCO, E.; SHEN, H.; FERRARI, M. Principles of nanoparticle design for overcoming biological barriers to drug delivery. **Nature biotechnology,** v. 33, n. 9, p. 941, 2015. ISSN 1546-1696.

CAMPEAU, P. M.; SCRIVER, C. R.; MITCHELL, J. J. A 25-year longitudinal analysis of treatment efficacy in inborn errors of metabolism. **Molecular genetics and metabolism,** v. 95, n. 1, p. 11-16, 2008. ISSN 1096-7192.

CAVENDER, C. P.; TURLEY, S. D.; DIETSCHY, J. M. Sterol metabolism in fetal, newborn, and suckled lambs and their response to cholesterol after weaning. **American Journal of Physiology-Endocrinology And Metabolism,** v. 269, n. 2, p. E331-E340, 1995. ISSN 0193-1849.

CHATTERJEE, S.; KUMARI, R. M.; NIMESH, S. Nanotoxicology: Evaluation of toxicity potential of nanoparticles. In: (Ed.) . **Advances in Nanomedicine for the Delivery of Therapeutic Nucleic Acids**: Elsevier, 2017. p.187-201.

DAVIDSON, C. D. et al. Chronic cyclodextrin treatment of murine Niemann-Pick C disease ameliorates neuronal cholesterol and glycosphingolipid storage and disease progression. **PLoS ONE,** v. 4, n. 9, p. e6951, 2009. ISSN 1932-6203.

DE CHAVES, E. I. P. et al. Uptake of lipoproteins for axonal growth of sympathetic neurons. **Journal of Biological Chemistry,** v. 275, n. 26, p. 19883-19890, 2000. ISSN 0021-9258.

DE DUVE, C. et al. Tissue fractionation studies. 6. Intracellular distribution patterns of enzymes in rat-liver tissue. **Biochemical Journal,** v. 60, n. 4, p. 604, 1955.

DESNICK, R. J.; SCHUCHMAN, E. H. Enzyme replacement and enhancement therapies: lessons from lysosomal disorders. **Nature Reviews Genetics,** v. 3, n. 12, p. 954, 2002. ISSN 1471-0064.

DIETSCHY, J.; TURLEY, S. Cholesterol metabolism in the central nervous system during early development and in the mature animal. **J Lipid Res,** v. 45, p. 1375-1397, 2004.

DIETSCHY, J. M.; TURLEY, S. D.; SPADY, D. K. Role of liver in the maintenance of cholesterol and low density lipoprotein homeostasis in different animal species, including humans. **Journal of lipid research,** v. 34, n. 10, p. 1637-1659, 1993. ISSN 0022-2275.

DONIDA, B. et al. Oxidative damage and redox in Lysosomal Storage Disorders: Biochemical markers. **Clinica Chimica Acta,** v. 466, p. 46-53, 2017. ISSN 0009-8981.

EL-HATTAB, A. W. Inborn errors of metabolism. **Clinics in perinatology,** v. 42, n. 2, p. 413-439, 2015. ISSN 0095-5108.

FORMARIZ, T. P. et al. Microemulsões e fases líquidas cristalinas como sistemas de liberação de fármacos. **Revista Brasileira de Ciências Farmacêuticas**, p. 301-313, 2005. ISSN 1516-9332.

FROZZA, R. L. et al. Characterization of trans-resveratrol-loaded lipid-core nanocapsules and tissue distribution studies in rats. **Journal of biomedical nanotechnology,** v. 6, n. 6, p. 694-703, 2010. ISSN 1550-7033.

FUTERMAN, A. H.; VAN MEER, G. The cell biology of lysosomal storage disorders. **Nature reviews Molecular cell biology,** v. 5, n. 7, p. 554, 2004. ISSN 1471-0080.

GANEM-QUINTANAR, A.; QUINTANAR-GUERRERO, D.; BURI, P. Monoolein: a review of the pharmaceutical applications. **Drug development and industrial pharmacy,** v. 26, n. 8, p. 809-820, 2000. ISSN 0363-9045.

GELPERINA, S. et al. Drug delivery to the brain using surfactant-coated poly (lactide-co-glycolide) nanoparticles: influence of the formulation parameters. **European Journal of Pharmaceutics and Biopharmaceutics,** v. 74, n. 2, p. 157-163, 2010. ISSN 0939-6411.

GEORGIEVA, J. V.; HOEKSTRA, D.; ZUHORN, I. S. Smuggling drugs into the brain: an overview of ligands targeting transcytosis for drug delivery across the blood ' brain barrier. **Pharmaceutics,** v. 6, n. 4, p. 557-583, 2014.

GOLAN, D. et al. Princípios de farmacologia: a base fisiopatológica da farmacoterapia. In: (Ed.) . **Princípios de farmacologia: a base fisiopatológica da farmacoterapia**, 2009.

GRIFFIN, L. D. et al. Niemann ' Pick type C disease involves disrupted neurosteroidogenesis and responds to allopregnanolone. **Nature medicine,** v. 10, n. 7, p. 704, 2004. ISSN 1546-170X.

GUSTAFSSON, J. et al. Cubic lipid− water phase dispersed into submicron particles. **Langmuir,** v. 12, n. 20, p. 4611-4613, 1996. ISSN 0743-7463.

HALLIWELL, B.; GUTTERIDGE, J. M. **Free radicals in biology and medicine**. Oxford University Press, USA, 2015. ISBN 0198717482.

HAMMERSCHMIDT, T. G. et al. Molecular and biochemical biomarkers for diagnosis and therapy monitorization of Niemann-Pick type C patients. **Int J Dev Neurosci,** v. 66, p. 18-23, May 2018. ISSN 1873-474X.

HAYASHI, H. et al. Glial lipoproteins stimulate axon growth of central nervous system neurons in compartmented cultures. **Journal of Biological Chemistry,** v. 279, n. 14, p. 14009-14015, 2004. ISSN 0021-9258.

HEESE, B. A. Current strategies in the management of lysosomal storage diseases. Seminars in pediatric neurology, 2008, Elsevier. p.119-126.

HOVAKIMYAN, M. et al. Combined therapy with cyclodextrin/allopregnanolone and miglustat improves motor but not cognitive functions in Niemann ' Pick Type C1 mice. **Neuroscience,** v. 252, p. 201-211, 2013. ISSN 0306-4522.

HSIN, Y.-H. et al. The apoptotic effect of nanosilver is mediated by a ROS-and JNK-dependent mechanism involving the mitochondrial pathway in NIH3T3 cells. **Toxicology letters,** v. 179, n. 3, p. 130-139, 2008. ISSN 0378-4274.

HYDE, S.; ANDERSSON, S. A cubic structure consisting of a lipid bilayer forming an infinite periodic minimum surface of the gyroid type in the glycerolmonooleat-water system. **Zeitschrift für Kristallographie-Crystalline Materials,** v. 168, n. 1-4, p. 213-220, 1984. ISSN 2196-7105.

JARDIM, L. B.; ASHTON-PROLLA, P. Erros inatos do metabolismo em crianças e recém-nascidos agudamente enfermos: guia para o seu diagnóstico e manejo. **J Pediatr (Rio J)** , v. 72, p. 63-70, 1996.

JIANG, X. et al. A sensitive and specific LC-MS/MS method for rapid diagnosis of Niemann-Pick C1 disease from human plasma. **Journal of lipid research**, p. jlr. D015735, 2011. ISSN 0022-2275.

KARTEN, B. et al. Generation and function of astroglial lipoproteins from Niemann ⸍ Pick type C1-deficient mice. **Biochemical Journal,** v. 387, n. 3, p. 779-788, 2005. ISSN 0264-6021.

KARTEN, B. et al. Cholesterol accumulates in cell bodies, but is decreased in distal axons, of Niemann ⸍ Pick C1 ⸌deficient neurons. **Journal of neurochemistry,** v. 83, n. 5, p. 1154-1163, 2002. ISSN 0022-3042.

KERWIN, B. A. Polysorbates 20 and 80 used in the formulation of protein biotherapeutics: structure and degradation pathways. **Journal of pharmaceutical sciences,** v. 97, n. 8, p. 2924-2935, 2008. ISSN 0022-3549.

KOGAN, A. et al. Formation and characterization of ordered bicontinuous microemulsions. **The Journal of Physical Chemistry B,** v. 113, n. 31, p. 10669-10678, 2009. ISSN 1520-6106.

KREUTER, J. Nanoparticulate systems for brain delivery of drugs. **Advanced drug delivery reviews,** v. 47, n. 1, p. 65-81, 2001. ISSN 0169-409X.

_ _ _ _ _ _ . Mechanism of polymeric nanoparticle-based drug transport across the blood-brain barrier (BBB) . **Journal of microencapsulation,** v. 30, n. 1, p. 49-54, 2013. ISSN 0265-2048.

KREUTER, J. et al. Direct evidence that polysorbate-80-coated poly (butylcyanoacrylate) nanoparticles deliver drugs to the CNS via specific mechanisms requiring prior binding of drug to the nanoparticles. **Pharmaceutical research,** v. 20, n. 3, p. 409-416, 2003. ISSN 0724-8741.

KREUTER, J. et al. Apolipoprotein-mediated transport of nanoparticle-bound drugs across the blood-brain barrier. **Journal of drug targeting,** v. 10, n. 4, p. 317-325, 2002. ISSN 1061-186X.

LACHMANN, R. H. Enzyme replacement therapy for lysosomal storage diseases. **Current opinion in pediatrics,** v. 23, n. 6, p. 588-593, 2011. ISSN 1040-8703.

LI, H. et al. GM2/GD2 and GM3 gangliosides have no effect on cellular cholesterol pools or turnover in normal or NPC1 mice. **Journal of lipid research,** v. 49, n. 8, p. 1816-1828, 2008. ISSN 0022-2275.

LIU, B. et al. Genetic variations and treatments that affect the lifespan of the NPC1 mouse. **Journal of lipid research,** v. 49, n. 3, p. 663-669, 2008. ISSN 0022-2275.

LIU, B. et al. Cyclodextrin overcomes the transport defect in nearly every organ of NPC1 mice leading to excretion of sequestered cholesterol as bile acid. **Journal of lipid research,** v. 51, n. 5, p. 933-944, 2010. ISSN 0022-2275.

LIU, B. et al. Reversal of defective lysosomal transport in NPC disease ameliorates liver dysfunction and neurodegeneration in the npc1−/− mouse. **Proceedings of the National Academy of Sciences,** v. 106, n. 7, p. 2377-2382, 2009. ISSN 0027-8424.

LIU, Y. et al. Alleviation of neuronal ganglioside storage does not improve the clinical course of the Niemann ' Pick C disease mouse. **Human molecular genetics,** v. 9, n. 7, p. 1087-1092, 2000. ISSN 1460-2083.

LJUSBERG-WAHREN, H.; NYBERG, L.; LARSSON, K. Dispersion of the cubic liquid crystalline phase: Structure, preparation and functionality aspects. **Chimica Oggi,** v. 14, n. 6, p. 40-43, 1996. ISSN 0392-839X.

LOPEZ, A. M. et al. Systemic administration of 2 ‚hydroxypropyl ‚β ‚ cyclodextrin to symptomatic Npc1 ‚deficient mice slows cholesterol sequestration in the major organs and improves liver function. **Clinical and Experimental Pharmacology and Physiology,** v. 41, n. 10, p. 780-787, 2014. ISSN 0305-1870.

LUTTON, E. Phase behavior of aqueous systems of monoglycerides. **Journal of the American Oil Chemists Society,** v. 42, n. 12, p. 1068-1070, 1965. ISSN 0003-021X.

LUZIO, J. P.; PRYOR, P. R.; BRIGHT, N. A. Lysosomes: fusion and function. **Nature reviews Molecular cell biology,** v. 8, n. 8, p. 622, 2007. ISSN 1471-0080.

MARRINK, S.-J.; TIELEMAN, D. P. Molecular dynamics simulation of a lipid diamond cubic phase. **Journal of the American Chemical Society,** v. 123, n. 49, p. 12383-12391, 2001. ISSN 0002-7863.

MARTIN-BANDERAS, L. et al. Role of nanotechnology for enzyme replacement therapy in lysosomal diseases. a focus on Gaucher ˛ s disease. **Current medicinal chemistry,** v. 23, n. 9, p. 929-952, 2016. ISSN 0929-8673.

MAUCH, D. H. et al. CNS synaptogenesis promoted by glia-derived cholesterol. **Science,** v. 294, n. 5545, p. 1354-1357, 2001. ISSN 0036-8075.

MONNAERT, V. et al. Behavior of α-, β-, and γ-cyclodextrins and their derivatives on an in vitro model of blood-brain barrier. **Journal of Pharmacology and Experimental Therapeutics,** v. 310, n. 2, p. 745-751, 2004. ISSN 0022-3565.

MURGIA, S. et al. Nanoparticles from lipid-based liquid crystals: emulsifier influence on morphology and cytotoxicity. **The Journal of Physical Chemistry B,** v. 114, n. 10, p. 3518-3525, 2010. ISSN 1520-6106.

NIEWEG, K.; SCHALLER, H.; PFRIEGER, F. W. Marked differences in cholesterol synthesis between neurons and glial cells from postnatal rats. **Journal of neurochemistry,** v. 109, n. 1, p. 125-134, 2009. ISSN 0022-3042.

ORY, D. S. et al. Intrathecal 2-hydroxypropyl-β-cyclodextrin decreases neurological disease progression in Niemann-Pick disease, type C1: a non-randomised, open-label, phase 1 ' 2 trial. **The Lancet,** v. 390, n. 10104, p. 1758-1768, 2017. ISSN 0140-6736.

PARENTI, G.; ANDRIA, G.; BALLABIO, A. Lysosomal storage diseases: from pathophysiology to therapy. **Annual review of medicine,** v. 66, p. 471-486, 2015. ISSN 0066-4219.

PATTERSON, M. C. A riddle wrapped in a mystery: understanding Niemann-Pick disease, type C. **The neurologist,** v. 9, n. 6, p. 301-310, 2003. ISSN 1074-7931.

PLATT, F. M. et al. Lysosomal storage diseases. **Nat Rev Dis Primers,** v. 4, n. 1, p. 27, Oct 1 2018. ISSN 2056-676X

PONTIKIS, C. C. et al. Cyclodextrin alleviates neuronal storage of cholesterol in Niemann-Pick C disease without evidence of detectable blood ꞌ brain barrier permeability. **Journal of inherited metabolic disease,** v. 36, n. 3, p. 491-498, 2013. ISSN 0141-8955.

QUAN, G. et al. Ontogenesis and regulation of cholesterol metabolism in the central nervous system of the mouse. **Developmental brain research,** v. 146, n. 1-2, p. 87-98, 2003. ISSN 0165-3806.

RAMIREZ, C. M. et al. Weekly cyclodextrin administration normalizes cholesterol metabolism in nearly every organ of the Niemann-Pick type C1 mouse and markedly prolongs life. **Pediatric research,** v. 68, n. 4, p. 309, 2010. ISSN 1530-0447.

REPETTO, G.; DEL PESO, A.; ZURITA, J. L. Neutral red uptake assay for the estimation of cell viability/cytotoxicity. **Nature protocols,** v. 3, n. 7, p. 1125, 2008. ISSN 1750-2799.

RIBAS, G. et al. Selective screening of Niemann ꞌ Pick type C Brazilian patients by cholestane-3β, 5α, 6β-triol and chitotriosidase measurements followed by filipin staining and NPC1/NPC2 gene analysis. **Clinica Chimica Acta,** v. 459, p. 57-62, 2016. ISSN 0009-8981.

RIBAS, G. S. et al. Oxidative stress in Niemann-Pick type C patients: a protective role of N-butyl-deoxynojirimycin therapy. **International Journal of Developmental Neuroscience,** v. 30, n. 6, p. 439-444, 2012. ISSN 0736-5748.

SAFTIG, P.; KLUMPERMAN, J. Lysosome biogenesis and lysosomal membrane proteins: trafficking meets function. **Nature reviews Molecular cell biology,** v. 10, n. 9, p. 623, 2009. ISSN 1471-0080.

SAUDUBRAY, J.-M. Clinical phenotypes: diagnosis/algorithms. **The metabolic and molecular bases of inherited disease**, p. 1327-1403, 2001.

SCRIVER, C. R. et al. **Metabolic and Molecular Bases of Inherited Disease, 4 Volume Set**. McGraw-Hill Professional Publishing, 2000. ISBN 0079130356.

SINGH, N. P. et al. A simple technique for quantitation of low levels of DNA damage in individual cells. **Experimental cell research,** v. 175, n. 1, p. 184-191, 1988. ISSN 0014-4827.

SLY, W. S. et al. Role of the 6-phosphomannosyl-enzyme receptor in intracellular transport and adsorptive pinocytosis of lysosomal enzymes. In: (Ed.) . **Methods in cell biology**: Elsevier, v.23, 1981. p.191-214. ISBN 0091-679X.

SOUZA, C. F.; SCHWARTZ, I. V.; GIUGLIANI, R. Triagem neonatal de distúrbios metabólicos. **Ciência & Saúde Coletiva,** v. 7, p. 129-137, 2002. ISSN 1413-8123.

STAATS, P. S. Complications of intrathecal therapy. **Pain Medicine,** v. 9, n. suppl_ 1, p. S102-S107, 2008. ISSN 1526-4637.

STORM, G. et al. Surface modification of nanoparticles to oppose uptake by the mononuclear phagocyte system. **Advanced drug delivery reviews,** v. 17, n. 1, p. 31-48, 1995. ISSN 0169-409X.

TEUBNER, M.; STREY, R. Origin of the scattering peak in microemulsions. **The Journal of Chemical Physics,** v. 87, n. 5, p. 3195-3200, 1987. ISSN 0021-9606.

THOMAS, R.; KERMODE, A. R. Enzyme enhancement therapeutics for lysosomal storage diseases: Current status and perspective. **Molecular Genetics and Metabolism**, 2018. ISSN 1096-7192.

TORCHILIN, V. P. Drug targeting. **European Journal of Pharmaceutical Sciences,** v. 11, p. S81-S91, 2000. ISSN 0928-0987.

VALLDEPERAS, M. et al. Sponge phases and nanoparticle dispersions in aqueous mixtures of mono-and diglycerides. **Langmuir,** v. 32, n. 34, p. 8650-8659, 2016. ISSN 0743-7463.

VAN VUGHT, F.; DE JONG, M. R. CYCLODEXTRINS FOR SENSING: SOLUTION, SURFACE, AND SINGLE MOLECULE CHEMISTRY. 2001.

VANCE, J. E.; KARTEN, B. Niemann-Pick C disease and mobilization of lysosomal cholesterol by cyclodextrin. **Journal of lipid research**, p. jlr. R047837, 2014. ISSN 0022-2275.

VANIER, M. T. Niemann-Pick disease type C. **Orphanet journal of rare diseases,** v. 5, n. 1, p. 16, 2010. ISSN 1750-1172.

_ _ _ _ _ _ . Complex lipid trafficking in Niemann-Pick disease type C. **Journal of inherited metabolic disease,** v. 38, n. 1, p. 187-199, 2015. ISSN 0141-8955.

VANIER, M. T.; LATOUR, P. Laboratory diagnosis of Niemann ' Pick disease type C: The filipin staining test. In: (Ed.) . **Methods in cell biology**: Elsevier, v.126, 2015. p.357-375. ISBN 0091-679X.

VITE, C. H. et al. Intracisternal cyclodextrin prevents cerebellar dysfunction and Purkinje cell death in feline Niemann-Pick type C1 disease. **Science translational medicine,** v. 7, n. 276, p. 276ra26-276ra26, 2015. ISSN 1946-6234.

WARD, S. et al. 2-hydroxypropyl-β-cyclodextrin raises hearing threshold in normal cats and in cats with Niemann-Pick type C disease. **Pediatric research,** v. 68, n. 1, p. 52, 2010. ISSN 1530-0447.

WASSIF, C. A. et al. High incidence of unrecognized visceral/neurological late-onset Niemann-Pick disease, type C1, predicted by analysis of massively parallel sequencing data sets. **Genetics in Medicine,** v. 18, n. 1, p. 41, 2016. ISSN 1530-0366.

WEHRMANN, Z. T. et al. Quantitative comparison of the efficacy of various compounds in lowering intracellular cholesterol levels in Niemann-Pick type C fibroblasts. **PLoS ONE,** v. 7, n. 10, p. e48561, 2012. ISSN 1932-6203.

WOLFRAM, J. et al. Safety of nanoparticles in medicine. **Current drug targets,** v. 16, n. 14, p. 1671-1681, 2015. ISSN 1389-4501.

YU, D. et al. Niemann ׳ Pick Disease Type C: Induced Pluripotent Stem Cell ׳ Derived Neuronal Cells for Modeling Neural Disease and Evaluating Drug Efficacy. **Journal of biomolecular screening,** v. 19, n. 8, p. 1164-1173, 2014. ISSN 1087-0571.

ZHAI, J.   et al. Amphiphilic brush polymers produced using the RAFT polymerisation method stabilise and reduce the cell cytotoxicity of lipid lyotropic liquid crystalline nanoparticles. **Faraday discussions,** v. 191, p. 545-563, 2016.

ANEXO I - Artigo de revisão publicado na *Clinica Chimica Acta (JCR: 2,926)* intitulado: *Oxidative damage and redox in Lysosomal Storage Disorders: Biochemical markers.*

Review

Oxidative damage and redox in Lysosomal Storage Disorders: Biochemical markers

CrossMark

Bruna Donida [a,*], Carlos Eduardo Diaz Jacques [a], Caroline Paula Mescka [b,c],
Daiane Grigolo Bardemaker Rodrigues [b], Desirèe Padilha Marchetti [a], Graziela Ribas [e],
Roberto Giugliani [c,d], Carmen Regla Vargas [a,b,c,*]

[a] Programa de Pós-Graduação em Ciências Biológicas: Bioquímica, UFRGS, Porto Alegre, RS, Brazil
[b] Programa de Pós-Graduação em Ciências Farmacêuticas, UFRGS, Porto Alegre, RS, Brazil
[c] Serviço de Genética Médica, HCPA, Porto Alegre, RS, Brazil
[d] Departamento de Genética, e Programa de Pós-Graduação em Genética e Biologia Molecular, Instituto de Biociências, UFRGS, Porto Alegre, RS, Brazil
[e] Programa de Pós-Graduação em Saúde da Criança e do Adolescente, UFRGS, Porto Alegre, RS, Brazil

ARTICLE INFO

ABSTRACT

Lysosomal Storage Disorders (LSD) comprise a heterogeneous group of >50 genetic disorders caused by mutations in genes that encode lysosomal enzymes, transport proteins or other gene products essential for a functional lysosomal system. As a result, abnormal accumulation of substrates within the lysosome leads to a progressive cellular impairment and dysfunction of numerous organs and systems. The exact mechanisms underlying the pathophysiology of LSD remain obscure. Previous studies proposed a relationship between oxidative stress and the pathogenesis of several inborn errors of metabolism, including LSD. Considering these points, in this paper it was reviewed oxidative stress and emerging antioxidant therapy in LSD, emphasizing studies with biological samples from patients affected by this group of conditions. These studies allow presuming that metabolites accumulated in LSD cause an increase of lysosomes' number and size, which may induce excessive production of reactive species and/or deplete the tissue antioxidant capacity, leading to damage in biomolecules. In vitro and in vivo evidence showed that cell oxidative process occurs in LSD and probably contributes to the pathophysiology of these disorders. In this context, it is possible to suggest that, in the future, antioxidants could come to be used as adjuvant therapy for LSD patients.

© 2017 Published by Elsevier B.V.

Contents

1. Introduction

Lysosomes, discovered by Christian de Duve > 50 years ago, are membrane-bound organelles that contain acid-active enzymes, which are involved in degradation of complex molecules and are also required for the digestion of the intracellular material during the process of autophagy [1]. Among these enzymes, about 50–60 are soluble and located in lysosomal lumen; seven of them are integral membrane proteins [2]. Mutations in genes that encode any of these proteins could cause Lysosomal Storage Disorders (LSD), which are characterized by an abnormal accumulation of substrates within the lysosome [1]. Taken together, LSD comprise > 50 genetic disorders with a collective frequency of 1:5000 live births [3]. Some LSD are characterized by a broad spectrum phenotype, with progressive cellular impairment and dysfunction of numerous organs and systems [1,4]. Clinical manifestations, which may manifest from early childhood until adulthood, may include neurocognitive decline, dysmorphia, hydrops fetalis, hepatosplenomegaly and musculoskeletal abnormalities [5].

Although the exact mechanisms of oxidative damage in LSD are not yet fully understood, it has been proposed that the lysosomal overload that occurs in these disorders can exacerbate the imbalance between formation and removal of reactive species [6]. These aspects will be discussed in details in this review, emphasizing studies from affected patients.

2. Free radicals, antioxidant compounds and oxidative stress biomarkers

Free radicals are chemical compounds that have an unpaired electron occupying a single atomic or molecular orbital. As a consequence, these molecules become unstable and highly reactive, causing several damages to cellular structures [7]. These radicals can be formed endogenously, mainly due to aerobic metabolism, or by exogenous sources such as alcohol, tobacco and drugs consumption, exposure to ionizing and electromagnetic radiation and atmospheric pollution [8,9]. The reactive oxygen and nitrogen species (ROS and RNS, respectively) comprise both radicals – like superoxide anion ($O_2^{\bullet-}$), hydroxyl radical ($HO\bullet$) and nitric oxide ($NO\bullet$) – and non-radical molecules, such as hydrogen peroxide (H_2O_2) and peroxynitrite ($ONOO^-$) [10,7].

At low levels, ROS and RNS are essential to many biochemical pathways; however when they are overproduced or improperly removed by antioxidant defenses, a pro-oxidant state may be generated [11]. The antioxidant defense systems include non-enzymatic antioxidants – such as bilirubin, melatonin, reduced glutathione (GSH), estrogens, vitamins and polyphenols – and antioxidant enzymes such as superoxide dismutase (SOD), catalase (CAT) and glutathione peroxidase (GPx) [7]. Under pathological conditions, the generation of reactive species can be greater than their neutralization by antioxidant defenses, what can provoke oxidation in biomolecules, such as proteins (leading to their inactivation), lipids (causing membrane instability) and DNA (inducing mutations), a process of damage known as oxidative stress [8].

3. Oxidative stress in Lysosomal Storage Disorders

Recent studies have shown the involvement of oxidative damage in the pathophysiology of several genetic diseases, including in LSD (Table 1). It should be noted that the primary biological consequence in LSD is the increase in the size and number of the lysosomes, in an attempt to retain the growing concentration of under graded macromolecules. These processes might trigger intracellular cascades, such as inflammation and oxidative stress, finally culminating into cell and tissue dysfunction [12]. In the following sections of this review, the findings of oxidative stress obtained from various LSD studies will be discussed.

3.1. Oxidative stress in mucopolysaccharidoses (MPS)

MPS are a subgroup of LSD and are caused by a deficiency in lysosomal enzymes involved in catabolism of glycosaminoglycans (GAG)

Table 1
Oxidative stress findings in LSD affected patients.

Disease	Defective protein	Main alterations
MPS I (Hurler, Scheie, Hurler/Scheie) (Pereira et al. [23])	α-L-iduronidase	Transitory decrease of SOD activity and increase of CAT activity during ERT treatment; high levels of MDA before and during ERT treatment.
MPS II (Hunter) (Filippon et al. [24]; Filippon et al. [29]; Jacques et al. [25])	Iduronate-2-sulfatase	Increase of lipid and protein damage biomarkers before and during short- and long-term ERT; mild alterations of antioxidant enzymes activities; high levels of RNS in long-term treated patients; DNA damage before and during ERT.
MPS IVA (Morquio-A) (Donida et al. [34]; Negretto et al. [35])	N-acetylgalactosamine-6-sulfate sulfatase	Oxidative DNA damage; decrease of GSH content; increased isoprostane levels in urine and high levels of protein damage in treated ERT patients.
Fabry (Biancini et al. [40]; Biancini et al. [46]; Chimenti et al. [48])	α-Galactosidase A	Increase of RNS and ROS contents; GSH metabolism alterations; lipid and protein damage; high levels of purine bases oxidation metabolites before and during ERT; overexpression of iNOS in myocardial cells.
Niemann-Pick C (Reddy et al. [59]; De Windt et al. [60]; Fu et al. [65]; Ribas et al. [64])	NPC-1 NPC-2	Upregulation of NADPH oxidase genes, in genes involved in Fe, Cu and Zn homeostasis; decrease of reduced Cq10; presence of high levels of lipid peroxidation and protein damage; antioxidant defenses mildly altered.
Gaucher (Deganuto et al. [72]; Moraitou et al. [74]; Moraitou et al. [77]; Zahran et al. [80])	β-glucosidase	Decreased antioxidant defenses and plasmalogens levels; increase of ROS and lipid peroxides in fibroblasts; high levels of NO• before ERT; decreasing of Zn, Cu and Se before and after ERT.

This table shows the main results about oxidative stress in LSD patients found in several studies. Left column gives the name of the disease, the middle column presents the deficient protein and the right column highlights the alterations found in each disease.

[13], especially heparan sulfate (HS), dermatan sulfate (DS), keratan sulfate (KS), chondroitin 6-sulfate (CS) and hyaluronan [13,14]. Combined, MPS have a prevalence of 1:25,000 live births, being the second most common group of LSD [15,16]. Clinical features of MPS patients may vary on a wide spectrum of degrees, with a chronic and progressive course [13,17]. Common symptoms of MPS include facial dysmorphism, joint stiffness and contractures, organomegaly and, for some of them, neurological impairment [17]. Treatment with enzyme replacement therapy (ERT) is available since the 2000s to MPS I, II, IVA and VI [18], which demonstrated to reduce GAG levels and improve life quality of patients [18,19,20,21,22].

Although the pathophysiology of MPS is not yet completely elucidated, oxidative stress has been increasingly recognized as a mechanism of cell damage. In 2008, Pereira et al. [23] detected a decrease in SOD activity in erythrocytes from MPS I patients after 12 weeks of treatment with ERT, while CAT activity increased after 4 weeks and kept high during the entire time of this study (24 weeks). Besides, before treatment, MPS I patients from this study did not present differences in the parameters evaluated in relation to control subjects, reinforcing the notion that the ERT could be responsible for such enzyme alterations. This hypothesis can be explained by alterations in antioxidant pathways as a consequence of modifications on cells' architecture and biochemistry which occur with the degradation of accumulated GAG by the recombinant enzyme. The authors did not observe alterations in the GSH content in MPS I patients, both before and during ERT. On the contrary, lipid peroxidation was found increased in these two conditions in relation to control individuals.

Lipid peroxidation was also verified by Filippon et al. [24] in MPS II untreated patients through the increase of malondialdehyde (MDA) in plasma. In this work, 15 days of ERT were capable to decrease the MDA concentrations of patients compared to the pre-treatment moment. Nevertheless, the concentrations of this biomarker remained increased compared to the control group, even after six months of ERT, suggesting that, like in MPS I, lipid damage do not reach normal levels despite the ERT effects. Increased lipid peroxidation, as well as high levels of reactive nitrogen species (NO• in plasma and nitrate + nitrite in urine) were also verified in MPS II patients under long-term ERT (about 5.2 years) [25]. In this work, Jacques and coworkers [25] found that di-tyrosine (a parameter of protein damage) and nitrate + nitrite levels are positively associated to urinary GAG concentrations, indicating again the role of GAG on these deleterious processes in patients.

On the other hand, although protein oxidative damage (evaluated by reduced sulfhydryl content and increased protein carbonylation) has been observed in plasma from MPS II patients under short-term ERT [24], these parameters were not altered in MPS II patients treated for a longer time [25], suggesting that the protein oxidative damage, which is increased in untreated MPS II patients in relation to controls, could be corrected with a longer time of therapy. In fact, it is important to mention that protein damage is harder and slower to be reverted compared to other oxidized biomolecules [26].

DNA damage in leucocytes, evaluated by the comet assay through the measurement of tail length of the nucleoids after electrophoresis, was also investigated in MPS II patients, before and during ERT. DNA and RNA are highly sensitive to oxidant species, particularly to HO• [27,28], and the oxidation in these biomolecules plays an important role in mutagenesis and carcinogenesis processes [7]. Filippon et al. [29] verified increased DNA damage in untreated MPS II patients, which was reduced, but did not reach normal values after three months of ERT. DNA damage in these patients was positively correlated with carbonylated proteins and also with MDA content, indicating a possible role of oxidative stress in DNA damage induction. Similarly, Negretto and coworkers [30] have found a strong correlation between MDA and DNA damage in MPS II patients submitted to ERT. MDA is a final product of lipid peroxidation, and it can act itself as an inductor of DNA damage [31].

In relation to antioxidant defenses, total antioxidant status (TAS), which measures unspecific and non-enzymatic defenses, was found

to be decreased in MPS II patients, before and during the first five months of ERT, being restored to the control levels at the sixth month of treatment. In what concerns antioxidant enzymes activities, SOD had a transient increase throughout ERT period, while CAT did not present significant alterations as compared to controls [24]. On the other hand, Jacques et al. [25] did not observe alterations in SOD, CAT, GPx and GR activities in MPS II patients under long-term ERT. Analyzed together, these results suggest that the content and production of ROS can be transient during the ERT period, since ROS can act as activators of signaling pathways, enhancing, this way, the expression of antioxidant enzymes [32,33], and that the beneficial effects of ERT, especially on the antioxidant defense system, are probably time-dependent.

Oxidative stress was also evidenced in MPS IVA patients undergoing ERT [34]. Reduction of the antioxidant GSH, as well as increased SOD activity in erythrocytes, not accompanied by an increased GPx activity, were detected in these patients. This excess of H_2O_2, produced by the imbalance between SOD and GPx reactions, can interact with transition metals to yield the radical OH•, which is extremely dangerous to the cell. These authors also verified increased lipid and protein damage, as well as higher levels of interleukin-6, which was inversely correlated with GSH, suggesting a possible link between inflammation and oxidative stress in MPS IVA disease [34]. DNA oxidative damage, investigated by the comet assay with the repair enzyme endonuclease III and also by the urinary concentrations of 8-hydroxy-2′-deoxyguanosine (8-OHdG), was increased in MPS IVA patients, indicating that both purine and pyrimidine bases are damaged by ROS in this disease. These results reinforce the importance of oxidative stress in MPS IVA patients even during ERT [34,35].

3.2. Oxidative stress in Fabry disease (FD)

FD is an X-linked inborn error of glycosphingolipid catabolism due to deficient activity of α-galactosidase A. This deficiency leads to accumulation of the enzyme substrates, mainly globotriaosylceramide (Gb3), in body fluids and lysosomes of vascular endothelium and most other tissues [36]. The incidence was estimated at 1:40,000 to 1:117,000 in male [37]. FD classic manifestation involves angiokeratomata, corneal opacity, neuropathic pain (acroparesthesias), intolerance to heat, inability to sweat and micro-albuminuria [38]. Inflammation and oxidative stress seem to be related to the pathophysiology of the FD [3], since lysosomes are quite vulnerable to oxidative stress as a natural consequence of the physiological conditions underlying this organelle [6,39].

In this context, Biancini et al. [40] have verified that Fabry patients under ERT presented high lipid oxidative damage, represented by increased levels of MDA, and high protein oxidation, since carbonyl plasma groups and urinary di-tyrosine levels were augmented compared to controls. Moreover, MDA and carbonyl content were positively correlated with Gb3, indicating that the main metabolite accumulated in this disorder may be inducing such damages. This is in accordance with the in vitro study performed by Shen and coworkers [41] demonstrating that Gb3 induces an increased expression of adhesion molecules and a higher production of reactive oxygen species in endothelial cells culture of Fabry patients.

Alterations in antioxidant defenses were also detected in Fabry patients, such as decrease in erythrocyte GSH content and GPx activity, contributing to a higher susceptibility to oxidative damage [40]. Biancini et al. [42] reported that the redox impairment also occurs in Fabry patients before ERT (demonstrated by altered GSH metabolism, high lipid peroxidation and higher NO• equivalents production). This way, oxidative damage could not be a consequence of ERT itself, being present in affected Fabry patients before initiating therapy.

A study performed by Moore et al. [43] has shown that intravenous infusion of ascorbate, a potent antioxidant, decreased cerebral hyperperfusion found in patients with FD treated with ERT. Also, they have

observed an increase of serum myeloperoxidase activity in these patients consistent with inflammatory process [43]. Myeloperoxidase is associated with vascular injury and increased risk of atherosclerosis [44]. Its elevation in serum indicates a significant increase in leukocyte priming which is being associated with inflammation and ROS generation [45].

Some studies have investigated the possible mechanisms of vascular alterations and cardiac impairment in FD. It has been proposed that reactive species of oxygen ($O_2^{•-}$) and nitrogen (NO• and $ONOO^-$) could not only act as vasodilators, but also increase the vulnerability to vascular atherosclerosis [43,46]. Furthermore, increased levels of homocysteine (Hcy), a sulfur-containing amino acid which is considered a risk factor in vascular diseases, were described in FD patients [47], as well as increased GSH levels and CAT activity. Considering that the most FD patients of this study were undergoing ERT, the activation of antioxidant defenses observed could be associated with the therapy. In other study, Chimenti et al. [48] verified that iNOS and nitrotyrosine expressions were increased in myocardial tissue from FD patients as compared to hypertrophic cardiomyopathy patients and normal controls. Moreover, 8-OHdG, that reflects the oxidative damage to DNA, was expressed in 25% of cardiomyocyte nuclei from FD patients, whereas it was absent in controls. These findings suggest that cardiac dysfunction in FD could be associated with increased myocardial NO• production and oxidative damage of cardiomyocyte myofilaments and DNA, causing cell dysfunction and death [48].

DNA damage was also verified in leukocytes from FD patients by Biancini et al. [49], who also detected increased ROS formation in these patients - measured by 2′,7′-Dichlorodihydrofluorescein diacetate (DCFH-DA) oxidation. DNA injuries observed in this work had an oxidative origin in purine bases and despite the chronic exposure to oxidative stress has induced repair mechanisms, they were not sufficient to correct DNA damage to normal levels [49].

3.3. Oxidative stress in Niemann-Pick C (NPC)

NPC is an atypical lysosomal storage disease resulting from mutations in one of two genes: *Npc1* (affected in about 95% of families) or *Npc2*. NPC is currently conceived as a lipid trafficking disorder and the impaired egress of cholesterol from the late endosomal/lysosomal compartment is a specific and key element of the pathogenesis. Other lipids, more especially sphingolipids, are also involved, and there are indications for further abnormalities [50]. NPC affect about 1:120,000 live births [51].

NPC is a neurovisceral disease with extreme clinical heterogeneity; about 90% of the patients present a progressive neurodegenerative involvement, with symptoms like: dystonia, dysarthria, dysphagia, ataxia, seizures, gelastic cataplexy, impairment of motor and intellectual function, dementia and premature death. The neuropathology of NPC is characterized by distended neurons, demyelinated axons, reactive astrocytes and microglia, as well as rapid and progressive neuronal loss [52,53,54,55,56]. Although neuronal damage is a major feature of NPC, most patients present considerable hepatic damage [57].

Oxidative stress occurrence was evidenced in NPC by the detection of two cholesterol oxidation products [3β,5α,6β-triol and 7-ketocholesterol (7-KC)] in plasma, which demonstrated to be associated with clinical symptoms onset and disease severity in the NPC1 subjects [58].

Additionally, microarray studies have shown that human NPC fibroblasts exhibit an apoptotic cascade activation and genes induction (like chromogranin A gene) related to the generation of ROS and RNS [59,60]. Chromogranin A protein is a component of Alzheimer's disease plaques and induces nitric oxide efflux from microglia (a key step in neurodegeneration). Likewise, components of the phagocytic NADPH oxidase (CYBB, NCF4), that can generate ROS, were upregulated in NPC fibroblasts. Correspondingly, a number of genes that respond to oxidative stress, such as genes involved in iron homeostasis and copper and zinc transport, were also upregulated in NPC fibroblasts, as well as components of the mitochondrial electron transport chain, what may indicate a compensatory response to a disruption in this chain. Disruption in steady state levels of iron and copper may play a role in oxidative damage, as observed in Alzheimer's disease [61,62].

Fibroblasts from NPC patients also presented increased ROS formation, lipid peroxidation and were more susceptible to cell death through apoptosis, in a process mediated by activation of the Nuclear Factor Kappa B (NF-κB) signaling pathway [63]. These effects were reduced when NPC fibroblasts were treated with allopregnanolone, a neurosteroid which is substantially diminished at birth and decreases further over time in NPC mice. Increased lipid and protein oxidation, measured by TBARS and carbonyl formation, respectively, were also detected in plasma from NPC untreated patients, probably as a consequence of increased ROS generation [64]. Taken together, these results suggest that oxidative stress might contribute to the tissue injury in NPC disease and that allopregnanolone treatment might be beneficial, at least in part, due to its ability to restore the intracellular redox state [63].

Imbalances in important antioxidant systems were also described in NPC disease by different authors. Fu and coworkers [65] showed a diminution in the reduced fraction of CoQ10 in serum of NPC patients when compared to control values. CoQ10 is important for production of chemical energy by the mitochondrial respiratory chain, and the imbalance between its oxidized/reduced forms suggests mitochondrial dysfunction (what can lead to decreased ATP production and increased ROS formation). Reduced CoQ10 is also important to protect membrane proteins, lipids and cholesterol against oxidative injury [66,67,68]. However, in the work of Fu and coworkers [65], the supplementation with CoQ10 was not effective in correcting the decreased fraction of reduced CoQ10, probably because the cycling of oxidized to reduced CoQ10 could be impaired in NPC. In the same work, measurement of serum trolox equivalent antioxidant capacity (TEAC) in NPC patients showed a significant decrease compared to age-matched controls [65].

Corroborating with these findings, it was verified that untreated NPC patients presented reduction of antioxidant defenses (TAS) in relation to healthy subjects, suggesting a poor ability of the tissues in modulating the damage associated with the increased ROS production [64]. The antioxidant activity of GPx was increased in these patients, probably as a compensatory response, since GPx protects cell membranes and essential proteins by removing H_2O_2 and lipid peroxides [7]. CAT activity demonstrated to be reduced in fibroblasts from NPC patients [63], but no differences were observed in erythrocytes [64]. No alterations in the GSH metabolism were described in NPC patients [63,64].

It was reported that NPC patients treated with miglustat, a small iminosugar molecule that acts as a competitive inhibitor of the enzyme glucosylceramide synthase, presented normal levels of TBARS and antioxidant defenses (TAS and erythrocyte GPx activity) in relation to untreated patients, although high levels of protein carbonyl have yet been observed [64]. These findings differ from previous works showing a reduction in TEAC and lower concentrations of reduced and total CoQ10 in miglustat-treated patients [65]. Although the effects of miglustat on antioxidant status need to be better investigated, it is possible that its beneficial effect on lipid damage could be associated with the reduction of intracellular lipid accumulation by this drug, through the inhibition of glucosylceramide synthase.

3.4. Oxidative stress in Gaucher disease (GD)

GD is an autosomal recessive LSD, with estimated overall frequencies of 1–2 in 100,000 live births [38]. All GD patients suffer from mutations in the *Gba* gene encoding the lysosomal beta-glucosidase enzyme (EC. 3.2.1.45), known as glucocerebrosidase (GBA) [69]. In healthy individuals, macrophages use GBA to break down dead cells and cellular debris, but when the enzyme is deficient, fats and carbohydrates accumulate in the macrophage lysosomes in the reticuloendothelial

system [36]. GD is a highly heterogeneous disease exhibiting a wide range of phenotypes. Three main forms have been identified and classified as types I, II and III, depending on their effects in the CNS, their symptomatology and severity. Type I, the most common, is non-neuronopathic, and shows highly variable signs and symptoms and a variable course. Types II and III are neuronopathic. All forms of the disease involve some degree of hepatosplenomegaly, anemia, thrombocytopenia, bone complications and abnormal energetic metabolism [70].

Cellular responses to oxidative stress are complex and coordinate processes involving several signal transducer proteins [71]. The study performed by Deganuto and coworkers [72] have verified significantly increased ROS levels in fibroblasts of Gaucher patients compared to controls, as well as enhanced protein carbonyls. Additionally, the treatment of GD fibroblasts with antioxidants, such as N-acetyl-cysteine (NAC) and dithiothreitol, or with β-glucosidase, caused a significant reduction in intracellular ROS concentrations. APE1/Ref-1 protein plays a central role in ROS-induced cellular effects, such as repairing oxidative damages in DNA and also controlling the activity of several important transcription factors [73]. Increased cytoplasmic amounts of APE1/Ref-1 were observed in GD fibroblasts, but these cells failed to upregulate the expression of this protein upon H_2O_2 treatment [72]. Both ROS and APE1/Ref-1 increases are related to glucosylceramide accumulation, being prevented by treatment of GD fibroblasts with Cerezyme® (recombinant β-glucosidase). The same effects can be induced in healthy fibroblasts with a specific blocker of β-glucosidase, conduritol-β-epoxide [72].

In 2008, Moraitou et al. [74] reported that red blood cell plasmalogen levels were significantly reduced in GD patients compared to non-affected individuals. Plasmalogens constitute 18% of the total phospholipid mass in humans, being abundant in neurons, cardiac and skeletal muscle, and between several functions attributed to these molecules is the protection against oxidative stress [75,76]. This group also verified increased lipid peroxidation and reduced TAS in GD patients, which were correlated with the low concentrations of plasmalogens presented by them. Moreover, negative correlations between plasmalogen levels and glucosylceramide, glucosylceramide/ceramide ratio and glucosylsphingosine were found [77]. So, the role of plasmalogens as "sacrificial antioxidants" has been proposed, once plasmalogens could be oxidized themselves sparing the oxidation of other vulnerable membrane lipids [77].

Since the 1990s, treatment of GD had included ERT using mannose-terminated recombinant human glucocerebrosidase imiglucerase [78]. In this line, the results of Roversi et al. [79] showed that GD patients treated by ERT had an improvement in the antioxidant capacity, which was increased immediately after recombinant enzyme infusion. It was observed higher CAT levels and lower levels of SOD in the blood of ERT-treated GD patients, and an increase in total GSH levels just after ERT.

Additionally, Zahran and coworkers [80] have analyzed the levels of cell-derived microparticles (MPs), lipid peroxide, NO• and trace elements (TEs) in patients with GD, before and after ERT. The results showed that the level of lipid peroxide was significantly higher in patients compared to controls, even after ERT. Although NO• levels were normalized in patients after ERT, zinc (Zn) and copper (Cu) were still diminished. This is important since essential TEs, such as Zn, Cu and selenium (Se), act as cofactors of SOD, CAT and GPX, contributing to both catalytic activity and spatial conformation of these antioxidant enzymes [81]. The percentages of various MPs were significantly higher in GD patients before and after ERT than in healthy individuals [80]. MPs are microvesicles of size < 1.0 mm, released from parent cells during cell activation or apoptosis, and their increase can be associated with oxidative stress [82]. Zahran et al. [80] have also observed positive correlations between chitotriosidase (a chitinase secreted by activated macrophages which is highly increased in GD) with both lipid peroxide and total MPs.

Recently, mutations in the Gba gene have been identified as a risk factor for the development of Parkinson's disease [83,84]. McNeill and coworkers [85] have studied cellular biochemical changes associated with Gba mutations that might predispose to neurodegeneration. The authors analyzed fibroblasts from GD patients and from heterozygous carriers of Gba mutation, with and without Parkinson's disease. Oxidative stress was assayed by single cell imaging of dihydroethidium, which demonstrated increased production of cytosolic ROS in fibroblasts from all studied patients. In the same work, it was reasoned that ambroxol hydrochloride, a small molecule that previously shown to improve glucosylceramidase function in GD, might ameliorate the cellular phenotypes in GD and Gba mutation heterozygotes. The findings indicated that Gba mutations were associated with oxidative stress and that ambroxol could improve lysosomal biochemistry in these cells [85].

4. Therapeutic strategies and antioxidants in LSD

The past two decades have been characterized by remarkable progress in LSD treatment, particularly with the development of innovative therapeutic approaches. These therapies include strategies that aim to increase the activity of a missing enzyme – ERT, hematopoietic stem cell transplantation (HSCT), pharmacological chaperones and gene therapy – and approaches based on reducing the substrates synthesis – substrate reduction therapy [86,87].

Therapies to increase enzyme levels on LSD are based on lysosomal enzymes property to be secreted and uptaken by neighboring cells on the mannose-6-phosphate pathway. After endocytic internalization, the enzyme is transported by endosomes to the lysosome, resulting in the breakdown of accumulated storage material [88]. ERT is conceptually the most successful, straightforward, relatively non-invasive and directly targets the primary enzyme deficiency. ERT is available for a small number of LSD, including non-neuronopathic Gaucher form [89], Fabry [90], MPS I [91], MPS II [92], MPS IV [93] and MPS VI [94]. Owing to the transient nature of ERT, it is typically administered weekly or every other week, which requires a significant time investment (4–5 h infusions) and resources. In addition, lysosomal enzymes generally do not cross the blood-brain barrier, limiting the value of ERT for LSD with significant CNS involvement [88,95]. It should be noted that this kind of treatment brings improvement but not a cure, as it can be observed in the MPS IVA patients under ERT that showed no improvement in 3-min stair climb test [96].

HSCT, using either bone marrow or cord blood, has also been utilized as a treatment for several LSD. The goal of HSCT is to provide a widespread and continuous source of the deficient enzyme from hematopoietic-derived cells with advantages compared to ERT on diseases with cognitive decline as MPS I – Hurler [95]. However, significant risks are associated with this approach, including harsh conditioning regimens and graft-versus-host disease. Although many advances in this treatment over the last 30 years have been reached, its use has been deferred in favor of ERT whenever it is available [97]. Gene therapy may overcome some of these problems, as it may allow constant delivery of the enzyme direct to target organs. LSD are considered good candidates for gene therapy, as they are single gene disorders and not subject to complex regulation mechanisms [98]. In addition, enzyme activity of only 15–20% of the normal level can be sufficient for clinical efficacy, even though different systems may need higher amounts of enzyme to be corrected [88].

Recently, several therapies have been combined in order to target diverse pathogenic mechanisms of LSD in a more effective manner. A promising strategy aims to provide a persistent source of the deficient enzyme, with HSCT and gene therapy, and also targeting a secondary consequence of disease with a more transient approach (substrate reduction, anti-inflammatories, pharmacological mimetic, etc.). This general strategy has resulted in both additive and synergistic effects thereby facilitating improved survival and quality of life [95,99].

Multiple secondary mechanisms play a role in LSD pathogenesis, including secondary metabolites accumulation, altered calcium homeostasis, inflammation, abnormal lipid trafficking, increased autophagy,
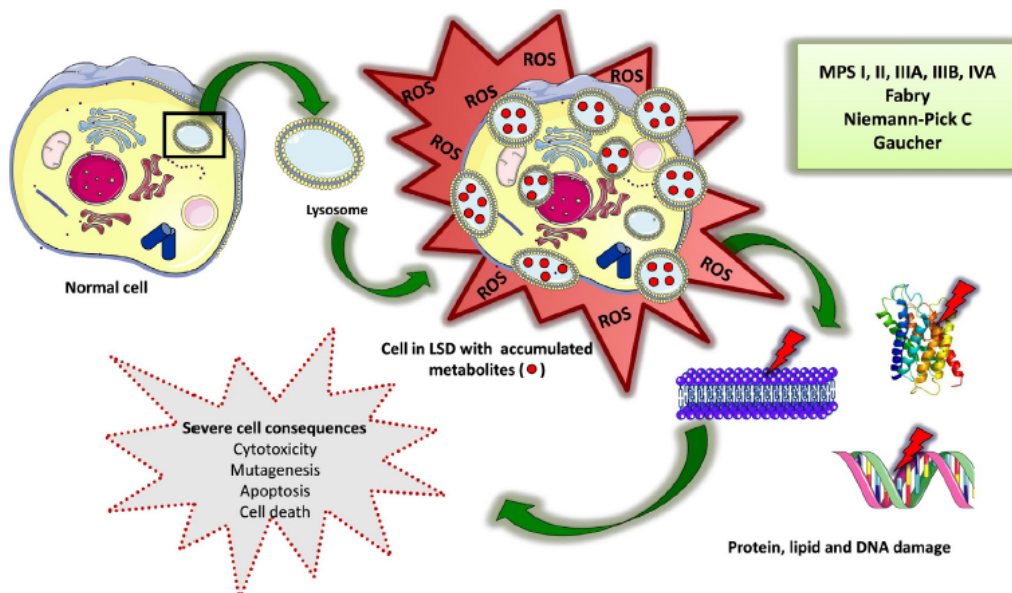
Fig. 1. Metabolites accumulated in LSD cause an increase of lysosomes' number and size, induce an excessive production of ROS/RNS which leads to damage in lipids, proteins, and DNA, causing severe cell consequences. *ROS reactive oxygen species, RNS reactive nitrogen species.*

unfolded protein response, autoimmunity and oxidative stress [95,99]. Contributing to the findings obtained from some in vitro and in vivo studies, in the last years, some works have been demonstrated significative alterations in oxidative stress biomarkers and biochemical profile by antioxidants in LSD-affected patients. In this context, Holmay et al. [100] have reported that acute intravenous administration of NAC, a membrane-permeable Cys precursor which serves as the rate limiting substrate for GSH biosynthesis [101], increased blood GSH redox ratios in patients with Parkinson and GD. It was also observed an increase in GSH brain concentrations, supporting the hypothesis that NAC enhances GSH synthesis in the brain and decreases the GSSG content. The GSSG dissociation by NAC, resulting in a NAC-GS complex and free GSH, could contribute to the transient nature of this change and to have an antioxidant protective effect in these disorders [102].

Matalonga et al. [103] have evaluated whether treatment with CoQ10 and an antioxidant cocktail (α-tocopherol, NAC and α-lipoic acid) were able to ameliorate the biochemical phenotype in cultured fibroblasts of MPS IIIA and IIIB patients. Upon CoQ10 treatment, none of the MPS IIIA fibroblasts enhanced their residual enzymatic activity, but the two B fibroblasts showed a statistically significant increase of their residual activity. The cocktail antioxidant treatment had no effect on the enzymatic activity in all tested fibroblasts cells. Moreover, MPS III A and B fibroblasts showed a GAG accumulation reduction after CoQ10 and antioxidant cocktail treatment with enhanced exocytosis levels. These results might be possible due to the role of CoQ10, α-tocopherol, NAC and α-lipoic acid in maintaining the structure and function of the lysosome, enabling membrane fluidity, protecting this organelle from ROS, acidifying intra- lysosomal medium and restoring calcium homeostasis, which is necessary for the enhanced exocytosis levels [104]. These results are encouraging as some cellular alterations observed in Sanfilippo syndrome can be partially restored by CoQ10 or other antioxidant treatment, but further studies, including those in mouse models are necessary before clinical trials can be considered.

Chemical chaperones have been considered an attractive therapeutic approach for LSD. They are a group of small-molecular-weight compounds that stabilize the conformation of proteins, increase the protein folding capacity of the endoplasmic reticulum and facilitate the trafficking of mutant proteins [105]. Wei et al. [106] have demonstrated that chemical/pharmacological chaperones [trimethylamine N-oxide dihydride (TMAO) and tauroursodeoxycholic acid (TUDCA)] can

alleviate oxidative stress, as well as to protect the cells from undergoing apoptosis by reducing the levels of P-eIF2a and caspase-3, which are apoptosis biomarkers.

The use of antioxidants as adjunctive therapy for some LSD has attracted increasing interest in recent years. One of these promising antioxidants is resveratrol, a natural polyphenol with several beneficial properties, such as anti-inflammatory, antioxidant and neuroprotective effects [107]. Seo and Kim [108] have evaluated the potential therapeutic effects of this compound on primary GD fibroblasts. It is already known that the accumulation of mutant glucocerebrosidase inside the endoplasmic reticulum, in this disease, can lead to a prolonged stress, with impairment in Ca^{2+} homeostasis and mitochondrial dysfunction. This cascade can activate apoptotic enzymes, such as Bax and caspases, leading to cell death [106,109,110]. Resveratrol treatment was able to decrease the expression of apoptotic enzymes and to increase the viability of type I GD cells, in a dose-dependent manner [108]. GD cells treated with resveratrol also exhibited a significant reduction in glucosylceramide concentration and a dose-dependent increase in the expression of acetyl-coenzyme A acetyltransferase 1, an enzyme involved in lipid metabolism. The increased expression of acetyl-coenzyme A acetyltransferase 1 indicates that acetyl-CoA, the byproduct of glucosylceramide degradation, can be used to produce acetoacetyl-CoA, which can be utilized to make molecules necessary for cell survival, growth, and/or proliferation via the mevalonate pathway [108].

The authors also observed an increase in the expression of E3-binding protein and citrate synthase, which are enzymes related to the carbohydrate metabolism and citric acid cycle. Therefore, resveratrol is involved not only in the reduction of apoptotic events and glucosylceramide levels in GD cells, but also is able to modulate the expression of enzymes linked to glucose and lipid metabolism [108].

5. Concluding remarks

LSD are caused by the defective activity of lysosomal enzymes, leading to accumulation of unmetabolized substrates. As a result, a variety of pathogenic cascades are activated such as oxidative stress, inflammation, altered lipid trafficking and autophagy. Some of these pathways are common to many LSD, whereas others are only altered in a subset of them. It is presumed that metabolites accumulated in LSD cause an increase of lysosomes' number and size, which may induce excessive

143

production of reactive species and/or deplete the tissue antioxidant capacity, leading to damage in biomolecules (lipids, proteins, and DNA) (Fig. 1).

In this review, it was presented in vitro and in vivo evidence that oxidative stress occurs in LSD, even when patients are undergoing therapy. Considering the deleterious effects provoked by the excess of oxidative species in the cells, it is possible to suggest that, in the future, antioxidants will probably represent promising adjuvant therapy for many of these disorders.

Conflict of interest

The authors declare that they have no conflict of interest.

Acknowledgements

References

[1] A.H. Futerman, G. van Meer, The cell biology of lysosomal storage disorders, Nat. Rev. Mol. Cell. 5 (2004) 554–565.

[2] P. Saftig, J. Klumperman, Lysosome biogenesis and lysosomal membrane proteins: trafficking meets function, Nat. Rev. Mol. Cell Biol. 10 (2009) 623–635.

[3] E.B. Vitner, F.M. Platt, A.H. Futerman, Common and uncommon pathogenic cascades in lysosomal storage diseases, J. Biol. Chem. 285 (2010) 20423–20427.

[4] B.A. Heese, Current strategies in the management of lysosomal storage diseases, Semin. Pediatr. Neurol. 15 (2008) 119–126.

[5] S.D.K. Kigma, O.A. Bodamer, F.A. Wijburg, Epidemiology and diagnosis of lysosomal storage disorders: challenges of screening, Best Pract. Res. Clin. Endocrinol. Metab. 29 (2015) 145–157.

[6] A. Terman, U.T. Brunk, Oxidative stress, accumulation of biological 'garbage', and aging, Antioxid. Redox Signal. 8 (2006) 197–204.

[7] B. Halliwell, J.M.C. Gutteridge, Free Radicals in Biology and Medicine, Oxford University, Oxford, 2007.

[8] B. Halliwell, Free radicals, antioxidants, and human disease: curiosity, cause or consequence? Lancet 344 (1994) 721–724.

[9] W. Dröge, Free radicals in the physiological control of cell function, Physiol. Rev. 82 (2002) 47–95.

[10] I. Fridovich, Fundamental aspects of reactive oxygen species, or what's the matter with oxygen, Ann. N. Y. Acad. Sci. 893 (1999) 13–18.

[11] B. Halliwell, Antioxidant in human health and disease, Annu. Rev. Nutr. 16 (1996) 33–50.

[12] L.A. Clarke, The mucopolysaccharidoses: a success of molecular medicine, Expert. Rev. Mol. Med. 10 (2008), e1. .

[13] E.F. Neufeld, J. Muenzer, The mucopolysaccharidoses, in: C.R. Scriver, A.L. Beaudet, W.S. Sly, D. Valle (Eds.), The Metabolic and Molecular Bases of Inherited Disease, eighth ed.McGraw-Hill Inc., New York 2001, pp. 3421–3452.

[14] V. Gieselmann, Lysosomal storage diseases, Biochim. Biophys. Acta 1270 (1995) 103–136.

[15] R. Pinto, C. Caseiro, M. Lemos, et al., Prevalence of lysosomal storage diseases in Portugal, Eur. J. Hum. Genet. 12 (2004) 87–92.

[16] F. Baehner, C. Schmiedeskamp, F. Krummenauer, et al., Cumulative incidence rates of the mucopolysaccharidoses in Germany, J. Inherit. Metab. Dis. 28 (2005) 1011–1017.

[17] I.D. Young, P.S. Harper, Incidence of Hunter's syndrome, Hum. Genet. 60 (1982) 391–392.

[18] B.A. Baldo, Enzymes approved for human therapy: indications, mechanisms and adverse effects, BioDrugs 29 (2015) 31–55.

[19] R. Giugliani, S. Herber, L. Lapagesse, C. de Pinto, G. Baldo, et al., Pediatr. Endocrinol. Rev. 12 (Suppl. 1) (2014) 152–158.

[20] S. Tomatsu, A.M. Montaño, H. Oikawa, et al., Mucopolysaccharidosis type IVA (Morquio A disease): clinical review and current treatment: a special review, Curr. Pharm. Biotechnol. 12 (2011) 931–945.

[21] T. Okuyama, A. Tanaka, Y. Suzuki, et al., Japan Elaprase® Treatment (JET) study: idursulfase enzyme replacement therapy in adult patients with attenuated Hunter syndrome (mucopolysaccharidosis II, MPS II), Mol. Genet. Metab. 99 (2010) 18–25.

[22] J.E. Wraith, L.A. Clarke, M. Beck, et al., Enzyme replacement therapy for mucopolysaccharidosis I: a randomized, placebo-controlled, multinational study of recombinant human α-L-iduronidase (laronidase), J. Pediatr. 144 (2004) 581–588.

[23] V.G. Pereira, A.M. Martins, C. Micheletti, V. D'Almeida, Mutational and oxidative stress analysis in patients with mucopolysaccharidosis type I undergoing enzyme replacement therapy, Clin. Chim. Acta 387 (2008) 75–79.

[24] L. Filippon, C.S. Vanzin, G.B. Biancini, et al., Oxidative stress in patients with mucopolysaccharidosis type II before and during enzyme replacement therapy, Mol. Genet. Metab. 103 (2011) 121–127.

[25] C.E.D. Jacques, B. Donida, C.P. Mescka, et al., Oxidative and nitrative stress and pro-inflammatory cytokines in Mucopolysaccharidosis type II patients: effect of long-term enzyme replacement therapy and relation with glycosaminoglycan accumulation, Biochim. Biophys. Acta 1862 (2016) 1608–1616.

[26] I. Dalle-Donne, G. Aldini, M. Carini, R. Colombo, R. Rossi, A. Milzani, Protein carbonylation, cellular dysfunction, and disease progression, J. Cell. Mol. Med. 10 (2006) 389–406.

[27] B. Tudek, A. Winczura, J. Janik, A. Siomek, M. Foksinski, R. Oliński, Involvement of oxidatively damaged DNA and repair in cancer development and aging, Am. J. Transl. Res. 2 (2010) 254–284.

[28] R. De Bont, N. van Larebeke, Endogenous DNA damage in humans: a review of quantitative data, Mutagenesis 19 (2004) 169–185.

[29] L. Filippon, C.A. Wayhs, D.M. Atik, et al., DNA damage in leukocytes from pretreatment mucopolysaccharidosis type II patients: protective effect of enzyme replacement therapy, Mutat. Res. 721 (2011) 206–210.

[30] G.W. Negretto, M. Deon, G.B. Biancini, M.G. Burin, R. Giugliani, C.R. Vargas, Glycosaminoglycans can be associated with oxidative damage in mucopolysaccharidosis II patients submitted to enzyme replacement therapy, Cell Biol. Toxicol. 30 (2014) 189–193.

[31] L.A. Van der Veen, M.F. Hashim, Y. Shyr, L.J. Marnett, Induction of frameshift and base pair substitution mutations by the major DNA adduct of the endogenous carcinogen malondialdehyde, Proc. Natl. Acad. Sci. U. S. A. 100 (2003) 14247–14252.

[32] R.K. Olsen, N. Cornelius, N. Gregersen, Redox signalling and mitochondrial stress responses: lessons from inborn errors of metabolism, J. Inherit. Metab. Dis. 38 (2015) 703–719.

[33] H.S. Marinho, C. Real, L. Cyrne, H. Soares, F. Antunes, Hydrogen peroxide sensing, signaling and regulation of transcription factors, Redox Biol. 2 (2014) 535–562.

[34] B. Donida, D.P. Marchetti, G.B. Biancini, et al., Oxidative stress and inflammation in mucopolysaccharidosis type IVA patients treated with enzyme replacement therapy, Biochim. Biophys. Acta 1852 (2015) 1012–1019.

[35] G.W. Negretto, M. Deon, M. Burin, et al., In vitro effect of genistein on DNA damage in leukocytes from mucopolysaccharidosis IVA patients, Mol. Genet. Metab. 111 (2014) 205–208.

[36] C.R. Scriver, W.A. Sly, A.L. Beaudet, D. Valle, The Metabolic and Molecular Bases of Inherited Disease, McGraw-Hill Inc., New York, 2001.

[37] R.J. Desnick, Y.A. Ioannou, C.M. Eng, α-Galactosidase A deficiency: Fabry disease, in: C.R. Scriver, W.A. Sly, A.L. Beaudet, D. Valle (Eds.), The Metabolic and Molecular Bases of Inherited Disease, McGraw-Hill Inc, New York 2001, pp. 3733–3774.

[38] M.J. Ferraz, W.W. Kallemeijn, M. Mirzaian, et al., Gaucher disease and Fabry disease: new markers and insights in pathophysiology for two distinct glycosphingolipidoses, Biochim. Biophys. Acta 1841 (2014) 811–825.

[39] U.T. Brunk, J. Neuzil, J.W. Eaton, Lysosomal involvement in apoptosis, Redox Rep. 6 (2001) 91–97.

[40] G.B. Biancini, C.S. Vazin, D.B. Rodrigues, et al., Globotriaosylceramide is correlated with oxidative stress and inflammation in Fabry patients treated with enzyme replacement therapy, Biochim. Biophys. Acta 2012 (1822) 226–232.

[41] J. Shen, X. Meng, D.F. Moore, et al., Globotriaosylceramide induces oxidative stress and up-regulates cell adhesion molecule expression in Fabry disease endothelial cells, Mol. Genet. Metab. 95 (2008) 163–168.

[42] G.B. Biancini, C.E. Jacques, T. Hammerschmidt, et al., Biomolecules damage and redox status abnormalities in Fabry patients before and during enzyme replacement therapy, Clin. Chim. Acta 461 (2016) 41–46.

[43] D.F. Moore, F. Ye, M.L. Brennan, et al., Ascorbate decreases Fabry cerebral hyperperfusion suggesting a reactive oxygen species abnormality: an arterial spin tagging study, J. Magn. Reson. Imaging 20 (2004) 674–683.

[44] R. Zhang, M.L. Brennan, X. Fu, et al., Association between myeloperoxidase levels and risk of coronary artery disease, JAMA 286 (2001) 2136–2142.

[45] S.D. Swain, T.T. Rohn, M.T. Quinn, Neutrophil priming in host defense: role of oxidants as priming agents, Antioxid. Redox Signal. 4 (2002) 69–83.

[46] E.P. Wei, H.A. Kontos, J.S. Beckman, Mechanisms of cerebral vasodilation by superoxide, hydrogen peroxide, and peroxynitrite, Am. J. Physiol. Heart Circ. Physiol. 271 (1996) H1262–H1266.

[47] K.B. Müller, L.C. Galdieri, V.G. Pereira, A.M. Martins, V. D'Almeida, Evaluation of oxidative stress markers and cardiovascular risk factors in Fabry disease patients, Genet. Mol. Biol. 35 (2012) 418–423.

[48] C. Chimenti, F.E. Scopelliti, E. Vulpis, et al., Increased oxidative stress contributes to cardiomyocyte dysfunction and death in patients with Fabry disease cardiomyopathy, Hum. Pathol. 46 (11) (2015) 1760–1768.

[49] G.B. Biancini, D.J. Moura, P.R. Manini, J.L. Faverzani, C.B. Netto, M. Deon, R. Giugliani, J. Saffi, C.R. Vargas, DNA damage in Fabry patients: an investigation of oxidative damage and repair, Mutat. Res. Genet. Toxicol. Environ. Mutagen. 784-785 (2015) 31–36.

[50] M.T. Vanier, Complex lipid trafficking in Niemann-Pick disease type C, J. Inherit. Metab. Dis. 38 (2015) 187–199.

[51] E. Mengel, H.H. Klünemann, C.M. Lourenço, et al., Niemann-Pick disease type C symptomatology: an expert-based clinical description, Orphanet J. Rare Dis. 8 (2013) 166.

[52] M. Baudry, Y. Yao, D. Simmons, J. Liu, X. Bi, Postnatal development of inflammation in a murine model of Niemann-Pick type C disease: immunohistochemical observations of microglia and astroglia, Exp. Neurol. 184 (2003) 887–903.

[53] H. Suzuki, T. Sakiyama, N. Harada, M. Abe, M. Tadokoro, Pathologic changes of glial cells in murine model of Niemann-Pick disease type C: immunohistochemical, lectin-histochemical and ultrastructural observations, Pediatr. Int. 45 (2003) 1–4.

[54] C.A. Paul, A.K. Boegle, R.A. Maue, Before the loss: neuronal dysfunction in Niemann-Pick Type C disease, Biochim. Biophys. Acta 1685 (2004) 63–76.

[55] S.L. Sturley, M.C. Patterson, W. Balch, L. Liscum, The pathophysiology and mechanisms of NP-C disease, Biochim. Biophys. Acta 1685 (2004) 83–87.

[56] S.U. Walkley, K. Suzuki, Consequences of NPC1 and NPC2 loss of function in mammalian neurons, Biochim. Biophys. Acta 1685 (2004) 48–62.

[57] L. Liscum, J.J. Klansek, Niemann-Pick disease type C, Curr. Opin. Lipidol. 9 (1998) 131–135.

[58] F.D. Porter, D.E. Scherrer, M.H. Lanier, et al., Cholesterol oxidation products are sensitive and specific blood-based biomarkers for Niemann-Pick C1 disease, Sci. Transl. Med. 2 (2010) 56ra81.

[59] J.V. Reddy, I.G. Ganley, S.R. Pfeffer, Clues to neurodegeneration in Niemann-Pick type C disease from global gene expression profiling, PLoS One 1 (2006), e19. .

[60] A. De Windt, M. Rai, L. Kytömäki, et al., Gene set enrichment analyses revealed several affected pathways in Niemann-Pick disease type C fibroblasts, DNA Cell Biol. 26 (2007) 665–671.

[61] M.A. Smith, P.L. Harris, L.M. Sayre, G. Perry, Iron accumulation in Alzheimer disease is a source of redox-generated free radicals, Proc. Natl. Acad. Sci. U. S. A. 94 (1997) 9866–9868.

[62] M.A. Lovell, J.D. Robertson, W.J. Teesdale, J.L. Campbell, W.R. Markesbery, Copper, iron and zinc in Alzheimer's disease senile plaques, J. Neurol. Sci. 158 (1998) 47–52.

[63] S. Zampieri, S.H. Mellon, T.D. Butters, M. Nevyjel, D.F. Covey, B. Bembi, A. Dardis, Oxidative stress in NPC1 deficient cells: protective effect of allopregnanolone, J. Cell. Mol. Med. 13 (2009) 3786–3796.

[64] G.S. Ribas, R. Pires, J.C. Coelho, et al., Oxidative stress in Niemann-Pick type C patients: a protective role of N-butyl-deoxynojirimycin therapy, Int. J. Dev. Neurosci. 6 (2012) 439–444.

[65] R. Fu, N.M. Yanjanin, S. Bianconi, W.J. Pavan, F.D. Porter, Oxidative stress in Niemann-Pick disease, type C, Mol. Genet. Metab. 101 (2–3) (2010) 214–218.

[66] R.E. Beyer, J. Segura-Aguilar, S. Di Bernardo, et al., The role of DT-diaphorase in the maintenance of the reduced antioxidant form of coenzyme Q in membrane systems, Proc. Natl. Acad. Sci. U. S. A. 93 (1996) 2528–2532.

[67] K.U. Ingold, V.W. Bowry, R. Stocker, C. Walling, Autoxidation of lipids and antioxidation by alpha-tocopherol and ubiquinol in homogeneous solution and in aqueous dispersions of lipids: unrecognized consequences of lipid particle size as exemplified by oxidation of human low density lipoprotein, Proc. Natl. Acad. Sci. U. S. A. 90 (1993) 45–49.

[68] V.W. Bowry, D. Mohr, J. Cleary, R. Stocker, Prevention of tocopherol-mediated peroxidation in ubiquinol-10-free human low density lipoprotein, J. Biol. Chem. 270 (1995) 5756–5763.

[69] A.D. Patrick, A deficiency of glucocerebrosidase in Gaucher's disease, Biochem. J. 97 (1965) 17c–18c.

[70] G.A. Grabowski, Gaucher disease: lessons from a decade of therapy, J. Pediatr. 144 (2004) S15–S19.

[71] T. Finkel, Oxidant signals and oxidative stress, Curr. Opin. Cell Biol. 15 (2003) 247–254.

[72] M. Deganuto, M.G. Pittis, A. Pines, et al., Altered intracellular redox status in Gaucher disease fibroblasts and impairment of adaptive response against oxidative stress, J. Cell. Physiol. 212 (2007) 223–235.

[73] G. Tell, G. Damante, D. Caldwell, M.R. Kelley, The intracellular localization of APE1/Ref-1: more than a passive phenomenon? Antioxid. Redox Signal. 7 (2005) 367–384.

[74] M. Moraitou, E. Dimitriou, D. Zafeiriou, C. Reppa, T. Marinakis, J. Sarafidou, H. Michelakakis, Plasmalogen levels in Gaucher disease, Blood Cells Mol. Dis. 41 (2008) 196–199.

[75] A.A. Farooqui, L.A. Horrocks, Plasmalogens: workhorse lipids of membranes in normal and injured neurons and glia, Neuroscientist 7 (2001) 232–245.

[76] N. Nagan, R.A. Zoeller, Plasmalogens biosynthesis and functions, Prog. Lipid Res. 40 (2001) 199–229.

[77] M. Moraitou, E. Dimitriou, N. Dekker, I. Monopolis, J. Aerts, H. Michelakakis, Gaucher disease: plasmalogen levels in relation to primary lipid abnormalities and oxidative stress, Blood Cells Mol. Dis. 53 (2014) 30–33.

[78] A.H. Futerman, J.L. Sussman, M. Horowitz, I. Silman, A. Zimran, New directions in the treatment of Gaucher disease, Trends Pharmacol. Sci. 25 (2004) 147–151.

[79] F.M. Roversi, L.C. Galdieri, B.H.C. Grego, et al., Blood oxidative stress markers in Gaucher disease patients, Clin. Chim. Acta 364 (2006) 316–320.

[80] A.M. Zahran, K.I. Elsayh, S.E.M. El-Deek, M.A.H. El-Baz, Oxidative stress, trace elements and circulating microparticles in patients with Gaucher disease before and after enzyme replacement therapy, Clin. Appl. Thromb. Hemost. 21 (2015) 58–65.

[81] S. Kalkan Ucar, M. Coker, E. Sozmen, S. Goksen Simsek, S. Darcan, An association among iron, copper, zinc, and selenium, and antioxidative status in dyslipidemic pediatric patients with glycogen storage disease types IA and III, J. Trace Elem. Med. Biol. 24 (2010) 42–45.

[82] O. Helal, C. Defoort, S. Robert, et al., Increased levels of microparticles originating from endothelial cells, platelets and erythrocytes in subjects with metabolic syndrome: relationship with oxidative stress, Nutr. Metab. Cardiovasc. Dis. 21 (2011) 665–671.

[83] E. Sidransky, M.A. Nalls, J.O. Aasly, et al., Multicenter analysis of glucocerebrosidase mutations in Parkinson's disease, N. Engl. J. Med. 361 (2009) 1651–1661.

[84] E. Sidransky, G. Lopez, The link between the GBA gene and parkinsonism, Lancet Neurol. 11 (2012) 986–998.

[85] A. McNeill, J. Magalhaes, C. Shen, Ambroxol improves lysosomal biochemistry in glucocerebrosidase mutation-linked Parkinson disease cells, Brain 137 (2014) 1481–1495.

[86] R.J. Desnick, E.H. Schuchman, Enzyme replacement and enhancement therapies: lessons from lysosomal disorders, Nat. Rev. Genet. 3 (2002) 954–966.

[87] G. Parenti, G. Andria, A. Ballabio, Lysosomal storage diseases: from pathophysiology to therapy, Annu. Rev. Med. 66 (2015) 471–486.

[88] U. Matte, V.L. Lagranha, T.G. de Carvalho, F.Q. Mayer, R. Giugliani, Cell microencapsulation: a potential tool for the treatment of neuronopathic lysosomal storage diseases, J. Inherit. Metab. Dis. 34 (2011) 983–990.

[89] J. Charrow, C.R. Scott, Long-term treatment outcomes in Gaucher disease, Am. J. Hematol. 90 (Suppl. 1) (2015) S19–S24.

[90] R. Schiffmann, C. Swift, X. Wang, D. Blankenship, M. Ries, A prospective 10-year study of individualized, intensified enzyme replacement therapy in advanced Fabry disease, J. Inherit. Metab. Dis. 38 (2015) 1129–1136.

[91] A.D. Domelles, L.L. de Camargo Pinto, A.C. de Paula, et al., Enzyme replacement therapy for Mucopolysaccharidosis Type I among patients followed within the MPS Brazil Network, Genet. Mol. Biol. 37 (2014) 23–29.

[92] A. Tylki-Szymańska, Mucopolysaccharidosis type II, Hunter's syndrome, Pediatr. Endocrinol. Rev. Suppl. 1 (2014) 107–113.

[93] D.D. Horovitz, T.S. Magalhães, A. Acosta, et al., Enzyme replacement therapy with galsulfase in 34 children younger than five years of age with MPS VI, Mol. Genet. Metab. 109 (2013) 62–69.

[94] J. Politei, A.B. Schenone, N. Guelbert, A. Fainboim, M. Szlago, Morquio disease (Mucopolysaccharidosis type IV-A): clinical aspects, diagnosis and new treatment with enzyme replacement therapy, Arch. Argent. Pediatr. 113 (2015) 359–364.

[95] J.A. Hawkins-Salsbury, A.S. Reddy, M.S. Sands, Combination therapies for lysosomal storage disease: is the whole greater than the sum of its parts? Hum. Mol. Genet. 20 (2011) R54–R60.

[96] C.J. Hendriksz, B. Burton, T.R. Fleming, et al., Efficacy and safety of enzyme replacement therapy with BMN 110 (elosulfase alfa) for Morquio A syndrome (mucopolysaccharidosis IVA): a phase 3 randomised placebo-controlled study, J. Inherit. Metab. Dis. 37 (2014) 979–990.

[97] T.C. Lund, Hematopoietic stem cell transplant for lysosomal storage diseases, Pediatr. Endocrinol. Rev. Suppl. 1 (2013) 91–98.

[98] D.P. Rastall, A. Amalfitano, Recent advances in gene therapy for lysosomal storage disorders, Appl. Clin. Genet. 8 (2015) 157–169.

[99] S. Ortolano, I. Viéitez, C. Navarro, C. Spuch, Treatment of lysosomal storage diseases: recent patents and future strategies, Recent Pat. Endocr. Metab. Immune. Drug Discov. 8 (2014) 9–25.

[100] M.J. Holmay, M. Terpstra, L.D. Coles, et al., N-acetylcysteine boosts brain and blood glutathione in Gaucher and Parkinson diseases, Clin. Neuropharmacol. 36 (2013) 103–106.

[101] S. Whillier, J.E. Raftos, B. Chapman, P.W. Kuchel, Role of N-acetylcysteine and cystine in glutathione synthesis in human erythrocytes, Redox Rep. 14 (2009) 115–124.

[102] J.C. Adair, J.E. Knoefel, N. Morgan, Controlled trial of N-acetylcysteine for patients with probable Alzheimer's disease, Neurology 57 (2001) 1515–1517.

[103] L. Matalonga, A. Arias, M.J. Coll, J. Garcia-Villoria, L. Gort, A. Ribes, Treatment effect of coenzyme Q(10) and an antioxidant cocktail in fibroblasts of patients with Sanfilippo disease, J. Inherit. Metab. Dis. 37 (2014) 439–446.

[104] F.M. Platt, B. Boland, A.C. van der Spoel, The cell biology of disease: lysosomal storage disorders: the cellular impact of lysosomal dysfunction, J. Cell Biol. 199 (2012) 723–734.

[105] Y. Suzuki, Chaperone therapy update: Fabry disease, GM1-gangliosidosis and Gaucher disease, Brain Dev. 35 (2013) 515–523.

[106] H. Wei, S.J. Kim, Z. Zhang, P.C. Tsai, K.E. Wisniewski, A.B. Mukherjee, ER and oxidative stresses are common mediators of apoptosis in both neurodegenerative and non-neurodegenerative lysosomal storage disorders and are alleviated by chemical chaperones, Hum. Mol. Genet. 17 (2008) 469–477.

[107] T. Yang, L. Wang, M. Zhu, L. Zhang, L. Yan, Properties and molecular mechanisms of resveratrol a review, Pharmazie 70 (2015) 501–506.

[108] C.H. Seo, J.B. Kim, Therapeutic potential of resveratrol in type I Gaucher disease, Phytother. Res. 29 (2015) 835–839.

[109] R. Bravo, T. Gutierrez, F. Paredes, et al., Endoplasmic reticulum: ER stress regulates mitochondrial bioenergetics, Int. J. Biochem. Cell Biol. 44 (2012) 16–20.

[110] E. Szegezdi, S. Logue, A. Gorman, A. Samali, Mediators of endoplasmic reticulum stress-induced apoptosis, EMBO Rep. 7 (2006) 880–885.

ANEXO II – Carta de aprovação do projeto.

COMISSÃO CIENTÍFICA

A Comissão Científica do Hospital de Clínicas de Porto Alegre analisou o projeto:

Projeto: 150468
Data da Versão do Projeto: 06/10/2015

Pesquisadores:
CARMEN REGLA VARGAS
ROBERTO GIUGLIANI
FERNANDA POLETTO
DESIREE PADILHA MARCHETTI

Título: Desenvolvimento de nanopartícula com B-ciclodextrina e vitamina B6 e avaliação in vitro de seu potencial terapêutico para tratamento da doença de Niemann-Pick C.

Este projeto foi APROVADO em seus aspectos éticos, metodológicos, logísticos e financeiros para ser realizado no Hospital de Clínicas de Porto Alegre.
Esta aprovação está baseada nos pareceres dos respectivos Comitês de Ética e do Serviço de Gestão em Pesquisa.

- Os pesquisadores vinculados ao projeto não participaram de qualquer etapa do processo de avalição de seus projetos.

- O pesquisador deverá apresentar relatórios semestrais de acompanhamento e relatório final ao Grupo de Pesquisa e Pós-Graduação (GPPG)

Porto Alegre, 03 de novembro de 2015.

Prof. José Roberto Goldim
Coordenador CEP/HCPA

ANEXO III – Termo de consentimento livre e esclarecido para pacientes Niemann-Pick C.

Termo de Consentimento Livre e Esclarecido: pacientes com doença de Niemann-Pick C

Projeto de Pesquisa: Desenvolvimento de nanopartícula com β-ciclodextrina e vitamina B_6 e avaliação *in vitro* de seu potencial terapêutico para tratamento da doença de Niemann-Pick C.

Você, portador de Niemann-Pick C, está sendo convidado(a) a participar deste projeto que tem por objetivo criar um novo tratamento para a sua doença. Este tratamento será baseado no desenvolvimento de um medicamento feito com partículas muito pequenas capazes de chegar no cérebro e diminuir o colesterol em excesso, o qual é o responsável pelos sintomas da doença.

Os dados necessários para a realização do projeto serão obtidos através de entrevistas realizadas com você (portador de Niemann-Pick C) durante consultas médicas no Centro de Pesquisa Clínica/HCPA e através da biópsia de pele (coleta de um pequeníssimo pedaço de pele) solicitada no momento da consulta com o seu médico, a qual é utilizada para o seu acompanhamento clínico. Caso sejam necessários dados adicionais estes serão obtidos no seu prontuário do Hospital.

Para participar do estudo será coletado sangue, urina e pele em frascos específicos. No momento da coleta de sangue poderá haver alguma dor em decorrência da punção da pele. Complicações de coleta de sangue são raras e geralmente simples. Se houver vazamento de sangue da veia no local da punção poderá se formar uma mancha roxa (hematoma) e um pequeno desconforto que desaparece em poucos dias. Para a coleta de fibroblastos, você receberá uma anestesia tópica (cremes anestésicos) e o procedimento se dará através da retirada de um pequeníssimo fragmento de pele através de uma biópsia. As coletas de sangue e biópsia de pele serão realizadas por profissionais especialmente treinados para este fim, o que diminui as chances de complicações. As coletas de urina serão feitas pelo próprio paciente ou com o auxílio de profissionais treinados.

Após o término deste estudo, os seus materiais biológicos coletados poderão ser descartados ou mantidos para futuras pesquisas, se isso for autorizado por você.

Com relação ao uso dos materiais biológicos, ao final deste estudo, você (marque com um X):

( ) autoriza o armazenamento.

( ) não autoriza o armazenamento, solicitando que sejam descartados.

Você tem direito à privacidade. Os resultados deste estudo poderão ser publicados em revistas científicas, mas o seu nome não será revelado. Por meio deste termo, você autoriza que os pesquisadores envolvidos neste estudo pesquisem os seus registros médicos a fim de obter as informações clínicas necessárias para a realização desta pesquisa. Sua participação no estudo é **voluntária**. **Se você decidir não participar do estudo, isto não afetará em nada o seu tratamento no hospital.** A participação pode também ser interrompida a qualquer momento por você mesmo(a). Em qualquer caso, não terá penalização.

É importante ressaltar que você não receberá nenhum tipo de pagamento pela participação no estudo e que todas as despesas relacionadas ao custo dos exames laboratoriais serão cobertas por verbas do próprio projeto de pesquisa, portanto, serão completamente gratuitas para você. Este estudo pode contribuir no futuro, para um tratamento mais efetivo para os pacientes com a doença de Niemann-Pick C. Não existe um prazo exato ou estipulado para que você receba os resultados do estudo, mas estes lhes serão informados assim que estiverem disponíveis.

Os pesquisadores responsáveis pelo estudo (Profª Drª Carmen Regla Vargas e a doutoranda Bruna Donida) estarão à disposição para o esclarecimento de qualquer dúvida durante todo o andamento da pesquisa, no serviço de Genética Médica do HCPA localizado no 3º andar, Fone: (51) 3359.8011. Ainda, para maiores informações, você pode contatar o Comitê de Ética em Pesquisa do HCPA, através do telefone (51) 3359.7640, das 8h às 17h, de segunda a sexta-feira.

Este documento será elaborado em duas vias, sendo que uma delas será entregue a você, participante da pesquisa, e a outra será mantida com o nosso grupo de pesquisa.

Pelo presente consentimento, declaro que fui devidamente informado sobre o projeto de pesquisa, de forma clara e detalhada, da liberdade de não participar do estudo e tive minhas dúvidas esclarecidas.

2

Data:_____

Nome do indivíduo e assinatura:_____

Nome do responsável legal e assinatura:_____

Nome do pesquisador e assinatura:_____

ANEXO IV – Termo de consentimento livre e esclarecido para indivíduos controle.

Termo de Consentimento Livre e Esclarecido: indivíduos controle

Projeto de Pesquisa: Desenvolvimento de nanopartícula com β-ciclodextrina e vitamina B_6 e avaliação *in vitro* de seu potencial terapêutico para tratamento da doença de Niemann-Pick C.

Você está sendo convidado(a) a participar deste projeto que tem por objetivo criar um novo tratamento para uma doença genética chamada de Niemann-Pick C. Este tratamento será baseado no desenvolvimento de um medicamento feito com partículas muito pequenas capazes de chegar no cérebro e diminuir o colesterol em excesso, o qual é o responsável pelos sintomas da doença. Para que este estudo seja realizado, é necessária uma comparação entre um grupo de pacientes que apresentam a doença com um grupo de pacientes que não apresentam. Você, portanto, está sendo convidado a participar deste estudo como controle, ou seja, como **NÃO** portador da doença de Niemann-Pick C.

Para participar do estudo será coletado sangue periférico, urina e um pequeno fragmento de pele (biópsia) em frascos específicos durante a consulta de rotina no Hospital de Clínicas de Porto Alegre. No momento da coleta de sangue poderá haver alguma dor em decorrência da punção da pele. Complicações de coleta de sangue são raras e geralmente são simples. Se houver vazamento de sangue da veia no local da punção poderá se formar uma mancha roxa (hematoma) e um pequeno desconforto que desaparece em poucos dias. Para a biópsia de pele, você receberá uma anestesia tópica (cremes anestésicos) e o procedimento se dará através da retirada de um pequeníssimo fragmento de pele através de uma biópsia. As coletas de sangue e a biópsia de pele serão realizadas por profissionais especialmente treinados para este fim, o que diminui as chances de complicações. As coletas de urina serão feitas pelo próprio indivíduo ou com o auxílio de profissionais treinados.

Após o término deste estudo, os seus materiais biológicos coletados poderão ser descartados ou mantidos para futuras pesquisas, se isso for autorizado por você. Com relação ao uso dos materiais biológicos, ao final deste estudo, você (marque com um X):

1

( ) autoriza o armazenamento.

( ) não autoriza o armazenamento, solicitando que sejam descartados.

Você tem direito à privacidade. Os resultados deste estudo poderão ser publicados em revistas científicas, mas o seu nome não será revelado. Sua participação no estudo é voluntária. A participação pode também ser interrompida a qualquer momento por você mesmo(a). Em qualquer caso, não terá penalização.

É importante ressaltar que você não receberá nenhum tipo de pagamento pela participação no estudo e que todas as despesas relacionadas ao custo dos exames laboratoriais serão cobertas por verbas do próprio projeto de pesquisa, portanto, serão completamente gratuitas para você. A sua participação neste estudo não trará benefício direto a você, porém, os dados advindos com a sua doação são de importância científica relevante para o estabelecimento de novos tratamentos para esta doença, bem como para o melhor entendimento da mesma.

Os pesquisadores responsáveis pelo estudo (Profª Drª Carmen Regla Vargas e a doutoranda Bruna Donida) estarão à disposição para o esclarecimento de qualquer dúvida durante todo o andamento da pesquisa, no serviço de Genética Médica do HCPA localizado no 3º andar, Fone: (51)3359.8011. Ainda, para maiores informações, você pode contatar o Comitê de Ética em Pesquisa do HCPA, através do telefone (51) 3359.7640, das 8h às 17h de segunda a sexta-feira.

Este documento será elaborado em duas vias, sendo que uma delas será entregue a você, participante da pesquisa, e a outra será mantida com o nosso grupo de pesquisa.

Pelo presente consentimento, declaro que fui devidamente informado sobre o projeto de pesquisa, de forma clara e detalhada, da liberdade de não participar do estudo e tive minhas dúvidas esclarecidas.

Data:_____

Nome do indivíduo e assinatura:_____

Nome do responsável legal e assinatura:_____

Nome do pesquisador e assinatura:_____

2

ANEXO V - Lista de artigos científicos publicados durante o doutorado

1. POLETTO, FERNANDA S.; DE OLIVEIRA, CATIÚSCIA P.; WENDER, HEBERTON; REGENT, DOROTHÉE; **DONIDA, BRUNA**; TEIXEIRA, SÉRGIO R.; GUTERRES, SÍLVIA S.; ROSSI-BERGMANN, BARTIRA; POHLMANN, ADRIANA R. How Sorbitan Monostearate Can Increase Drug-Loading Capacity of Lipid-Core Polymeric Nanocapsules. *Journal of Nanoscience and Nanotechnology (Print)*, v. 15, p. 827-837, 2015.

2. BIANCINI, GIOVANA B.; JACQUES, CARLOS E.; HAMMERSCHMIDT, TATIANE ; DE SOUZA, HERYK M.; **DONIDA, BRUNA**; DEON, MARION; VAIRO, FILIPPO P.; LOURENÇO, CHARLES M.; GIUGLIANI, ROBERTO; VARGAS, CARMEN R. Biomolecules damage and redox status abnormalities in Fabry patients before and during enzyme replacement therapy. *Clinica Chimica Acta (Print)*, v. 461, p. 41-46, 2016.

3. JACQUES, CARLOS E.D.; **DONIDA, BRUNA**; MESCKA, CAROLINE P.; RODRIGUES, DAIANE G.B.; MARCHETTI, DESIRÈE P.; BITENCOURT, FERNANDA H.; BURIN, MAIRA G.; DE SOUZA, CAROLINA F.M.; GIUGLIANI, ROBERTO; VARGAS, CARMEN R. Oxidative and nitrative stress and pro-inflammatory cytokines in Mucopolysaccharidosis type II patients: effect of long-term enzyme replacement therapy and relation with glycosaminoglycan accumulation. *Biochimica et Biophysica Acta. Molecular Basis of Disease*, v. 1862, p. 1608-1616, 2016.

4. MARCHETTI, DESIRÈE P.; **DONIDA, BRUNA**; DEON, MARION; JACQUES, CARLOS E.; JARDIM, LAURA B.; VARGAS, CARMEN R. In vitro effect of N-acetyl-L-cysteine on glutathione and sulfhydryl levels in X-linked adrenoleukodystrophy patients. *Clinical and Biomedical Research*, v. 37, p. 33-37, 2017.

5. **DONIDA, BRUNA**; JACQUES, CARLOS E.D.; MESCKA, CAROLINE P.; RODRIGUES, DAIANE G.B.; MARCHETTI, DESIRÈE P.; RIBAS, GRAZIELA; GIUGLIANI, ROBERTO; VARGAS, CARMEN R. Oxidative damage and redox in Lysosomal Storage Disorders: Biochemical markers. *Clinica Chimica Acta (Print),* v. 466, p. 46-53, 2017.

6. **DONIDA, BRUNA**; MARCHETTI, DESIRÈE P.; JACQUES, CARLOS E. D.; RIBAS, GRAZIELA; DEON, MARION; MANINI, PAULA; DA ROSA, HELEN T.; MOURA, DINARA J.; SAFFI, JENIFER; GIUGLIANI, ROBERTO; VARGAS, CARMEN R. Oxidative profile exhibited by Mucopolysaccharidosis type IVA patients at diagnosis: Increased keratan urinary levels. *Molecular Genetics and Metabolism Reports*, v. 11, p. 46-53, 2017.

7. VANZIN, CAMILA S.; MESCKA, CAROLINE P.; **DONIDA, BRUNA**; MARCHETTI, DESIRÈE P.; JACQUES, CARLOS E.; HAUSCHILD, TATIANE; FAVERZANI, JÉSSICA L.; DEON, MARION; MOURA, DINARA J.; SAFFI, JENIFER; COELHO, DANIELLA D.M.; WAJNER, MOACIR ; WYSE, ANGELA T. S.; VARGAS, CARMEN R. DNA damage in homocystinuria: 8-oxo-7,8-dihydro-2 -deoxyguanosine levels in cystathionine-²-synthase deficient patients

and the in vitro protective effect of N-acetyl-L-cysteine. *Clinical and Biomedical Research*, v. 38, p. 50-57, 2018.

8. MARCHETTI, DESIRÈE P.; **DONIDA, BRUNA**; JACQUES, CARLOS E.; DEON, MARION; HAUSCHILD, TATIANE C.; KOEHLER-SANTOS, PATRICIA; COELHO, DANIELLA D.M.; COITINHO, ADRIANA S.; JARDIM, LAURA B.; VARGAS, CARMEN R. Inflammatory profile in X-linked adrenoleukodystrophy patients: Understanding disease progression. *Journal of Cellular Biochemistry*, v. 119, p. 1223-1233, 2018.

9. BOHN, DENISE R.; LOBATO, FRANCIELLI O.; THILL, ALISSON S.; STEFFENS, LUIZA; RAABE, MARCO; **DONIDA, BRUNA**; VARGAS, CARMEN R.; MOURA, DINARA J.; BERNARDI, FABIANO; POLETTO, FERNANDA. Artificial cerium-based proenzymes confined in lyotropic liquid crystals: synthetic strategy and on-demand activation. *Journal of Materials Chemistry B*, v. 6, p. 4920-4928, 2018.

10. **DONIDA, BRUNA**; TAUFFNER, BÁRBARA; RAABE, MARCO; IMMICH, MAIRA F.; DE FARIAS, MARCELO A.; COUTINHO, DIEGO D.S.; MACHADO, ANDRYELE Z.; KESSLER, REJANE G.; PORTUGAL, RODRIGO V.; BERNARDI, ANDRESSA; FROZZA, RUDIMAR; MOURA, DINARA J.; POLETTO, FERNANDA; VARGAS, CARMEN R. Monoolein-based nanoparticles for drug delivery to the central nervous system: A platform for Lysosomal Storage Disorder treatment. *European Journal of Pharmaceutics and Biopharmaceutics*, v. 133, p. 96-103, 2018.